# DEVELOPMENT OF DOX AND siRNA LOADED SURFACE MODIFIED CHITOSAN NANOPARTICLES FOR TREATMENT OF COLORECTAL CANCER: IN-VITRO & IN-VIVO EVALUATION

By

Ms. TAIHASEEN ALIM MOMIN

Under the Supervision of

Dr. ARVIND GULBAKE

Thesis Submitted to



For the Degree of

Doctor of Philosophy

2024

# DEVELOPMENT OF DOX AND siRNA LOADED SURFACE MODIFIED CHITOSAN NANOPARTICLES FOR TREATMENT OF COLORECTAL CANCER: in-vitro & in-vivo EVALUATION
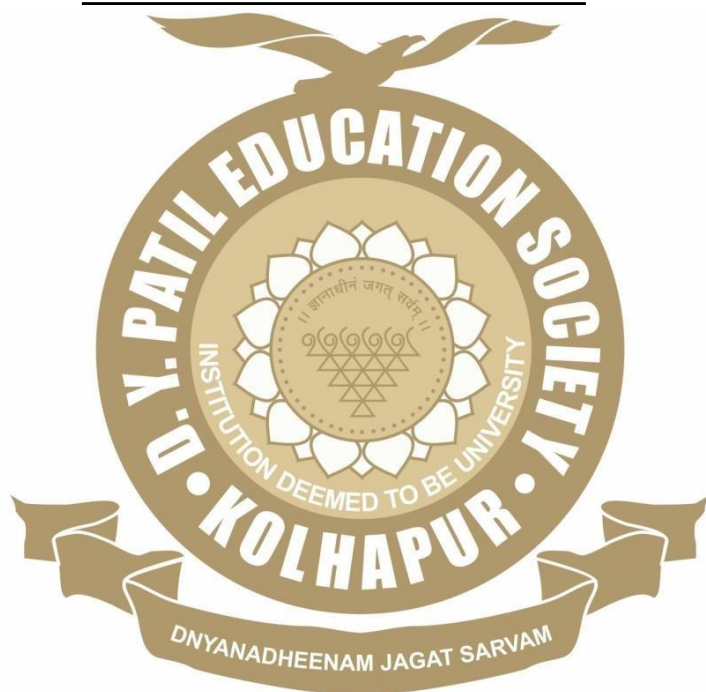
A Thesis Submitted to

## D. Y. PATIL EDUCATION SOCIETY
## (DEEMED TO BE UNIVERSITY)

For the Degree of

## DOCTOR OF PHILOSOPHY
## In
### BIOTECHNOLOGY

By

## Ms. TAIHASEEN ALIM MOMIN
**M. Sc.**

Under the Supervision of

## Dr. ARVIND GULBAKE
**M. Pharm., Ph. D.**

**FORMER COORDINATOR AND ASSISTANT PROFESSOR,
RESEARCH AND DEVELOPMENT, CENTRE FOR
INTERDISCIPLINARY RESEARCH,
D.Y. PATIL EDUCATION SOCIETY (DEEMED TO BE UNIVERSITY)
KOLHAPUR**

**2024**

# DECLARATION

I hereby declare that the thesis entitled, "**DEVELOPMENT OF DOX AND siRNA LOADED SURFACE MODIFIED CHITOSAN NANOPARTICLES FOR TREATMENT OF COLORECTAL CANCER: IN-VITRO & IN-VIVO EVALUATION**" submitted for the award of the degree of **Doctor of Philosophy** in the faculty of Science of the D. Y. Patil Education Society (Deemed to be University), Kolhapur is completed and written by me, has not previously formed the basis for the award of any Degree or Diploma or other similar titles of this or any other University in India or any other country or examining body to the best of my knowledge. Further, I declare that I have not violated any of the provisions under the Copyright and Piracy/ Cyber/ IPR Act amended from time to time.

**Research Student**

**Place:** Kolhapur

**Date:** 15/01/2024

*momin*

**(Ms. Taihaseen Alim Momin)**

# CERTIFICATE

This is to certify that the thesis entitled, "**DEVELOPMENT OF DOX AND siRNA LOADED SURFACE MODIFIED CHITOSAN NANOPARTICLES FOR TREATMENT OF COLORECTAL CANCER: IN-VITRO & IN-VIVO EVALUATION**", which is being submitted herewith for the award of the degree of **Doctor of Philosophy** in **BIOTECHNOLOGY** under the faculty of Science of D. Y. Patil Education Society (Deemed to be University), Kolhapur, is the result of the original research work completed by **Ms. TAIHASEEN ALIM MOMIN** under my supervision and guidance and to the best of my knowledge and belief, the work embodied in this thesis has not formed earlier the basis for the award of any degree or similar title of this or any other University or examining body.
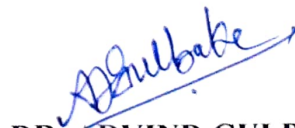
**Place**: Kolhapur

**Date**: 15/01/2024

**Research Director & Dean**

**PROF. C. D. LOKHANDE**
Centre for Interdisciplinary Research,
D.Y. Patil Education Society
(Deemed to be University),
Kolhapur.

**Research Guide**

**DR. ARVIND GULBAKE**
Former Coordinator and
Assistant Professor,
Research and Development,
Centre For Interdisciplinary Research,
D.Y. Patil Education Society
(Deemed To Be University) Kolhapur

# ACKNOWLEDGEMENT

# CONTENTS

# LIST OF FIGURES

# LIST OF TABLES

# LIST OF ABBREVIATIONS

| | |
|---|---|
| **Abs** | Absorbance |
| **Ab** | Antibody |
| **BSA** | Bovine serum albumin |
| **CEA** | Carcinoembryonic antigen |
| **Ch** | Chitosan |
| **ChNPs** | Chitosan nanoparticles |
| **CMAb** | Carcinoembryonic antigen targeted mononoclonal antibody |
| **CRC** | Colorectal cancer |
| **DAPI** | 4'6-diamidino-2-phenylindole |
| **DD** | Degree of deacetylation |
| **DD** | Drug delivery |
| **DDS** | Drug delivery system |
| **DW** | Distilled water |
| **DOX** | Doxorubicin |
| **ELISA** | Enzyme linked immunosorbant assay |
| **EPR** | Enhanced Permeability and Retention |
| **EtBr** | Ethidium Bromide |
| **FT-IR** | Fourier transform infrared spectroscopy |
| **H&E** | Hematoxylin and eosin |
| **HRP** | Horse reddish peroxidase |
| **HT-29** | Human-colon carcinoma cell line |
| **MAb** | Monoclonal antibody |
| **MDR** | Multidrug resistance |
| **mg** | Microgram |
| **µl** | Microlitre |
| **µm** | Micrometer |
| **ml** | Mililitre |

| | |
|---|---|
| **MTT** | 3-(4,5-dimethylthiazol-2-yl)-2,5-diphenyl tetrazolium bromide dye |
| **mw** | Molecular weight |
| **NCCS** | National Centre for Cell Science |
| *nm* | Nanometer |
| **NPs** | Nanoparticles |
| **PBS** | Phosphate buffer saline |
| **PDI** | Polydispersity Index |
| **RNAi** | RNA interference |
| **Rpm** | Rotation per minute |
| **SEM** | Scanning electron microscopy |
| **siRNA** | Small interfering RNA |
| **TE** | Tris-EDTA buffer |
| **TAE** | Tris-acetate-EDTA |
| **TEM** | Transmission electron microscopy |
| **TMB** | 3,3',5,5'-Tetramethylbenzidine |
| **TPP** | Sodium tripolyphosphate |
| **UV-Vis** | UV visible spectrophotometry |
| **VEGF** | Vascular endothelial growth factor |

# LIST OF PATENTS, PUBLICATIONS AND CONFERENCES ATTAINED

➢ **Patent (Granted 01)**

- Process for embedding oleic acid coated superparamagnetic iron oxide nanoparticles in lipidic nanoparticles for enhancing hyperthermic efficiency Dr. A. Gulbake, Mr. S. S. Harugale, **Miss. T. Momin**, Prof. C. D. Lokhande, Dr. V. V. Bhosale, Application No.201921019463

➢ **Articles in International Journals**

- **T. Momin**, S. Harugale, A. Gulbake, A. Gulbake - Recent trends in siRNA delivery for treatment of colorectal cancer. Int J App Pharm, 11, Special Issue 2, (2019), 31-36.

- **Momin T**., Gulbake A. Development and characterization of doxorubicin and siRNA encapsulated chitosan nanoparticles. Int J App Pharm, 12, Special Issue 4, (2020) 53-56.

- Nanotechnology and regenerative medicine, Chapter 22, accepted in Nanomedicine, Nanotheranostics and Nanobiotechnology: Fundamentals and Applications, CRC Press,Taylor & Francis Group.

➢ **Conference/Seminar/Workshop Participation & Presentations**

# 1.    STATEMENT OF THE PROBLEM

In world, colorectal cancer (CRC) is the fourth leading and common cause of cancer-related death**.** The current cancer therapies, consists of surgery combined with chemotherapy and/or radiotherapy. Although, conventional drug delivery systems (DDS) has serious side effects and several limitations such as acquired multi-drug resistance (MDR), non-specificity, poor bio-distribution and bioavailability with low therapeutic index and high toxicity. Therefore, there is a lot of scope to develop novel therapeutics to improve the efficacy of chemotherapeutic agents and reduce drug resistance.

siRNA therapeutics have shown potential advantages over the off-target delivery of conventional chemotherapeutic agents via specific gene-silencing mechanisms. A major problem associated with siRNA delivery is poor bioavailability due to degradation of siRNA by serum nucleases. Therefore, practical applications require targeted carriers that deliver drugs or siRNA therapeutics to target sites via oral or intravenous administration and increase cellular uptake. A combination of chemotherapy and gene therapy that specifically targets cancer cells has emerged as a promising strategy for cancer treatment.

## 1.1 Colorectal cancer

In the 21$^{st}$ century, cancer is the major leading cause of death. Several genetic alterations and cellular abnormalities are involved in the development of cancer. According to the WHO, 17.5 million deaths and 27 million new cancer cases are projected to occur by 2050 (Saraswathy and Gong, 2014, Cardoso et al., 2012). Cells from the lining of colon and rectum proliferate abnormally, are non-cancerous in the early stage and 100% curable but become uncontrolled and develop into adenomatous polyps and then tumors in 10-20 years. In CRC, genetic mutations lead to high cellular heterogeneity that exhibits variability between tumors (Pereira et al., 2018, Chandran et al., 2017).

### 1.1.1 Current treatments

There are several conventional treatments for CRC. For example, (1) open surgery to remove the primary local tumor along with nearby healthy tissue and lymph nodes, (2) high energy radiation therapy to target cancer and (3) chemotherapy with various chemotherapeutic agents to kill cancer cells, but they have limited tissue

specificity and are severely cytotoxic in healthy cells (Li et al., 2016). Depending on the stage of cancer development combination of these treatments is used. But, these conventional treatments do not have a 100% guaranteed cure and with 50% recurrence rate showing side effects like pain, nausea, gastro-intestinal distrubance, mouth ulcer, skin rash, atrophy, vascular and neural damage etc. (Lee et al., 2016, Pereira et al., 2018, Siahmansouri et al., 2016).

### 1.1.2 Limitations of current treatments overcomes by Drug Delivery (DD)

Although the use of chemotherapeutic drugs has several disadvantages such as lack of selectivity, low antitumor efficiency, short plasma half-life due to rapid blood clearance and acquired MDR. Hence, there is a need to develop targeted DDS that specifically acts on the target site (Parveen and Sahoo, 2010, Sun et al., 2018). The most important application of nanotechnology is the development of nanoscale targeted delivery which improves the therapeutic efficiency of conventional chemotherapeutics. A different tissue or cell-specific receptor and antigen can offer a useful target in cancer treatment (Cardoso et al., 2012). Targeted DD has a unique advantage such as reducing toxicity to normal cells and improving in the therapeutic index for cancer cells. As in other cancers, conventional chemotherapy is not as effective in CRC because the effective concentration of the drug does not reach the target site. So, pharmaceutical technologists and researchers have been working on ways to deliver the drug to the target tumor tissue more efficiently (Jain et al., 2010, Siahmansouri et al., 2016). Multidrug resistance has several mechanisms that include p-gp glycoprotein efflux transporters, DNA damage repair, acidic tumor microenvironment and reduced intracellular accumulation of drug and detoxification of drug by enzymes. For the past three decades, nanoparticulate DDSs have been studied and shown advantages in cancer treatment over conventional therapeutics (Khdair et al., 2016). The problems associated with MDR circumvents by one of the most promising approach is RNA interference (RNAi) technology (Rudzinski et al., 2016). Recently, combining chemotherapy and gene therapy has the potential to provide target selectivity and synergy to reduce the development of drug resistance (Liu et al., 2018).

## 1.2 Role and benefits of Nanotechnology in Drug Delivery

Nanomedicine is an interdisciplinary field of nanotechnology that plays a major role in targeted therapy. The use of nanoscale DDS has emerged as a widely studied approach to improve cancer delivery and treatment. Two commercially available nanoparticulate DDSs, (Doxil®) liposomal DOX and (Abraxane®) albumin-based taxol NPs have rekindled interest in DD (Karra and Benita, 2012). Various nanocarrier systems are used for DD. Polymeric NPs, liposomes, hydrogels and self-assembled nanofibers possess passive and active tumor-targeting capabilities that minimize toxicity, overcome drug resistance and increase therapeutic index. Among these nanocarriers, NPs have received much attention due to their unique properties (Siddharth et al., 2017, Saraswathy and Gong, 2014, Siahmansouri et al., 2016).



**Figure 1.1 Advantages of nanocarriers in drug delivery**

Nanoparticulate DDS offers numerous advantages including engineered size and surface area, sustained drug release, pharmacokinetics and bio-distribution enhancement, decrease in side effects and programmed particles degradation (Pavitra et al., 2021). Advantages of nanocarriers in DD are shown in Figure 1.1.

Furthermore, the characteristically loose neovasculature of growing tumors exhibits greater accumulation and slower clearance of NPs. This effect is referred to as the "enhanced permeability and retention (EPR) effect". The penetration of NPs with the entrapped drug to the tumor tissue is highly affected by their small size and leaky nature of tumor neovasculature (Hellmers et al., 2013, Karra and Benita, 2012, Pavitra et al., 2021). Essential physicochemical properties of NPs are their size ranging from 1−1000 nm, shape, surface charge and compactness. These properties of NPs offer many advantages in DD by improving bioavailability, biodistribution, mucoadhesion, stability of drug against chemical and enzymatic degradation and sustained and controlled release of the drug to the target site. In addition, specific ligands can be used to surface-modify these NPs to reduce side effects and improve therapeutic efficacy, thus delivering drug to target tumor tissues (Jonassen et al., 2012, Parveen and Sahoo, 2010, Masarudin et al., 2015, Pavitra et al., 2021).

Polymeric NPs are divided into biodegradable and non-biodegradable categories based on their basic chemical composition. Generally, polymeric NPs consist of a core-shell structure. Polymeric NPs have a polymeric backbone and are composed of monomers of simple one or more biodegradable, biocompatible organic molecules. Now a day, various synthetic and natural polymers are explored for the preparation of NPs such as, polylactide (PLA), polyethylene glycol (PEG), polyglycolide (PGA), polycaprolactone, polyacrylate, poly alkyl cyanoacrylate (PCA), polyethyleneimine (PEI), poly (L-lysine) (PLL) and its derivatives have been used for drug and siRNA delivery. Among the recently investigated polymeric materials for NPs fabrication, chitosan (Ch) possesses unique properties and characteristics that make it desirable as a potential NPs carrier (Karra and Benita, 2012, Abdul Ghafoor Raja et al., 2015).

## 1.3 Chitosan biopolymer as an efficient nanocarrier

Chitosan is a linear natural polysaccharide composed of D-glucosamine and N-acetyl–D-glucosamine units linked by β-(1-4) glycosidic bonds. It can be obtained by deacetylation and by alkaline or enzymatic hydrolysis of chitin which occurs naturally in crustaceans shells, insects exoskeletons, arachnids and also in the fungal cell wall (de Pinho Neves et al., 2014, Almalik et al., 2013). The Ch has a pKa value of ~6.3−6.5 and is affected by the degree of N-acetylation. Due to protonation of the amine group Ch is readily soluble in an acidic environment. Thus, the more cationic nature of Ch binds readily to negatively charged cell membranes and exhibits mucoadhesive properties that improve drug transport (Pant and Negi, 2018, Gomathi et al., 2017) and also promotes ionic cross-linking with multivalent anions, such as sodium tripolyphosphate (TPP), glutaraldehyde (Yang et al., 2010, Ibrahim et al., 2018). The resulting positive charge enables the preparation of ChNPs by ionic gelation. Some factors that influence the properties of ChNPs are the concentration and molecular weight of Ch, the TPP : Ch ratio, the ionic strength and the pH of the medium used to prepare the NPs (Jonassen et al., 2012). It is listed as a GRAS (Generally Recognized As Safe) and used as a food additive in Italy, Japan and Finland. It has been described as having low toxicity in-vitro and in-vivo (Cao et al., 2019, Alameh et al., 2018, Souto et al., 2016).

### 1.3.1 Chitosan properties

Ch is a cationic, nontoxic, semi-crystalline, biodegradable, biocompatible, bioadhesive, non-immunogenic, hemostatic, fungistatic biopolymer. Because of these properties ChNPs have received much attention for the delivery of drugs, proteins, peptides, antigens, genes and oligonucleotides by intravenous, oral and mucosal route administration (Venkatesan et al., 2013, Gomathi et al., 2017, Huang et al., 2004, Fan et al., 2012, Nogueira-Librelotto et al., 2016, Sahu et al., 2010).

### 1.3.1.1 Basic characteristics of chitosan

The amino and carboxyl groups of Ch molecules can bind with glycoproteins in mucus to form hydrogen bonds, resulting in adhesive effects, prolonging drug retention time and continuous drug release in-vivo and improving drug bioavailability.

- **Biodegradability and safety of chitosan**

Biodegradability of Ch has a major role in DDSs. Appropriate molecular weight Ch is cleared by the kidney, whereas excess molecular weight Ch is degraded into fragments suitable for renal elimination. The higher degree of deacetylation shows faster the degradation rate. Ch is mainly degraded by chemical and enzymatic catalysis and enzyme catalysis depends on the availability of Ch-amino groups.

- **Antitumor effect of chitosan**

Ch can act directly on tumor cells to disrupt cell metabolism, inhibit cell proliferation and induce apoptosis. It also plays an anti-tumor role that boosts the body's immune function (Cao et al., 2019).

### 1.3.1.2 Chitosan nanoparticles characteristics

ChNPs are drug carriers with great development potential with the advantages of improved drug solubility and stability, enhanced potency, reduced toxicity and slow/controlled drug release. Their small size allows them to cross biological barriers (such as the blood-brain barrier) in vivo, delivering drugs to sites of injury and increasing their efficacy. The modified NPs also have other properties such as: Improved Drug Targeting. Biodegradable NPs are an increasing research focus because they can produce water and carbon dioxide in-vivo through enzymatic action without side effects.

- **Sustained/controlled release characteristics**

Drugs contained by ChNPs can be released over time due to Ch breakdown and erosion, resulting in a distinct sustained-release effect. Different types of NPs can be used to control the drug release rate because Ch with different molecular weights and degrees of deacetylation have different degradation rates and times. Ch can be adjusted to provide a sustained/controlled release.

- **Modification of chitosan NPs**

A growing number of studies are focusing on Ch modification to increase the targeting and bioavailability of ChNPs. The pH sensitivity, thermosensitivity and targeting accuracy are all characteristics of modified ChNPs. ChNPs are used for targeted therapy because their positive charge has selective adsorption and neutralizing

effects on tumor cell surfaces. It has a targeting role for the liver, spleen, lung and colon cancer as a drug carrier.

- **Chitosan nanoparticles metabolic process in-vivo**

The NPs are detected as foreign substances and absorbed by antibodies (Abs) produced by the human body. Plasma proteins, lipoproteins, immunological proteins and complement C proteins are all adsorbed on NPs, speeding up the reticuloendothelial system rearrangement. Macrophages ingest NPs, which are then removed from the body's circulation. Plasma protein deposited on the NPs surface forms a bridge between NPs and macrophages. The ability of NPs to adsorb plasma proteins is regulated by their surface charge which influences the NPs transfer intensity via macrophage. The NPs with polarity and high surface potential are engulfed less and have a longer circulating period. Ch is primarily destroyed in the colon by lysozyme and bacterial enzyme catalysis. The kidneys remove the Ch that has been absorbed into the blood and the rest is excreted. The degree of deacetylation and molecular weight of Ch has an impact on Ch breakdown rate in-vivo. Ch has good biocompatibility and biodegradability as a non-viral carrier which has led to an increase in the use of ChNPs in gene delivery. The use of double-stranded short interfering RNA (siRNA) to silence genes has been extensively explored as a potential therapy for diseases caused by genetic abnormalities. However, its use is limited due to its rapid degradation and poor cellular uptake (Wang et al., 2011). Ch is a widely studied polymer in the field of non-viral gene therapy. Its positive charges allow it to bind with siRNA and form complexes or NPs under slightly acidic circumstances. Furthermore, because Ch is biocompatible and biodegradable it can be administered intraperitoneally or intravenously. This polymer is a good starting point for NPs development but it still needs to be improved to mediate high gene silencing, particularly after intravenous administration (Ragelle et al., 2014, Narmani and Jafari, 2021).

- **Enhanced siRNA Release**

The release of biologically active nucleic acids in cells is critical, as is the efficient entry of siRNA carriers into target cells. The carrier is trapped in early endosomes during endocytosis and undergoes gradual maturation into late endosomes to pH 5-6 through proton assembly via the ATPase proton pump. Later, endosomes eventually associate with lysosomes, resulting in a harsh, enzyme-rich

environment at pH 4–5. Carriers should be designed to escape endosomes prior to fusion with lysosomes. The proton sponge effect allowed Ch-based formulations to successfully escape endosomes. After encapsulation of the carrier within the endosome, the amine group of Ch which has a pKa of ~6.5, is gradually protonated in the more acidified endosomal environment. The influx of water and chloride is attributed to an increase in cationic ions entering the endosome to neutralize its charge, causing osmotic swelling and eventual physical rupture of the endosome, releasing Ch carriers into the cytoplasm (Cao et al., 2019, Chuan et al., 2019).

## 1.4 ChNPs preparation by ionic gelation method

For the preparation of ChNPs researchers used a variety of methods including ionic gelation, microemulsion, reverse micelle, coacervation spray-drying, precipitation, synthesis with carboxymethyl cellulose, formulations using glutaraldehyde, synthesis with alginate, template polymerization with poly(hydroxyethyl methacrylate), polyelectrolyte complex are some of the methods used for ChNPs preparation (Gomathi et al., 2017, de Pinho Neve et al., 2014, Berger et al., 2004, Nasti et al., 2009, Al-Qadi et al., 2012, Rampino et al., 2016).

Because of its simplicity, non-toxicity and lack of organic solvents, the high temperature and sonication ionic gelation method is a widely used method for ChNPs (Berger et al., 2004, Nasti et al., 2009, Al-Qadi et al., 2012, Rampino et al., 2016, de Pinho Neve et al., 2014, Kiilll et al., 2017). Among the various methods developed to prepare ChNPs, the ionic gelation technique has received much attention due to its non-toxic, organic solvent-free, simple and controlled design. Ionic gelation relies on ionic interactions between positively charged Ch primary amino groups and negatively charged polyanionic groups (such as TPP). TPP is the most commonly used ionic crosslinker due to its non-toxic and multivalent properties (Fan et al., 2012). In this approach, NPs are made by mixing a TPP solution (pH 7-9) with an acidic Ch solution (pH 4-6) (de Pinho Neve et al., 2014, Kiilll et al., 2017). The weight ratio of Ch to TPP is probably the most critical factor in controlling particle size, shape and surface charge. However, the concentration and molecular weight (mw) of Ch and the ionic strength and pH of the medium all play important roles (Almalik et al., 2013). Since the biological fate of NPs is determined by their size, there is great interest in controlling

the average size and polydispersity of NPs. Ionic strength, mixing process, Ch and TPP concentrations, degree of Ch deacetylation (DD), temperature and pH are all factors that influence the average Ch/TPP particle size. Ch chains contract more at pH 5 than in more acidic solutions due to the increased amount of hydrogen bonding (Masarudin et al., 2015, Sawtarie et al., 2017, Calvo et al., 1997).

At pH values below pKa 6.5, the primary amine residues of Ch are protonated and complexed with anionic substances such as the phosphate groups of nucleic acids and allows the formation of NPs through electrostatic interactions between both functional groups (Sadio et al., 2014). Peptides, proteins, plasmid DNA (pDNA), insulin and siRNA have all been encapsulated using ChNPs. The potential of Ch in the development of controlled-release medication delivery devices has been thoroughly investigated (Venkatesan et al., 2013). Cationic polysaccharides such as Ch can interact electrostatically with siRNAs to generate stable, positively charged polyplexes, whereas positively charged nanocarriers are the most efficient intracellular delivery of nucleic acids. Cationic polysaccharides such as Ch can interact electrostatically with siRNAs to generate stable, positively charged polyplexes, whereas positively charged nanocarriers provide the most efficient intracellular delivery of nucleic acids. There are two reasons for this, 1) binding with negatively charged nucleic acids shields them from degradation by nucleases 2) it creates a net positive charge that enhances complex interactions with the cell's anionic surface (Serrano-Sevilla et al., 2019, Chuan et al., 2019).

## 1.5 Small Interfering RNA (siRNA)

Many siRNA molecules have been shown to effectively block various signaling pathways involved in cell proliferation and cell death using RNAi therapeutics. However, efficient delivery of siRNAs to target cells, tissues or organs has proven challenging. Due to their polyanionic structure and relatively large mw, naked siRNAs are rapidly destroyed by serum ribonucleases and are largely unable to cross cell membranes (Saraswathy and Gong, et al., 2014, Sun et al., 2016). Double-stranded RNA helices trigger RNAi, a potent and highly specific gene silencing event. Introduction of 21-23 base-pair siRNAs into cells results in degradation of target messenger RNA (mRNA) and reduction of target protein levels (Rudzinski et al., 2016, Sun et al., 2016). Chemical modifications of siRNA can be used to address these issues, but have drawbacks such as reduced mRNA hybridization, increased cytotoxicity and

increased non-specific effects. To take advantage of the interesting potential applications of successful siRNA delivery, an effective system is required that can protect and deliver siRNA to the cytoplasm of target cells. Ch has many advantages such as low toxicity and immunogenicity, good biodegradability, biocompatibility and positive charge that can readily form polyelectrolyte complexes with negatively charged nucleotides through electrostatic interactions (Katas and Alpar, 2006, Sun et al., 2016).

### 1.5.1 Characteristics of ideal nanocarrier for siRNA delivery

Considering the intravenous route, which is one of the more direct routes to drug targets (tumor tissue, tumor endothelial blood vessels), an ideal carrier should possess the following properties: (1) biocompatibility, (2) size should be less than 200 nm. It is small enough to penetrate a range of tissues. In addition, the delivery system allows siRNA containing particles to enter cells via receptor-mediated endocytosis, facilitate intracellular trafficking and reticuloendothelial system (RES) clearance must be reduced, (3) The carrier should be stable enough in physiological fluids to avoid nucleic acid degradation, (4) The carrier must avoid opsonization and uptake by macrophages, maintain a high retention time and be able to reach and enter cells. All of these features are desirable for creating potent siRNA delivery systems (Li et al., 2017, Serrano-Sevilla et al., 2019, Ragelle et al., 2014).

### 1.5.2 Gene silencing mechanism of siRNA

An endoribonuclease called Dicer degrades long dsRNAs and converts them into short interfering RNAs or siRNAs. However, siRNA can be generated and directly transported into cells without using the Dicer process. Once siRNA enters the cell, it is incorporated into a protein complex known as the RNA Induced Silencing Complex (RISC). Argonaute 2 is a versatile protein of the RISC complex that unfolds siRNA prior to cleaving the sense strand. The antisense strand of activated RISC searches for complementary mRNA and when a single-stranded siRNA (part of the RISC complex) binds to it, it causes cleavage of the mRNA. The mRNA is then identified as defective and is thereby destroyed. Active RISC complexes destroy more mRNA targets and propagate gene silencing. It even needs to be administered with/in a suitable carrier. This allows delivery of siRNAs with improved therapeutic efficacy and target

specificity (Cavallaro et al., 2017). The gene silencing mechanism of siRNA is shown schematically in Figure 1.2.
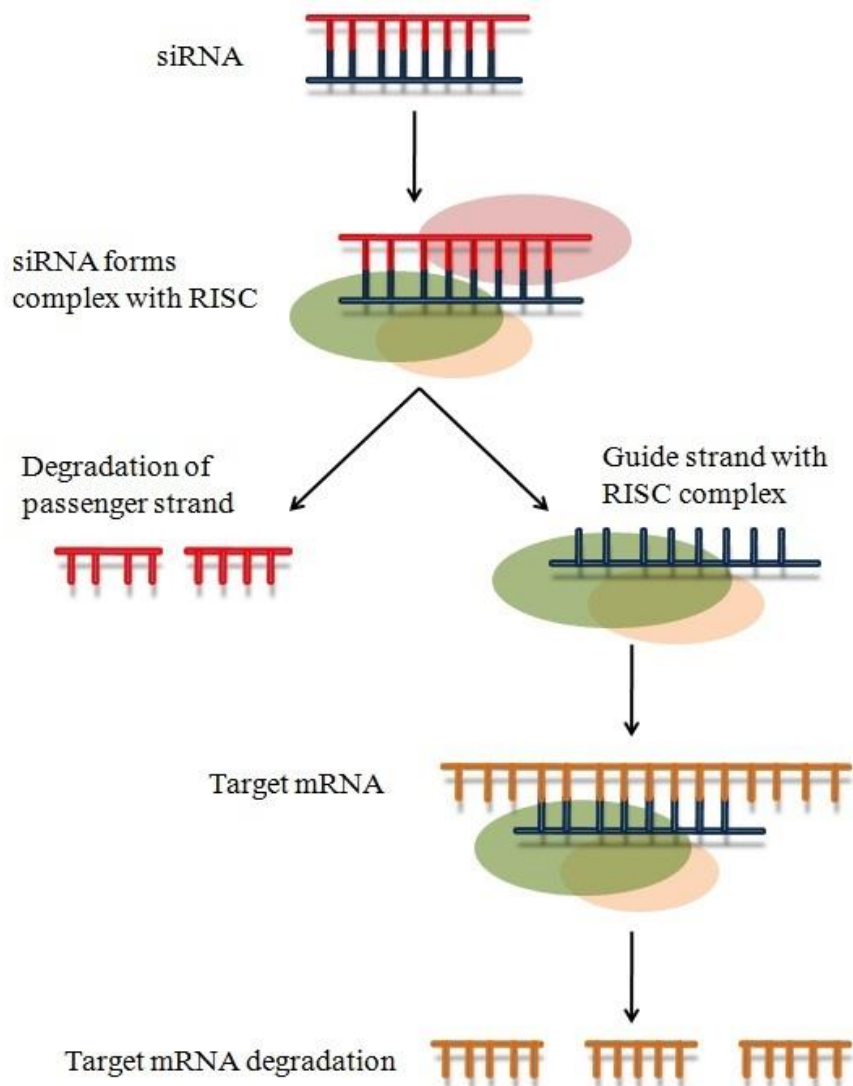


**Figure 1.2 Gene silencing mechanism of siRNA**

**1.5.3 Vascular endothelial growth factor (VEGF) gene silencing by siRNA**

With advances in RNAi technology, siRNAs targeting the VEGF gene have been intensively studied and termed anti-VEGF therapy. The success of bevacizumab in 2004 demonstrated that VEGF can be used as a target for angiogenic therapy. Bevasiranib, the first therapeutic siRNA, is progressing into a Phase III clinical trial for the treatment of exudative neovascular age-related macular degeneration (AMD) targeting VEGF. AGN-745, a second therapeutic siRNA targeting VEGF, is the second to enter clinical trials and its early results on safety and efficacy

are encouraging. A variety of innovative anti-VEGF medicines are currently in phase III clinical studies and could be available in the next few years.

Recently, many anti-angiogenic treatments have been demonstrated, such as the delivery of siRNAs that knock out specific pro-angiogenic genes. Among these targets, VEGF has received much interest due to its important involvement in tumor angiogenesis (Liu et al., 2018, Li et al., 2016).

Angiogenesis is a key factor in cancer cell survival, proliferation, migration and metastasis. Anti-VEGF technology was developed to prevent new blood vessel formation and deprive tumors of oxygen and nutrients. Increased production of pro-angiogenic factors is triggered by tumor cells that secrete VEGF. The National Comprehensive Cancer Network (NCCN) has identified it as a molecular therapy for CRC (Lan et al., 2017, Chekhonin et al., 2013, Wang et al., 2011).

The VEGF target was chosen to deliver chemotherapeutic medicines in tandem, resulting in a combined anticancer impact. However, naked siRNAs are fragile, particularly susceptible to destruction by nucleases and may not be taken up by cells due to their negatively charged surface, resulting in unsuccessful transfection. Furthermore, efficient transfection into cells requires intact siRNAs, which can trigger the RNAi process for targeted gene silencing. As a result, nanoscale delivery systems have become widespread and have emerged as an ideal option for co-loading chemotherapeutic agents and siRNA and protecting the siRNA from degradation (Liu et al., 2018, Li et al., 2016).

Co-administration of siRNA and chemotherapeutic drug is a promising strategy to improve therapeutic efficacy. Due to the inherent complexity of tumor therapy and its complex mechanism of action, in recent years combination therapy has been widely used. Significant research shows that combining chemotherapy and gene therapy improves the efficacy of treatment, reduces the side effects of chemotherapeutics, sensitizes tumor cells to the drugs and alleviates the long-standing problem of MDR (Sun et al., 2018).

For systemic or intravenous (IV) administration of siRNA there is a need of efficient carrier. Tekmira Pharmaceuticals Corporation developed RNAi therapeutic using lipid nanocarriers, to treat hypercholesterolemia, TKM-ApoB was designed using siRNA against ApoB mRNA. Several clinical studies have explored the use of siRNAs

in combination with other chemotherapeutic agents with promising results (Amjad et al., 2017). In addition to monoclonal antibodies (MAbs) that bind to VEGF and decrease tumor angiogenesis such as bevacizumab (Avastin®) and Ziv-aflibercept (Zaltrap®), anti-VEGF siRNA has tremendous potential for decreasing tumor angiogenesis (Lee et al., 2016).

## 1.6 Doxorubicin (DOX)

Doxorubicin is an anthracycline antibiotic produced from Streptomyces peucetius var. caesius, an actinobacterium. The medication has anticancer action across breast, ovarian, lung and bladder cancers (Yoncheva et al., 2019). Doxorubicin is a glycoside antibiotic that suppresses cell proliferation and DNA synthesis. Doxorubicin is a member of the $20^{th}$ WHO essential medication list (EML) for adults and the $6^{th}$ for children includes essential pharmaceuticals in cytotoxic and adjuvant medicine. It's given by IV infusion (Zare et al., 2018).

It is a water-soluble and one of the most commonly used anticancer agent to treat various cancers. DOX is a potent cytotoxic agent for normal tissues and its cumulative dose-dependent cardiotoxicity has been extensively reported by various studies.  Being hydrophilic, it binds to DNA by intercalation and triggers a cascade of biochemical processes in tumor cells, leading to death. Conventional drugs are normally easily discharged from tumors but when encapsulated in a nanostructure their storage in tumor tissue can be greatly increased (Unsoy et al., 2014, Nogueira-Librelotto et al., 2016, Li et al., 2016).

However, problems such as the development of resistance, acute cardiotoxicity, poor penetration and limited distribution to solid tumors have led researchers to consider other injection methods. Cell membranes are negatively charged, encapsulating DOX in positively charged nanocarriers would promotes cell adhesion and uptake (Souto et al., 2016, Janes et al., 2001). Targeting DOX via polymeric NPs is also an alternative strategy for cancer therapy to reduce toxicity. Due to its positive charge attracted to negatively charged cell membranes, cell adhesion and potential cellular uptake of ChNPs should be efficient in addition to tailored administration (Sahu et al., 2010, Unsoy et al., 2014).

Multidrug resistance, which lowers the therapeutic efficacy of chemotherapeutics is a major issue. The resistance of tumor cells is usually linked to

transport proteins that use DOX as a substrate. The activity of these proteins is directly related to drug accumulation in tumor cells and the cytotoxic potential of the drug. P-glycoprotein, an efflux transporter is one of them but others have also been discovered to contribute to DOX efflux. The incorporation of DOX in nanocarrier has the potential to overcome cell resistance. Furthermore, it has been demonstrated that using siRNAs that target specific genes reduces resistance issues (Yoncheva et al., 2019, Butt et al., 2016). Combining siRNA with encapsulated anticancer medicines is a viable way to boost treatment efficacy (Butt et al., 2016).

## 1.7 Advantages of co-delivery

According to research, combining two or more therapeutic approaches with different mechanisms of action can effectively maintain their unique benefits while considerably improving cancer treatment (Sun et al., 2018). Various drug combinations have already been clinically tested. The use of different therapeutic agents with different molecular targets may slow the cancer adaptation process. And if targets the same biological pathway, they can work together to improve outcomes, improving therapeutic efficacy and target specificity. In recent decades, gene therapy has emerged as a powerful treatment due to the genetic links associated with tumor development and progression. While preliminary preclinical and clinical trials are encouraging, the molecular complexity of cancer implies that using a single therapeutic gene to stop the course of most malignancies may be insufficient. As a result, nucleic acid and anticancer medication combinations that are appears to be more promising (Saraswathy and Gong, 2014).

New therapeutic practices, such as combinational therapy have been developed to combat cancer's high mortality rate. A combination of chemotherapy and gene therapy has been suggested as a way to generate synergistic effects, increase target selectivity and prevent the emergence of cancer treatment resistance (Liu et al., 2018). Diagrammatic representation of Drug and siRNA-loaded targeted nanocarrier is shown in Figure 1.3.
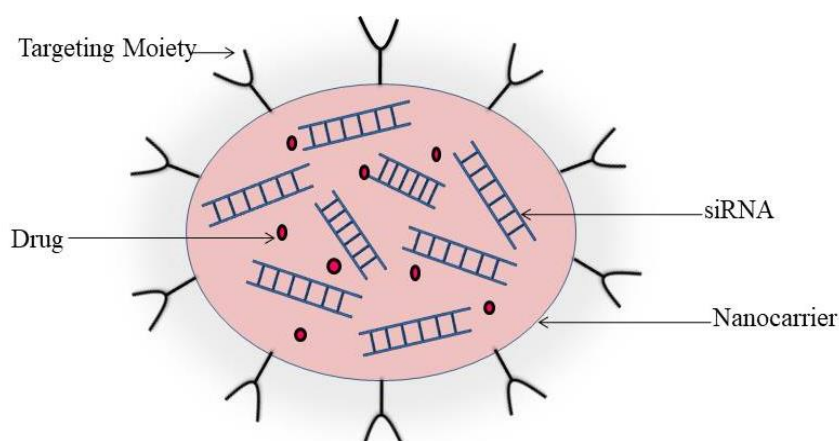
**Figure 1.3 Drug and siRNA-loaded targeted nanocarrier**

## 1.8 Advantages of targeted delivery

Other approaches rely on targeting moieties that promote NPs uptake within resistant cells via particular receptor-mediated binding and endocytosis. The active targeting of nanoscaled delivery systems for cancer treatment has received special attention. Active targeting of nanoscale delivery systems is a concept based on the high expression of specific cancer antigens on the cell surface, where successful selective targeting of cancer cells not only leads to highly efficient therapy, but also significantly. It is gaining in importance because it is now well known that it leads to reductions in systemic toxicity (Karra and Benita, 2012).

Masking/camouflage of NPs against reticuloendothelial system (RES) actions requires surface modification. RES does not identify surface-protected polymeric NPs (such as peptide or protein nanocarriers) that improve the half-life of such nanosystems in the bloodstream. The surface of NPs can be conjugated with various functional groups with the aim of modulating their biodistribution and biological effects through internalization (cellular uptake), a process known as functionalization (Mogoşanu et al., 2016). Additionally, specific ligands can be surface functionalized with these NPs to achieve site specific targeting, improve therapeutic efficacy and reduce chemotherapy side effects (Parveen and Sahoo, 2010). Passive targeting is affected by physicochemical variables such as NPs size distribution, shape, surface charge, hydrophilicity and NPs chemistry. On the other hand, passive tumor targeting is often insufficient to induce high levels of in-vivo accumulation of anticancer drugs. Nanocarriers are routinely used to address this defect. Peptides, Abs, aptamers and other

small molecules (such as folic acid) can be conjugated with various nanocarriers to bind to overexpressed specific receptors on cancer cell surfaces. Cellular uptake of targeted nanocarriers is often significantly higher than their non-targeted counterparts due to receptor-mediated endocytosis (Saraswathy and Gong, 2014).

### 1.8.1 Basic Components of Targeted Nanocarrier

The majority of active tumor-targeted delivery systems consist of main components such as 1) ligand which binds to a specific overexpressed epitope, 2) linker molecule or functional group between carrier and ligand, 3) Drugs and/or imaging probes encapsulated or chemically bound within the scaffold.

Various methods and functional groups can be used to covalently or non-covalently attach targeting ligands to the surface of NPs. MAbs are one of the most commonly conjugated ligands to NPs and the methods discussed below were mostly published with MAbs. However, given the availability of functional groups suitable for conjugation, several of the covalent techniques discussed might potentially be applied to other ligands as well (Cardoso et al., 2012).

### 1.8.2 Covalent Ligand Conjugation approach

The most prevalent groups present on the NPs surface, amines and carboxylic acids can be employed for interaction with ligands for direct coupling of Abs to the NPs surface. Various methods have been reported for conjugating Abs to NPs. Carbodiimide chemistry combines the carboxyl groups of the NPs with the primary amine groups of the Abs in the presence of 1-ethyl-3-(3-dimethylaminopropyl) carbodiimide (EDC) and N-hydroxysuccinimide (NHS). And resultant interaction occurs with a stable amide bond. MAbs against specific tumor antigens can be a viable platform for conjugated NPs targeting with high affinity and specificity if the antigen is positively identified and not expressed at high levels elsewhere in the body. Local and systemic delivery of MAbs conjugated NPs are commonly used to achieve aggressive tumor targeting (Cardoso et al., 2012).

### 1.8.3 Monoclonal Antibodies (MAbs) as targeting moiety

Cell-targeted therapies combining unique recognition entities such as Abs improve therapeutic efficacy while reducing systemic side effects. Due to their high affinity, specificity and adaptability MAbs were the first class of target molecules to be developed. The efficacy of targeting NPs accumulation to specific cells, tissues or

organs remains challenging due to the complexity and disability of the body. Effective targeting requires dual-focus strategies, improved target/receptor understanding and parallel development of targeting systems. Recombinant Abs with optimized properties such as antigen-binding affinity, molecular structure and dimerization state can be designed and fused to different effector moieties to improve cell-specific potency. In 1975, the first MAb was produced by mouse hybridoma technology. To optimize specificity, surface markers (antigens or receptors) on target cells should preferably be unique and uniformly expressed or overexpressed compared to normal cells. The conjugation method should be effective, establish a stable relationship, control the number of immobilized Abs and ensure that activity of Abs remains of intact. Covalent binding has a decisive advantage as compared to physical adsorption, binding prevents the adsorbed Ab from being displaced by blood components. The Fc region of the Abs used for covalent conjugation, leaving the Fab region of the antigen-binding site facing the medium and maintaining its full function (Cardoso et al., 2012, Karra and Benita, 2012).

### 1.8.4 Antibody Structure

Antibodies are functional molecules with two identical domains for antigen recognition (Fab fragments) and two identical domains for effector activity (Fc fragments) and Abs biodistribution linked via a flexible hinge region. It has a similar basic structure with a Y shape. At these sites, two pairs of polypeptide chains fold into a tight globular domain. Each heavy and light chain is structurally similar and has certain interchangeable moieties. Key changes in the variable region are found in the three short hypervariable sequences involved in antigen binding known as complementarity determining regions (CDRs) corresponding to the Fab portions of the light and heavy chains. Abs has high affinity and specificity for binding to target molecules. Antigen-binding proteins are proteins that bind antigens within a region with great specificity and differ between Abs (Cardoso et al., 2012).

## 1.9 Carcinoembryonic antigen (CEA) a receptor overexpressed on CRC cells

Tailored therapy for CRC may reduce chemotherapy side effects and improve treatment efficacy. Carcinoembryonic antigen is an example of a receptor found on the surface of many cancer cells, including CRC. CEA is a cell surface glycoprotein first

discovered in human colon cancer tissue extracts by Gold and Freeman. This glycoprotein is involved in cell adhesion. CEA is known to be expressed in healthy adult tissues, albeit at low levels only on the luminal surface of cells. The expression pattern is much greater and always aberrant in CRC as it is expressed at the basal and outer plasma membranes. CEA is one of the research targets for cancer therapy because it is overexpressed in primary and metastatic carcinomas (Pereira et al., 2018).

Targeted delivery is a rapidly growing and highly promising area of cancer research. Recently, scientists have invested great efforts in developing and testing targeted nanocarriers to improve therapeutic efficacy and avoid non-specific toxicities associated with conventional chemotherapy by altering the bio-distribution profile of therapeutics. Indeed, targeted delivery can enhance systemic delivery to the target site and increase drug accumulation at the target site while limiting damage to normal cells (Karra and Benita, 2012).

## 1.10 CHOICE OF TOPIC WITH REASONING

Chemotherapeutic agents are not specific for tumor cells and accumulate in healthy tissues also. However, off-target delivery of chemotherapeutics to tumor sites leading to severe side effects is a major cause of chemotherapy failure.

- Angiogenic factor VEGF will be efficiently inhibited by siRNA which will inhibit the tumor progression in CRC.

- Sustained/controlled release of chemotherapeutic drug and siRNA-loaded surface-modified ChNPs will improves drug solubility, stability and enhanced efficacy.

- Biodegradable, biocompatible, cationic nature, surface-modified ChNPs will enhance the entrapment efficiency which will deliver drug and siRNA at the targeted site efficiently.

- Surface modification with ligand will enhance targeting ability and increase cellular uptake of siRNA and drug which would be helpful for the treatment of CRC.

**Based on the above concern, the present thesis has the following objectives:**

- To prepare and characterize chemotherapeutic drug and siRNA loaded surface modified ChNPs for the treatment of colorectal cancer.

- To evaluate in-vitro chemotherapeutic drug and siRNA release profile from surface modified ChNPs.

- To study cell cytotoxicity and cellular uptake of chemotherapeutic drug and siRNA-loaded surface modified ChNPs on human colorectal cancer cell line HCT-116/ HT-29.

- To evaluate the in-vivo tumor targeting and regression potential of chemotherapeutic drug and siRNA loaded surface modified ChNPs in a colorectal cancer animal model.

# References

❖ Abdul Ghafoor Raja M, Katas H, Jing Wen T. Stability, intracellular delivery, and release of siRNA from chitosan nanoparticles using different cross-linkers. PLoS One. 2015 Jun 11;10(6):1-19.

❖ Alameh M, Lavertu M, Tran-Khanh N, Chang CY, Lesage F, Bail M, Darras V, Chevrier A, Buschmann MD. siRNA delivery with chitosan: Influence of chitosan molecular weight, degree of deacetylation, and amine to phosphate ratio on in vitro silencing efficiency, hemocompatibility, biodistribution, and in vivo efficacy. Biomacromolecules. 2018 Jan 8;19(1):112-131.

❖ Almalik A, Donno R, Cadman CJ, Cellesi F, Day PJ, Tirelli N. Hyaluronic acid-coated chitosan nanoparticles: Molecular weight-dependent effects on morphology and hyaluronic acid presentation. J Control Release. 2013 Dec 28;172(3):1142-1150.

❖ Al-Qadi S, Grenha A, Remuñán-López C. Chitosan and its derivatives as nanocarriers for siRNA delivery. J Drug Deliv Sci Technol. 2012 Jan 1;22(1):29-42.

❖ Amjad MW, Kesharwani P, Amin MC, Iyer AK. Recent advances in the design, development, and targeting mechanisms of polymeric micelles for delivery of siRNA in cancer therapy. Prog Polym Sci. 2017 Jan 1;64:154-181.

❖ Berger J, Reist M, Mayer JM, Felt O, Peppas NA, Gurny RJ. Structure and interactions in covalently and ionically crosslinked chitosan hydrogels for biomedical applications. Eur J Pharm Biopharm. 2004 Jan 1;57(1):19-34.

❖ Butt AM, Amin MC, Katas H, Abdul Murad NA, Jamal R, Kesharwani P. Doxorubicin and siRNA codelivery via chitosan-coated pH-responsive mixed micellar polyplexes for enhanced cancer therapy in multidrug-resistant tumors. Mol Pharm. 2016 Dec 5;13(12):4179-4190.

❖ Calvo P, Remunan- Lopez C, Vila- Jato JL, Alonso MJ. Novel hydrophilic chitosan- polyethylene oxide nanoparticles as protein carriers. J Appl Polym Sci. 1997 Jan 3;63(1):125-132.

❖ Cao Y, Tan YF, Wong YS, Liew MW, Venkatraman S. Recent advances in chitosan-based carriers for gene delivery. Mar Drugs. 2019 Jun;17(6):381.

❖ Cardoso M, N Peca I, CA Roque A. Antibody-conjugated nanoparticles for therapeutic applications. Curr Med Chem. 2012 Jul 1;19(19):3103-3127.

❖ Cavallaro G, Sardo C, Craparo EF, Porsio B, Giammona G. Polymeric nanoparticles for siRNA delivery: Production and applications. Int J Pharm. 2017 Jun 20;525(2):313-333.

❖ Chandran SP, Natarajan SB, Chandraseharan S, Shahimi MS. Nano drug delivery strategy of 5-fluorouracil for the treatment of colorectal cancer. J Cancer Res Pract. 2017 Jun 1;4(2):45-48.

❖ Chekhonin VP, Shein SA, Korchagina AA, Gurina OI. VEGF in tumor progression and targeted therapy. Curr Cancer Drug Targets. 2013 May 1;13(4):423-443.

❖ Chuan D, Jin T, Fan R, Zhou L, Guo G. Chitosan for gene delivery: Methods for improvement and applications. Adv Colloid Interface Sci. 2019 Jun 1;268:25-38.

❖ de Pinho Neves AL, Milioli CC, Müller L, Riella HG, Kuhnen NC, Stulzer HK. Factorial design as tool in chitosan nanoparticles development by ionic gelation technique. Colloids Surf A Physicochem Eng Asp. 2014 Mar 20;445:34-39.

❖ Fan W, Yan W, Xu Z, Ni H. Formation mechanism of monodisperse, low molecular weight chitosan nanoparticles by ionic gelation technique. Colloids Surf B Biointerfaces. 2012 Feb 1;90:21-27.

❖ Gomathi T, Sudha PN, Florence JA, Venkatesan J, Anil S. Fabrication of letrozole formulation using chitosan nanoparticles through ionic gelation method. Int J Biol Macromol. 2017 Nov 1;104:1820-1832.

❖ Hellmers F, Ferguson P, Koropatnick J, Krull R, Margaritis A. Characterization and in vitro cytotoxicity of doxorubicin-loaded γ-polyglutamic acid-chitosan composite nanoparticles. Chem Eng J. 2013 Jun 15;75:72-78.

❖ Huang M, Khor E, Lim LY. Uptake and cytotoxicity of chitosan molecules and nanoparticles: effects of molecular weight and degree of deacetylation. Pharm Res 2004 Feb;21(2):344-353.

❖ Ibrahim HM, Farid OA, Samir A, Mosaad RM. Preparation of chitosan antioxidant nanoparticles as drug delivery system for enhancing of anti-cancer drug. Key Eng Mater 2018 Jan;759:92-97.

❖ Jain A, Jain SK, Ganesh N, Barve J, Beg AM. Design and development of ligand-appended polysaccharidic nanoparticles for the delivery of oxaliplatin in colorectal cancer. Nanomedicine. 2010 Feb 1;6(1):179-190.

❖ Janes KA, Fresneau MP, Marazuela A, Fabra A, Alonso MJ. Chitosan nanoparticles as delivery systems for doxorubicin. J Control Release. 2001 Jun 15;73(2-3):255-267.

❖ Jonassen H, Kjøniksen AL, Hiorth M. Stability of chitosan nanoparticles cross-linked with tripolyphosphate. Biomacromolecules. 2012 Nov 12;13(11):3747-3756.

❖ Karra N, Benita S. The ligand nanoparticle conjugation approach for targeted cancer therapy. Curr Drug Metab. 2012 Jan 1;13(1):22-41.

❖ Katas H, Alpar HO. Development and characterisation of chitosan nanoparticles for siRNA delivery. J Control Release. 2006 Oct 10;115(2):216-225.

❖ Khdair A, Hamad I, Alkhatib H, Bustanji Y, Mohammad M, Tayem R, Aiedeh K. Modified-chitosan nanoparticles: Novel drug delivery systems improve oral bioavailability of doxorubicin. Eur J Pharm Sci. 2016 Oct 10;93:38-44.

❖ Kiilll CP, da Silva Barud H, Santagneli SH, Ribeiro SJ, Silva AM, Tercjak A, Gutierrez J, Pironi AM, Gremião MP. Synthesis and factorial design applied to a novel chitosan/sodium polyphosphate nanoparticles via ionotropic gelation as an RGD delivery system. Carbohydr Polym. 2017 Feb 10;157:1695-1702.

❖ Lan J, Li H, Luo X, Hu J, Wang G. BRG1 promotes VEGF-A expression and angiogenesis in human colorectal cancer cells. Exp Cell Res. 2017 Nov 15;360(2):236-242.

❖ Lee SY, Yang CY, Peng CL, Wei MF, Chen KC, Yao CJ, Shieh MJ. A theranostic micelleplex co-delivering SN-38 and VEGF siRNA for colorectal cancer therapy. Biomaterials. 2016 Apr 1;86:92-105.

❖ Li L, Hu X, Zhang M, Ma S, Yu F, Zhao S, Liu N, Wang Z, Wang Y, Guan H, Pan X. Dual tumor-targeting nanocarrier system for siRNA delivery based on pRNA and modified chitosan. Mol Ther Nucleic Acids. 2017 Sep 15;8:169-83.

❖ Li T, Shen X, Geng Y, Chen Z, Li L, Li S, Yang H, Wu C, Zeng H, Liu Y. Folate-functionalized magnetic-mesoporous silica nanoparticles for drug/gene codelivery to potentiate the antitumor efficacy. ACS Appl Mater Interfaces. 2016 Jun 8;8(22):13748-13758.

❖ Liu C, Liu T, Liu Y, Zhang N. Evaluation of the potential of a simplified co-delivery system with oligodeoxynucleotides as a drug carrier for enhanced antitumor effect. Int J Nanomedicine. 2018 Apr 20;13:2435-2445.

❖ Masarudin MJ, Cutts SM, Pietersz GA, Evison BJ, Phillips DR, Pigram PJ. Factors determining the stability, size distribution, and cellular accumulation of small, monodisperse chitosan nanoparticles as candidate vectors for anticancer drug delivery: application to the passive encapsulation of [14C]-doxorubicin. Nanotechnol Sci Appl. 2015 Dec 11;8:67-80.

❖ Mogoşanu GD, Grumezescu AM, Bejenaru C, Bejenaru LE. Polymeric protective agents for nanoparticles in drug delivery and targeting. Int J Pharm. 2016 Aug 30;510(2):419-429.

❖ Narmani A, Jafari SM. Chitosan-based nanodelivery systems for cancer therapy: Recent advances. Carbohydr Polym. 2021 Nov 15;272:118464.

❖ Nasti A, Zaki NM, De Leonardis P, Ungphaiboon S, Sansongsak P, Rimoli MG, Tirelli N. Chitosan/TPP and chitosan/TPP-hyaluronic acid nanoparticles: systematic optimisation of the preparative process and preliminary biological evaluation. Pharm Res. 2009 Aug;26(8):1918-1930.

❖ Nogueira-Librelotto DR, Scheeren LE, Vinardell MP, Mitjans M, Rolim CM. Chitosan-tripolyphosphate nanoparticles functionalized with a pH-responsive amphiphile improved the in vitro antineoplastic effects of doxorubicin. Colloids Surf B Biointerfaces. 2016 Nov 1;147:326-335.

❖ Pant A, Negi JS. Novel controlled ionic gelation strategy for chitosan nanoparticles preparation using TPP-β-CD inclusion complex. Eur J Pharm Sci. 2018 Jan 15;112:180-185.

❖ Parveen S, Sahoo SK. Evaluation of cytotoxicity and mechanism of apoptosis of doxorubicin using folate-decorated chitosan nanoparticles for targeted delivery to retinoblastoma. Cancer Nanotechnol. 2010 Dec 1;1(1-6):47-62.

❖ Pavitra E, Dariya B, Srivani G, Kang SM, Alam A, Sudhir PR, Kamal MA, Raju GS, Han YK, Lakkakula BV, Nagaraju GP. Engineered nanoparticles for imaging and drug delivery in colorectal cancer. Semin cancer Biol. 2021 Feb 1;69:293-306.

❖ Pereira I, Sousa F, Kennedy P, Sarmento B. Carcinoembryonic antigen-targeted nanoparticles potentiate the delivery of anticancer drugs to colorectal cancer cells. Int J Pharm. 2018 Oct 5;549(1-2):397-403.

❖ Ragelle H, Riva R, Vandermeulen G, Naeye B, Pourcelle V, Le Duff CS, D'Haese C, Nysten B, Braeckmans K, De Smedt SC, Jérôme C. Chitosan nanoparticles for siRNA delivery: optimizing formulation to increase stability and efficiency. J Control Release. 2014 Feb 28;176:54-63.

❖ Rampino A, Borgogna M, Bellich B, Blasi P, Virgilio F, Cesàro A. Chitosan-pectin hybrid nanoparticles prepared by coating and blending techniques. Eur J Pharm Sci. 2016 Mar 10;84:37-45.

❖ Rudzinski WE, Palacios A, Ahmed A, Lane MA, Aminabhavi TM. Targeted delivery of small interfering RNA to colon cancer cells using chitosan and PEGylated chitosan nanoparticles. Carbohydr Polym. 2016 Aug 20;147:323-332.

❖ Sadio A, Gustafsson JK, Pereira B, Gomes CP, Hansson GC, David L, Pêgo AP, Almeida R. Modified-chitosan/siRNA nanoparticles downregulate cellular CDX2 expression and cross the gastric mucus barrier. PLoS One. 2014 Jun 12;9(6):e99449.

❖ Sahu SK, Mallick SK, Santra S, Maiti TK, Ghosh SK, Pramanik P. In vitro evaluation of folic acid modified carboxymethyl chitosan nanoparticles loaded with doxorubicin for targeted delivery. J Mater Sci Mater Med. 2010 May;21(5):1587-1597.

❖ Saraswathy M, Gong S. Recent developments in the co-delivery of siRNA and small molecule anticancer drugs for cancer treatment. Mater Today. 2014 Jul 1;17(6):298-306.

❖ Sawtarie N, Cai Y, Lapitsky Y. Preparation of chitosan/tripolyphosphate nanoparticles with highly tunable size and low polydispersity. Colloids Surf B Biointerfaces. 2017 Sep 1;157:110-117.

❖ Serrano-Sevilla I, Artiga Á, Mitchell SG, De Matteis L, de la Fuente JM. Natural polysaccharides for siRNA delivery: Nanocarriers based on chitosan, hyaluronic acid, and their derivatives. Molecules. 2019 Jan;24(14):2570.

❖ Siahmansouri H, Somi MH, Babaloo Z, Baradaran B, Jadidi-Niaragh F, Atyabi F, Mohammadi H, Ahmadi M, Yousefi M. Effects of HMGA2 siRNA and doxorubicin dual delivery by chitosan nanoparticles on cytotoxicity and gene expression of HT-29 colorectal cancer cell line. J Pharm Pharmacol. 2016 Sep; 68(9):1119-1130.

❖ Siddharth S, Nayak A, Nayak D, Bindhani BK, Kundu CN. Chitosan-Dextran sulfate coated doxorubicin loaded PLGA-PVA-nanoparticles caused apoptosis in doxorubicin resistance breast cancer cells through induction of DNA damage. Sci Rep. 2017 May 19;7(1):1-10.

❖ Souto GD, Farhane Z, Casey A, Efeoglu E, McIntyre J, Byrne HJ. Evaluation of cytotoxicity profile and intracellular localisation of doxorubicin-loaded chitosan nanoparticles. Anal Bioanal Chem. 2016 Aug;408(20):5443-5455.

❖ Sun P, Huang W, Jin M, Wang Q, Fan B, Kang L, Gao Z. Chitosan-based nanoparticles for survivin targeted siRNA delivery in breast tumor therapy and preventing its metastasis. Int J Nanomed. 2016 Sep 27;11:4931-4945.

❖ Sun Q, Wang X, Cui C, Li J, Wang Y. Doxorubicin and anti-VEGF siRNA co-delivery via nano-graphene oxide for enhanced cancer therapy in vitro and in vivo. Int J Nanomed. 2018 Jun 27;13:3713-3728.

❖ Unsoy G, Khodadust R, Yalcin S, Mutlu P, Gunduz U. Synthesis of Doxorubicin loaded magnetic chitosan nanoparticles for pH responsive targeted drug delivery. Eur J Pharm Sci. 2014 Oct 1;62:243-250.

❖ Venkatesan C, Vimal S, Hameed AS. Synthesis and characterization of chitosan tripolyphosphate nanoparticles and its encapsulation efficiency containing Russell's viper snake venom. J Biochem Mol Toxicol. 2013 Aug;27(8):406-411.

❖ Wang JJ, Zeng ZW, Xiao RZ, Xie T, Zhou GL, Zhan XR, Wang SL. Recent advances of chitosan nanoparticles as drug carriers. Int J Nanomed. 2011 Apr 11;6:765-774.

❖ Yang SJ, Lin FH, Tsai KC, Wei MF, Tsai HM, Wong JM, Shieh MJ. Folic acid-conjugated chitosan nanoparticles enhanced protoporphyrin IX accumulation in colorectal cancer cells. Bioconjug Chem. 2010 Apr 21;21(4):679-689.

❖ Yoncheva K, Merino M, Shenol A, Daskalov NT, Petkov PS, Vayssilov GN, Garrido MJ. Optimization and in-vitro/in-vivo evaluation of doxorubicin-loaded chitosan-alginate nanoparticles using a melanoma mouse model. Int J Pharm. 2019 Feb 10;556:1-8.

❖ Zare M, Samani SM, Sobhani Z. Enhanced intestinal permeation of doxorubicin using chitosan nanoparticles. Adv Pharm Bull. 2018 Aug;8(3):411.

## SUMMARY

The chapter "review of literature" intends to present the overall review on ChNPs, ChNPs mediated co-delivery and targeted co-delivery for CRC and other cancer treatments.

## 2.1 Review of literature

➢ **Sun et al., [2018]** explored the potential of engineered GO nanocarriers for siRNA and DOX delivery. In-vitro study results revealed that VEGF mRNA and VEGF protein expression was significantly reduced with markedly inhibition of tumor in in-vivo. These results suggest that GPF mediated co-delivery of siRNA and DOX may have promising applications in the clinical practices.

➢ **Pereira et al., [2018]** developed paclitaxel loaded PLGA-PEG-NPs by nanoprecipitation. To target CEA in intestinal epithelial cells NPs were surface functionalized with CMAb (PLGA-PEG-NPs-CMAb). The targeting ability of functionalized NPs were studied on CEA-expressing Caco-2 cells in comparison with non CEA-expressing SW480 cells. Overall, surface-functionalized PLGA-PEG-NPs containing CMAb have been successfully engineered as nanocarriers for paclitaxel and interact with CEA-expressing cells. This specific interaction allows these NPs to be used as targeting systems for the treatment of CRC.

➢ **Liu et al., [2018]** chose siRNA with a VEGF target for co-delivery resulting in a combined anticancer impact. Anti-VEGF medicines may sensitize cancer cells to chemotherapeutic agent by limiting blood supply, increase penetration and even directly kill cancer cells through gene therapy. Furthermore, siRNA with complete structure is required for efficient transfection into cells, which could kick start the RNAi process for targeted gene silencing. As a result, nanoscale delivery systems were widely used and proved to be an ideal option for co-loading of chemotherapeutic agent and siRNA and protecting siRNA from degradation.

➢ **Sadreddini et al., [2017]** designed a carboxymethyldextran (CMD)-ChNPs to encapsulate snail siRNA and DOX. The co-delivery of siRNA and DOX in HCT-116 cells by CMD-ChNPs showed significant changes in EMT genes in which downregulation of MMP-9 and vimentin, upregulation of E-cadherin, apoptotic cell

death and migration inhibition were observed. Therefore, it can be considered as an effective anticancer treatment for CRC.

➤ **Amjad et al., [2017]** developed folic acid (FA), DOX, siRNA conjugated cholic acid-polyethyleneimine polymer to form CA-PEI-FA, D-CA-PEI-FA, D-CA-PEI-FA-S micelles respectively. The presence of FA enhanced the antitumor activity of micelles. D-CA-PEI-FA and D-CA-PEI-FA-S micelles inhibit tumor growth in Nu/Nu mice. Histological analysis of mice treated with D-CA-PEI-FA or D-CA-PEI-FA-S revealed a low density of cancer cells and a high degree of apoptosis and necrosis in the tumor tissues. The developed CA-PEI-FA nanoconjugates are capable of achieving targeted co-delivery of DOX and siRNA.

➤ **Kiilll et al., [2017]** studied the viability of Ch2PP6 NPs, cRGDfV solution and cRGDfV-loaded-Ch2PP6-NPs for 24 h and 48 h on Caco-2 cells. This study indicated that for protein/peptide delivery Ch and PP NPs are a more attractive combination due to their biocompatibility, low toxicity and immunogenicity. All materials used in this study didn't show any cytotoxic effect on Caco-2 cells.

➤ **Svenson et al., [2016]** developed PLGA nanopharmaceuticals attached to siRNA via an intracellularly cleavable disulfide linkage (PLGA-siRNA). These nanopharmaceuticals induce prolonged circulation, prolong tumor-specific knockdown with uniform accumulation throughout the tumor in homozygous NCR female nude mice.

➤ **Li et al., [2016]** developed FA receptors targeting magnetic mesoporous silica NPs (MSN) for co-administration of VEGF-shRNA and DOX (M-MSN-(DOX)/PEI-FA/VEGF-shRNA). In-vitro assay for antitumor activity showed significant inhibition of HeLa cell proliferation. Intracellular DOX accumulation suggests that M-MSN (DOX)/PEI-FA are more readily absorbed than off-target M-MSN-(DOX). These examined data showed that M-MSN/PEI-FA/VEGF-shRNA induced a significant decrease in VEGF expression compared with cells treated with other nanocomplexes. The invasive and migratory phenotypes of HUVECS were significantly reduced after culture with HeLa cells treated with MSN/PEI-FA/VEGF-shRNA nanocomplex.

➢ **Rudzinski et al., [2016]** developed ChNPs and PEG-ChNPs for targeting siRNA to β-catenin mRNA in HCT-116 cells. Compare ChNPs and PEG-ChNPs with liposome based approach (Lipofectamine 2000) to determine if these NPs can reduce β-catenin protein levels in-vitro. The results of this study showed that ChNPs and PEG-ChNPs can successfully enter HCT-116 cells and reduce the levels of proteins that promote tumor progression. These or similar NPs have been considered useful for the treatment of CRC.

➢ **Butt et al., [2016]** prepared mixed micelles loaded with DOX by thin-layer hydration method and coated with Ch, complexed with MDR-inhibiting siRNA, targeted by FA conjugation. In vitro studies showed enhanced pH-dependent DOX release at acidic tumor pH, increased cytotoxicity in 4T1 and 4T1-mdr cells compared with free DOX and further enhanced downregulation of the mdr-1 gene after treatment with siRNA-complex polyplexes. In addition, co-administration of polyplexes resulted in the highest accumulation of DOX, showed a significant reduction in tumor volume in female Balb/c mice with 4T1 and 4T1-mdr tumors compared with free DOX group and improved survival time. This study concluded that polyplex co-distribution of siRNA and DOX has good potential as targeted nanocarriers for the treatment of MDR cancer.

➢ **Lee et al., [2016]** showed that the SN38/USPIO-loaded siRNA-PEG micelle passively targeted tumor regions, synergistically enhanced VEGF silencing and showed that the therapy successfully suppressed tumor growth. In addition, SN38/USPIO-loaded siRNAPEG micelleplexes function as negative contrast agents in T2-weighted magnetic resonance imaging (MRI), resulting in a powerful tool for the diagnosis and treatment of CRC.

➢ **Siahmansouri et al., [2016]** used CMD-ChNPs to encapsulate HMGA2 siRNA and DOX. The effect of co-delivery on viability and gene expression in HT-29 cells was assessed. ChNPs/siRNA/DOX/CMD could more effectively induce tumor cell death and significantly reduce the expression of HMGA2, vimentin, MMP9 and increase the expression of E-cadherin. These results indicate that the concomitant administration of siRNA and anticancer drugs has a significant impact on the treatment of CRC.

➢ **Abdul Ghafoor Raja et al., [2015]** demonstrated the stability and efficacy of siRNA-loaded ChNPs with various cross-linking agents such as TPP, dextran sulfate (DS) and polyglutamic acid (PGA) by ionic gelation. In DLD1 cells, siRNA loaded Ch-TPP/DS/PGA showed siRNA release with low concentration-dependent cytotoxicity. But, TPP-ChNPs-siRNA successfully delivered siRNA into the cytoplasm of DLD-1 cells. From this study, concluded that TPP-ChNPs are biocompatible and the most efficient non-viral gene delivery system.

➢ **Mansouri et al., [2006]** modified Ch with FA to improve gene transfection efficiency. They looked into the properties of FA for gene therapy and discovered that FA-ChNPs had low cell toxicity and could successfully condense DNA. The findings revealed that FA-ChNPs could be used as a nonviral gene carrier.

➢ **Katas and Alpar [2006]** investigated three siRNA binding techniques: simple complexation, ionic gelation (siRNA trapping) and siRNA adsorption onto the surface of prefabricated ChNPs to generate Ch based nanocarriers.

➢ **Calvo et al., [1997]** prepared ChNPs by ionic gelation method and found that 0.5 mg/ml concentration of Ch was appropriate to form NPs while aggregation of NPs was observed at 1 mg/ml of Ch.

## 2.2 Conclusions

In this review, we summarized the potential of ChNPs in drug and siRNA delivery in CRC as well as in other cancer treatments. In-vitro and in-vivo results reported by many investigators indicate that drugs and siRNA-loaded nanocarriers for treating CRC have anti-tumor activity by targeting specific genes involved in MDR.

In the future, it is necessary to develop new therapeutics that specifically target the overexpressed receptors on CRC cells. These receptors increase apoptosis and kill cancer cells by reducing side effects in normal cells and accumulating NPs precisely in tumor cells only. In preclinical studies, active targeting may predominate in the future design of nanocarriers for siRNA delivery and co-delivery.

# References

❖ Abdul Ghafoor Raja M, Katas H, Jing Wen T. Stability, intracellular delivery, and release of siRNA from Ch nanoparticles using different cross-linkers. PLoS One. 2015 Jun 11;10(6):1-19.

❖ Amjad MW, Kesharwani P, Amin MC, Iyer AK. Recent advances in the design, development, and targeting mechanisms of polymeric micelles for delivery of siRNA in cancer therapy. Prog Polym Sci. 2017 Jan 1;64:154-181.

❖ Butt AM, Amin MC, Katas H, Abdul Murad NA, Jamal R, Kesharwani P. Doxorubicin and siRNA codelivery via chitosan-coated pH-responsive mixed micellar polyplexes for enhanced cancer therapy in multidrug-resistant tumors. Mol Pharm. 2016 Dec 5;13(12):4179-4190.

❖ Calvo P, Remunan- Lopez C, Vila- Jato JL, Alonso MJ. Novel hydrophilic chitosan- polyethylene oxide nanoparticles as protein carriers. J Appl Polym Sci. 1997 Jan 3;63(1):125-132.

❖ Katas H, Alpar HO. Development and characterisation of chitosan nanoparticles for siRNA delivery. J Control Release. 2006 Oct 10;115(2):216-225.

❖ Kiilll CP, da Silva Barud H, Santagneli SH, Ribeiro SJ, Silva AM, Tercjak A, Gutierrez J, Pironi AM, Gremião MP. Synthesis and factorial design applied to a novel chitosan/sodium polyphosphate nanoparticles via ionotropic gelation as an RGD delivery system. Carbohydr Polym. 2017 Feb 10;157:1695-1702.

❖ Lee SY, Yang CY, Peng CL, Wei MF, Chen KC, Yao CJ, Shieh MJ. A theranostic micelleplex co-delivering SN-38 and VEGF siRNA for colorectal cancer therapy. Biomaterials. 2016 Apr 1;86:92-105.

❖ Li T, Shen X, Geng Y, Chen Z, Li L, Li S, Yang H, Wu C, Zeng H, Liu Y. Folate-functionalized magnetic-mesoporous silica nanoparticles for drug/gene codelivery to potentiate the antitumor efficacy. ACS Appl Mater Interfaces. 2016 Jun 8;8(22):13748-13758.

❖ Liu C, Liu T, Liu Y, Zhang N. Evaluation of the potential of a simplified co-delivery system with oligodeoxynucleotides as a drug carrier for enhanced antitumor effect. Int J Nanomedicine. 2018 Apr 20;13:2435-2445.

❖ Mansouri S, Cuie Y, Winnik F, et al. Characterization of folate chitosan-DNA nanoparticles for gene therapy. Biomaterials. 2006 Mar;27(9):2060–2065.

❖ Pereira I, Sousa F, Kennedy P, Sarmento B. Carcinoembryonic antigen-targeted nanoparticles potentiate the delivery of anticancer drugs to colorectal cancer cells. Int J Pharm. 2018 Oct 5;549(1-2):397-403.

❖ Rudzinski WE, Palacios A, Ahmed A, Lane MA, Aminabhavi TM. Targeted delivery of small interfering RNA to colon cancer cells using chitosan and PEGylated chitosan nanoparticles. Carbohydr Polym. 2016 Aug 20;147:323-332.

❖ Sadreddini S, Safaralizadeh R, Baradaran B, Aghebati-Maleki L, Hosseinpour-Feizi MA, Shanehbandi D, Jadidi-Niaragh F, Sadreddini S, Kafil HS, Younesi V, Yousefi M. Chitosan nanoparticles as a dual drug/siRNA delivery system for treatment of colorectal cancer. Immunol Lett. 2017 Jan 1;181:79-86.

❖ Siahmansouri H, Somi MH, Babaloo Z, Baradaran B, Jadidi-Niaragh F, Atyabi F, Mohammadi H, Ahmadi M, Yousefi M. Effects of HMGA2 siRNA and doxorubicin dual delivery by chitosan nanoparticles on cytotoxicity and gene expression of HT-29 colorectal cancer cell line. J Pharm Pharmacol. 2016 Sep;68(9):1119-1130.

❖ Sun Q, Wang X, Cui C, Li J, Wang Y. Doxorubicin and anti-VEGF siRNA co-delivery via nano-graphene oxide for enhanced cancer therapy in vitro and in vivo. Int J Nanomed. 2018 Jun 27;13:3713-3728.

❖ Svenson S, Case RI, Cole RO, Hwang J, Kabir SR, Lazarus D, Lim Soo P, Ng PS, Peters C, Shum P, Sweryda-Krawiec B. Tumor selective silencing using an RNAi-conjugated polymeric nanopharmaceutical. Mol Pharm. 2016 Mar 7;13(3):737-747.

## Summary

In the 21$^{st}$ century, cancer is a life-threatening problem. For the development of targeted therapeutics anticancer cancer drug DOX, VEGF siRNA and for surface modification CEA MAb (CMAb) was selected. This therapeutics mainly targeted CRC by binding with overexpressed carcinoembryonic antigen on the surface of CRC cells. This strategy eliminates side effects due to site-specific delivery and enhances therapeutic potential due to the synergistic effect of DOX and VEGF siRNA.

This chapter describes the rationale for the choice of the anticancer drug, target gene and targeting ligand. Drug substances are rarely administered as chemical entities but are almost given in some kind of formulations. Pre-formulation is a research activity that involves applying biopharmaceutical principles to the physicochemical parameters of drug to develop optimal DDS. Characterization of drug molecules is a critical step in the pre-formulation stage of product development. Therefore, a pre-formulation study of the selected drug, DOX was carried out which included tests for identification, solubility profile and analysis of DOX in physiological buffers. Also, give detailed product information, qualitative analysis of the other excipients such as VEGF siRNA and CMAb.

## 3.1 Doxorubicin Hydrochloride (DOX)

DOX is an anthracycline produced by the fungus *Streptomyces peucetius var. caesius*. DOX is the most important antitumor agent which displays broader activity against different types of human solid tumors.

### 3.1.1 Chemistry

The DOX anthracycline antibiotics contain sugar daunosamine attached to a tetracyclic ring structure. This cytotoxic agent acted as electron accepting and donating agents due to presence of quinone and hydroquinone moieties.

### 3.1.1.1 Structural and physicochemical properties

The structure of DOX is shown in Figure 3.1 and their physicochemical properties written in Table 3.1.
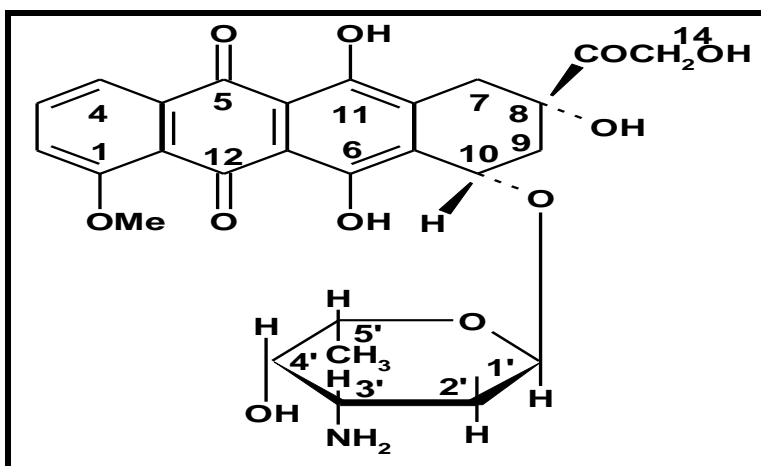
**Figure 3.1: Chemical Structure of DOX**

**Table 3.1: Physicochemical properties of DOX**

| Category | Antineoplastic antibiotics, Cytotoxic |
|---|---|
| Molecular formula | $C_{27}H_{29}NO_{11}$ and its hydrochloride salt $C_{27}H_{29}NO_{11}.HCl$ |
| Solubility | DOX is soluble in water, normal saline, methanol, acetonitrile, tetrahydrofuran and insoluble in chloroform, ether and other organic solvents. |
| pH | In between 4.0 to 5.5 in a solution containing 5 mg per ml. |
| Storage | DOX should be stored in well-closed, sterile, airtight, tamper-proof containers. |

### 3.1.2 Mechanism of Action

DOX inhibits the progression of DNA topoisomerase II (an enzyme that plays an important role in the transcription and replication process by an unwinding of supercoiled DNA) by forming a cleavable complex with DNA and topoisomerase II. DOX damages DNA also by the generation of free radicals, metal ion chelation and intercalation of the anthracycline portion which results in inhibition of DNA synthesis and function (Haskell, 1990; Chabner et al., 1989; Dorr et al., 1980). By asset of quinone groups, anthracyclines produce free radicals in normal and malignant tissues. The interaction of DOX with iron has significantly stimulated the production of free radicals (Myers, 1988).

### 3.1.3 Absorption, Fate and Excretion

Doxorubicin is most commonly administered intravenously because it is poorly absorbed by the gastrointestinal route. But, rapidly enter in blood, liver, spleen, kidneys, heart, lungs and they do not cross the blood-brain barrier but cross the placenta. DOX is eliminated by metabolic conversion into aglycones and inactive products. The binding of the DOX with plasma and proteins is very rapid and their highest concentration is found in the liver. About 5% of a dose is excreted in urine within 5 days.

### 3.1.4 Therapeutic uses

➢ Recommended dose of DOX is 60-75 mg/m$^2$, administered as a single rapid intravenous infusion and repeated after 21 days.

➢ DOX is effective in malignant lymphomas, breast metastatic carcinoma, sarcomas and for the successful treatment of lymphomas.

### 3.1.5 Adverse effects

The most common severe adverse effects of the DOX are cardiomyopathy, myelosuppression, tissue necrosis, hyperuricemia, skin rash, urticarial, facial flushing, alopecia and hyper-pigmentation of fingers, Mucositis, diarrhea, urticarial lesions, pruritus, anaphylactic skin rash, hepatitis, neurotoxic (Reynolds, 1989).

## 3.2 Drug identification tests

A pre-formulation study of the selected drug, DOX was kindly supplied as a gift sample by Sun Pharma Advanced Research co. Ltd., India. The DOX was identified accordingly by different Pharmacopoeial tests i.e. chemical test, melting point, Infrared (IR) spectra and absorbance maxima ($\lambda_{max}$), solubility profile, analysis of DOX in physiological buffers.

### 3.2.1 Chemical Test

DOX (about 2 mg) was dissolved in 0.5 ml of nitric acid and then 0.5 ml of water was added and heated for 2 min. After mixture was cooled 0.5 ml of silver nitrate solution was added.

### 3.2.2 Solubility Studies

Solubility is the spontaneous interaction of two or more substances to form a homogeneous dispersion (James, 1986). The solubility of DOX was determined in various polar and non-polar solvents. For the qualitative solubility studies, the DOX (10 mg) was suspended in a series of different solvents (10 ml) and then shaken for a fixed time interval (10 min).

### 3.2.3 Melting Point

A capillary melting point apparatus was used to determine the melting point of the DOX.

### 3.2.4 Absorption Maxima ($\lambda_{max}$)

When solution exposed to UV region of the spectrum organic molecules absorb light of particular wavelength (Silverstein et al., 1981). Absorption maxima of DOX were determined by scanning the 0.001% w/v solution of the DOX in PBS (7.4) in the range of 300 to 800 nm using a UV-Visible spectrophotometer.

### 3.2.5 Infrared (IR) Spectrum

An IR spectrum is a valuable tool used to determine organic structure and verification by using electromagnetic radiation with frequencies between 4000 and 500 cm$^{-1}$. The IR spectrum of compound provides information about the functional groups present in that compound. The DOX sample was scanned using an IR spectrophotometer and spectrum was compared with the standard IR spectrum (Florey, 1980) of pure DOX.

### 3.2.6 Preparation of Calibration Curve of DOX at pH 7.4 and pH 5.5 in PBS

1. **Stock solution preparation**

An accurately weighed quantity of DOX (5 mg) was transferred in 50 ml volumetric flask and the DOX was dissolved in a minimum quantity of PBS and final volume was made up to 50 ml with PBS to get a 100 µg/ml concentration of DOX.

2. **Quantification**

The aliquots of 0.2, 0.4, 0.6 up to 2.0 ml were pipetted out from the stock solution and transferred into 10 ml of volumetric flasks and the final volume was

made up to 10 ml with PBS. For quantification of DOX against blank solution, the absorbance of each of solution was measured with spectrophotometer at $\lambda_{max}$ 480 nm.

## 3.4 Vascular endothelial growth factor (VEGF) siRNA for gene silencing

Angiogenesis is the formation of new blood vessels and plays an important role in tumor growth and progression. VEGF is one of the most important and specific factors involved in angiogenesis. With the development of RNAi technology, siRNAs targeting VEGF have been extensively studied and have come to be referred to as anti-VEGF therapeutics. Treatment with VEGF antagonists is included in NCCN guidelines as a molecular therapy for CRC (Lan et al., 2017, Chekhonin et al., 2013, Liu et al., 2018, Lee et al., 2016).

The efficacy of siRNA is determined by its design and sequencing. While it is impossible to quantify, establishing some basic design parameters will assure optimal efficacy for the sequence chosen. The following is a general guideline for selection of target and siRNA sequences are:

1.     The siRNA should be directed towards a 50-100 nucleotide sequence downstream of the ATG start codon in the mRNA.

2.     Avoid nucleotide repetitions of four or more.

3.     Avoid sequences that have more similarity with other genes.

4.     In general, highly functional siRNAs have a G-C content ranging from 36 % to 52 %.

5.     The projected melting temperatures ($T_m$) can be used to determine relative thermodynamic stability and the ability to create internal hairpins (Groebe and Uhlenbeck, 1988, Groebe and Uhlenbeck, 1989).

In our design, a VEGF targeted siRNA was selected to be co-delivered with DOX, resulting in a synergistic anticancer effect.

**3.4.1 Product Information**

**The targeting human VEGF siRNA was purchased from Santacruz Biotech, India**

**Product -** VEGF siRNA (h) is a target-specific 19-25 nt siRNA designed to knock down gene expression.

**Chromosomal Location -** Genetic locus: VEGFA (human) mapping to 6p21.1.

**Applications -** VEGF siRNA (h) is recommended for the inhibition of VEGF expression in human cells.

**3.4.2 Analytical Methods of siRNA**

It is necessary that the quantity, purity and integrity of siRNA can be determined by different analytical methods. Due to the absorptivity of purines and pyrimidine, spectroscopic methods have been used to determine the quantity and purity of siRNA. While the integrity of the siRNA is a measure of its length and structural integrity, it can be assessed by utilizing electrophoretic mobility assays such as gel electrophoresis.

**3.4.2.1 Analysis of siRNA using UV Spectrophotometry**

When purines and pyrimidines solution exposed to UV region of the spectrum absorbs light of particular wavelength. Absorption maxima of siRNA were determined by scanning the siRNA suspension in TE buffer in the range of 220 to 320 nm using a UV-Visible spectrophotometer.

**3.4.2.2 Gel Electrophoresis**

Electrophoresis process is used to detect, quantify, purify and evaluate nucleic acid fragments. The principle of gel electrophoresis is based on when a charged molecule is placed in an electric field, it will move to the oppositely charged electrode according to its charge. Nucleic acids in a gel matrix flow towards the anode due to the high negative charge of the phosphate backbone (McMaster and Carmichael, 1977). The agarose gel was run in an electrophoresis buffer containing ions that conduct current and maintain pH. Agarose is a seaweed polymer made up of repeating agarobiose (Land D-galactose) subunits found in Gelidium and Gracilaria (Lee et al., 2012). Melting the agarose and pouring it into the slab is a simple way to

make the gel. During gelation, non-covalent interactions between agarose chains generate a network of holes that dictate the molecular sieving qualities of a gel. Different techniques are available for detecting siRNA bands. After staining with a suitable dye, the nucleic acids can be observed under UV light ($2500$ W/cm$^2$). The most frequent dye used in this application is ethidium bromide (EtBr). After irradiation with UV light, the EtBr can intercalate between base pairs, resulting in the stability of the phenyl moiety and increase in fluorescence of orange shade at a wavelength 605 nm (Higuchi et al., 1992, Haines et al., 2015). For EtBr visualization, 200 ng of RNA is usually necessary. This is usually accomplished with the use of a UV transilluminator. After filtering UV radiation with an orange filter, the light transmitted by fluorescing nucleotides can be measured. The velocity of migration of RNA in the gel is determined by its length or number of nucleotides, also siRNA fragmentation, loss in integrity and molecular weight can be observed using gel electrophoresis, which is a required method for determining siRNA quality. siRNA that has been partially degraded looks like low mw and the absence of sharp bands causes smearing. On the other hand, a degraded siRNA generates a diffused pale band. As a result, using RNA marker molecules or control helps in determining the size and interpreting data assures that the gel was properly run.

## 3.5 Carcinoembryonic antigen targeted monoclonal antibody (CMAb) for surface modification

Cancer cells exhibit cell surface molecules that are over-expressed only in cancerous tissue than in normal cells. One of the potential hurdles in the development of a targeting strategy is that normal cells also express these cell surface markers, though in smaller numbers and hence some amount of the carrier with its cargo can internalize into normal cells. This can have serious implications and will interfere with normal cellular functions, thereby transforming into a toxic entity (Hanahan and Weinberg, 2000). Hence, the identification of superior targeting moieties for the treatment of cancers continues. Targeted NPs promote NPs internalization in resistant cells through specific receptor-mediated endocytosis (Ruoslahti, 2010, Hanahan and Weinberg, 2000). Active targeting mediated by nanoscaled delivery systems with surface accessibility to the specific cancer antigens has gained major attention and this selective targeting of cancer cells reduced systemic toxicities which results in highly efficient treatments (Karra and Benita, 2012).

The selection of Abs as target-recognition ligands that bind to the NPs surface is critical for optimal design of target NPs. It should have high affinity and specificity for the appropriate target surface marker. Ideally, surface markers (antigens or receptors) should be unique and overexpressed in target cells over normal cells to maximize specificity (Cardoso et al., 2012). CEA receptors are overexpressed on the surface of CRC cells (Tiernan et al., 2013).

Monoclonal antibodies are the first class of target molecules and have been favored for their high affinity, specificity and versatility (Sanz et al., 2004, Van Dijk and Van De Winkel, 2001). Effective targeting requires dual focus strategies, improved target/receptor understanding and simultaneous development of targeting systems. Some therapeutic conjugates are currently in clinical development or in clinical practice. Recombinant Abs are engineered with optimized properties such as antigen-binding affinity, molecular structure and dimerization state and fused to different effector moieties to improve cell-targeting ability and potency (Sanz et al., 2004, Köhler and Milstein, 1975).

### 3.5.1 Product Information

**CEA (H-8) provided as a gift sample from Santacruz Biotechnology, Inc., India.**

**Source -** CEA (H-8) is a mouse monoclonal antibody raised against amino acids 35-334 and maps near the N-terminus of CEA of human origin.

**Molecular weight:** 80-200 kDa.

**Applications –**

CEA (H-8) is recommended for the detection of human CEA by immunohistochemistry (including paraffin-embedded sections) (starting dilution 1:50, dilution range 1:50-1:500) and solid-phase ELISA (initial dilution 1:30, dilution range 1:30-1:3000).

## 3.6 Results and discussion

The drug DOX was received as a gift sample from Sun Pharma Advanced Research co. Ltd., India. To confirm the identity and purity of the DOX gift sample various tests were performed.

### 3.6.1 Chemical Test

The formation of white precipitate was observed in chemical test which is same as reported in the IP.

### 3.6.2 Melting Point

The melting point was found to be 205°C determined using the melting point apparatus which is the same as reported in the IP.

### 3.6.3 Solubility Studies

The solubility parameters of the DOX determine the method to be followed or solvent to be employed for designing and developing a formulation. Qualitative solubility of DOX was determined in various solvents, which showed that the DOX is soluble in distilled water, in PBS (pH 7.4), (pH 5.5) and insoluble in diethyl ether and chloroform. Table 3.2 shows observations of qualitative solubility by the visible inspection.

### 3.6.4 Absorption Maxima ($\lambda_{max}$)

The $\lambda_{max}$ of the DOX was recorded while scanning a 0.001% w/v drug solution within a range of 300-800 nm using a double beam spectrophotometer. The value of $\lambda_{max}$ was found to be 480 nm in the buffer solutions of pH 7.4 shown in Figure 3.2

**Table 3.2: Solubility Profile of DOX in Various Solvents**

| Solvent | Solubility of DOX |
|---------|-------------------|
| Distilled water | ++++ |
| Phosphate Buffer Saline (PBS) pH 7.4 | ++++ |
| Phosphate Buffer Saline (PBS) pH 5.5 | ++++ |
| Chloroform | + |
| Ether | + |

++++ Soluble, + insoluble
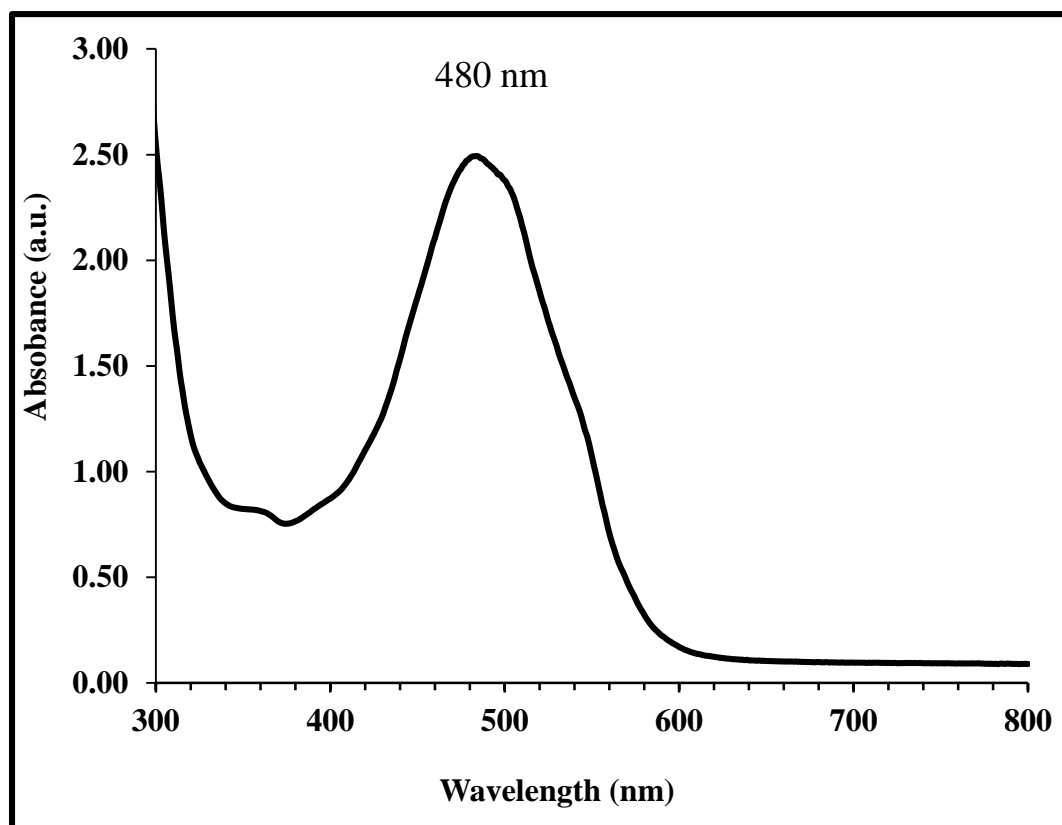
**Figure 3.2: Absorption Maxima (λ_max) of DOX**

### 3.6.5 Infrared (IR) Spectrum

The IR spectrum of the DOX was found to be identical to that reported in the literature, confirming the identity and purity of the DOX sample (Figure 3.3 (a), (b)). The IR spectrum of the DOX sample showed characteristic peaks at 3560-3160, 3160-2300, 1724, 1613 and 1580, 1282, 1115, 1071 and 1008 cm-1 (Table 3.3), which are in concordance with the standard IR spectrum of the DOX given in IP.
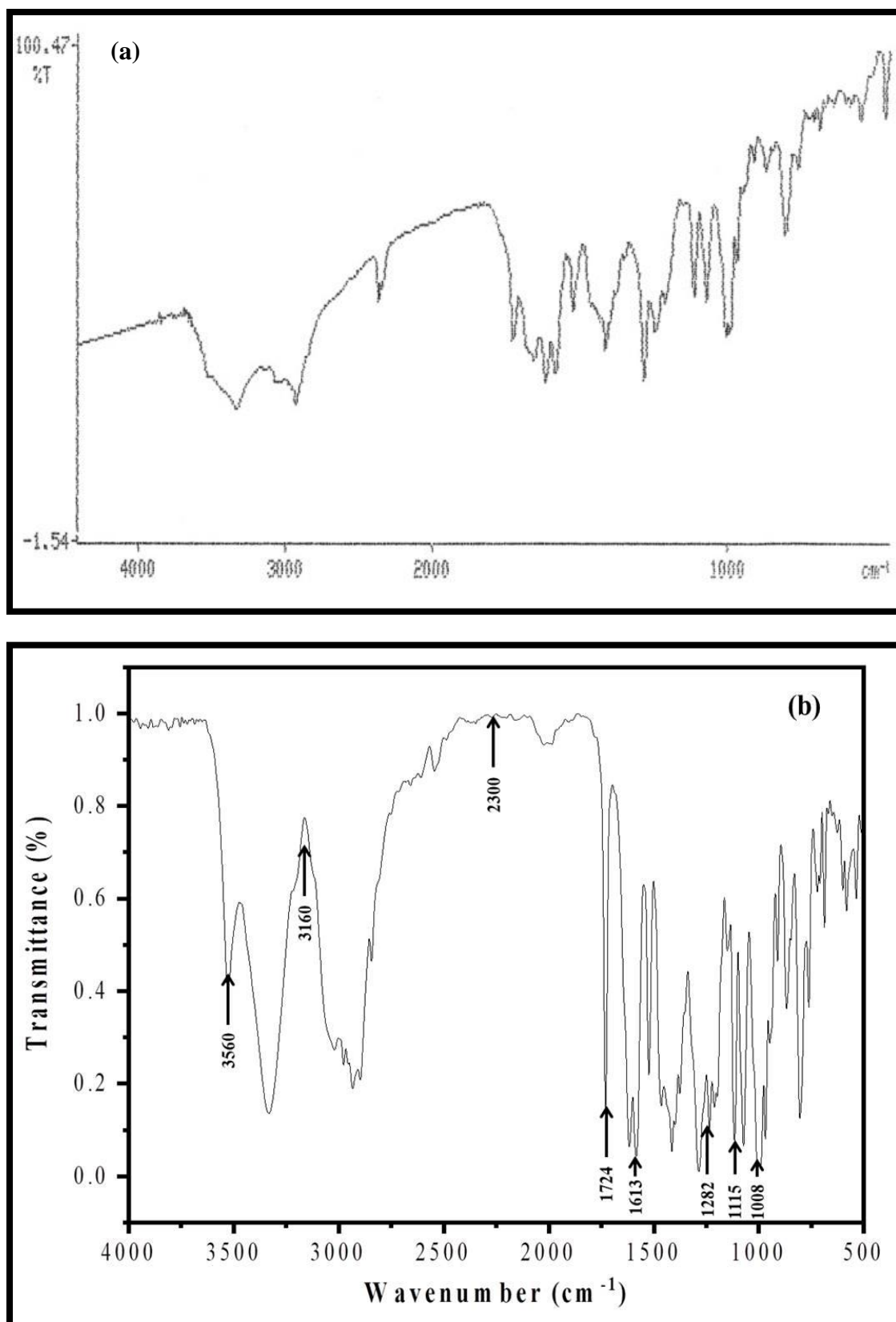
**Figure 3.3: (a) Reference IR Spectrum of DOX (Florey, 1980), (b) IR spectrum of DOX (Gift Sample)**

**Table 3.3: IR absorption band of DOX (Gift Sample)**

| IR Absorption Band, cm$^{-1}$ | Assignments |
|---|---|
| 3560-3160, 3160-2300 | O-H stretching (hydrogen-bonded) $NH_3^+$ stretching and OH stretching (hydrogen-bonded) |
| 1724 | C=O (ketone) |
| 1613 and 1580 | C=O stretching (Intra hydrogen-bonded quinone) |
| 1282 | C-O (tertiary alcohol) |
| 1115 | C-O (tertiary alcohol) |
| 1071 | C-O (secondary alcohol) |
| 1008 | C-O (primary alcohol) |

**3.6.6 Preparation of Calibration Curve of DOX at pH 7.4 and pH 5.5 in PBS**

The calibration curve of DOX was constructed at pH 7.4 and at pH 5.5 and it was observed that the DOX in a concentration of 2-20 μg/ml obeys Beers-Lambert's law. The calibration curve data were subjected to statistical analysis and parameters like the equation for straight line and correlation coefficient. The linearly regressed calibration curve was plotted (Figure 3.4 (a), (b)) and calculated correlation coefficient, which was found to be 0.9966 at pH 7.4, 0.9982 at pH 5.5 showing good linearity between concentration and absorbance within the concentration range of 2-20 μg/ml. Hence, it can be stated that the estimation procedures selected are stable and reliable and are being used for the calculation of DOX concentration wherever applicable.
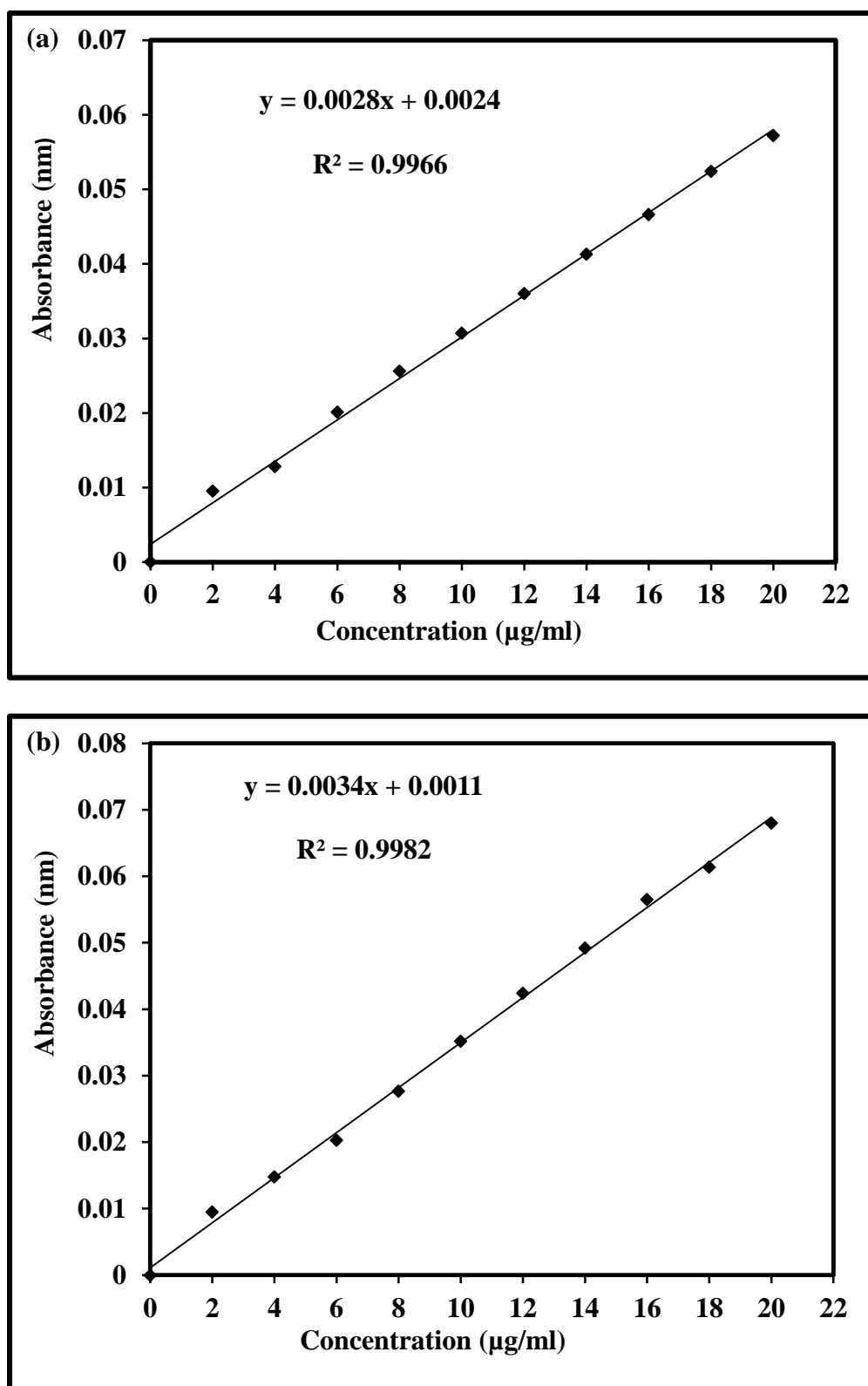
**Figure 3.4: Calibration Curves of DOX in PBS at (a) pH 7.4 and (b) pH 5.5 at 480nm**

Various other physicochemical parameters of the DOX were determined and compared with the standard values and shown in Table 3.4.

**Table 3.4: Various Tests for Identification of DOX**

| Parameters | Standard value (I.P.) | Observed Value |
|---|---|---|
| **Physical appearance** | Red crystalline powder | Fully complied |
| **Solubility** | Soluble in distilled water, PBS pH 7.4 and insoluble in chloroform and ether | Fully complied |
| **Melting point** | 205°C | 205°C |
| **U.V. spectroscopy** | The light absorption of 0.001% w/v solution of DOX exhibits maximum at 480 nm | The light absorption of 0.001% w/v solution of the DOX sample exhibited a maximum of 480 nm |
| **IR spectroscopy** | IR spectrum of drug exhibited peaks of OH, C-H and N-O stretching at 3230, 3105 and 1375 cm$^{-1}$ respectively | Fully complied |

**3.6.7 Analysis of siRNA using UV Spectrophotometry**

The VEGF siRNA was purchased from Santacruz Biotech, India. The product information was listed. The $\lambda_{max}$ of the siRNA were recorded while scanning siRNA suspension in TE buffer within a range of 220-320 nm using a double beam spectrophotometer. The value of $\lambda_{max}$ was found to be 260 nm in TE buffer shown in Figure 3.5.
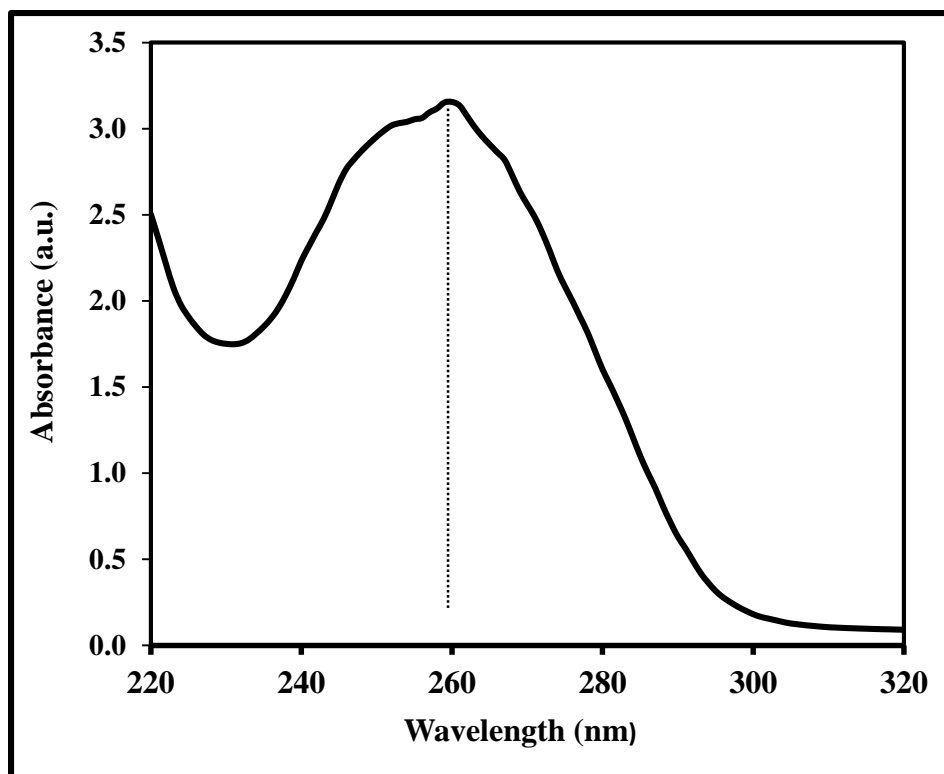
**Figure 3.5: Absorption Maxima (λ$_{max}$) of siRNA**

## 3.7 Conclusions

The drug identification tests revealed that the DOX gift sample complies with the official standard and is pure. The purity of siRNA can be determined by UV Spectrophotometry showed λ$_{max}$ at 260 nm which is similar to the standard absorption maxima of RNA. Also, discussed principle of gel electrophoresis and experiment were performed in next chapter. The targeting mechanism of Abs was discussed in detail.

# References

❖ Cardoso M, N Peca I, CA Roque A. Antibody-conjugated nanoparticles for therapeutic applications. Curr Med Chem. 2012 Jul 1;19(19):3103-3127.

❖ Chabner BA, Myers CE. Clinical pharmacology of cancer chemotherapy. Cancer: principles and practice of oncology. V. T. J. DeVita, S. Hellman, and S. A. Rosenberg, eds. (Philadelphia:J. B. Lippencott Co.), 1989; 1:287-328.

❖ Chekhonin VP, Shein SA, Korchagina AA, Gurina OI. VEGF in tumor progression and targeted therapy. Curr Cancer Drug Targets. 2013 May 1;13(4):423-443.

❖ Dorr, R. T. and Fritz, R. In: Cancer Chemotherapy Handbook, Elsevier Science Publishing Co. Inc., New York. 1980;435.

❖ Florey, K. (1980) Analytical Profiles of Drug Substance, 9,245.

❖ Groebe DR, Uhlenbeck OC. Characterization of RNA hairpin loop stability. Nucleic Acids Res. 1988 Dec 23;16(24):11725-11735.

❖ Groebe DR, Uhlenbeck OC. Thermal stability of RNA hairpins containing a four-membered loop and a bulge nucleotide. Biochemistry. 1989 Jan 1;28(2):742-747.

❖ Haines AM, Tobe SS, Kobus HJ, Linacre A. Properties of nucleic acid staining dyes used in gel electrophoresis. Electrophoresis. 2015 Mar;36(6):941-944.

❖ Hanahan D, Weinberg RA. The hallmarks of cancer. Cell. 2000 Jan 7;100(1):57-70.

❖ Haskell, C. M. In: Cancer Treatment, W B Saunders Co., Philadelphia. 1990. 99.

❖ Higuchi R, Dollinger G, Walsh PS, Griffith R. Simultaneous amplification and detection of specific DNA sequences. Biotechnology. 1992 Apr;10(4):413-417.

❖ James KC. Solubility and related properties. Drugs and the pharmaceutical sciences. 1986;28.

❖ Karra N, Benita S. The ligand nanoparticle conjugation approach for targeted cancer therapy. Curr Drug Metab. 2012 Jan 1;13(1):22-41.

❖ Köhler G, Milstein C. Continuous cultures of fused cells secreting antibody of predefined specificity. Nature. 1975 Aug 7;256(5517):495-497.

❖ Lan J, Li H, Luo X, Hu J, Wang G. BRG1 promotes VEGF-A expression and angiogenesis in human colorectal cancer cells. Exp Cell Res. 2017 Nov 15;360(2):236-242.

❖ Lee PY, Costumbrado J, Hsu CY, Kim YH. Agarose gel electrophoresis for the separation of DNA fragments. J Vis Exp. 2012 Apr 20;(62):3923.

❖ Lee SY, Yang CY, Peng CL, Wei MF, Chen KC, Yao CJ, Shieh MJ. A theranostic micelleplex co-delivering SN-38 and VEGF siRNA for colorectal cancer therapy. Biomaterials. 2016 Apr 1;86:92-105.

❖ Liu C, Liu T, Liu Y, Zhang N. Evaluation of the potential of a simplified co-delivery system with oligodeoxynucleotides as a drug carrier for enhanced antitumor effect. Int J Nanomed. 2018 Apr 20;13:2435-2445.

❖ McMaster GK, Carmichael GG. Analysis of single-and double-stranded nucleic acids on polyacrylamide and agarose gels by using glyoxal and acridine orange. Proc Natl Acad Sci. 1977 Nov 1;74(11):4835-4838.

❖ Myers CE. Role of iron in anthracycline action. In: Hacker M, Lazo J,Tritton T, eds. Organ Directed Toxicities of Anticancer Drugs. Boston, Mass: Martinus Nijhoff; 1988:17–30.

❖ Reynolds, J. E. F. In: Martindale The Extra Pharmacopoeia, 28th ed., London: Royal Pharmaceutical Society of Great Britain, 1989:209.

❖ Ruoslahti E, Bhatia SN, Sailor MJ. Targeting of drugs and nanoparticles to tumors. J Cell Biol. 2010 Mar 22;188(6):759-768.

❖ Sanz L, Blanco B, Alvarez-Vallina L. Antibodies and gene therapy: teaching old 'magic bullets' new tricks. Trends Immunol. 2004 Feb 1;25(2):85-91.

❖ Silverstein RM. GC Bassler and TC Morrill. In: Spectrophotometric Identification of Organic Compounds, 4th Ed., John Wiley and Sons, USA. 1981:105.

❖ Tiernan JP, Perry SL, Verghese ET, West NP, Yeluri S, Jayne DG, Hughes TA. Carcinoembryonic antigen is the preferred biomarker for in vivo colorectal cancer targeting. Br J Cancer. 2013 Feb;108(3):662-667.

❖ Van Dijk MA, Van De Winkel JG. Human antibodies as next generation therapeutics. Curr Opin Chem Biol. 2001 Aug 1;5(4):368-374.

**Summary**

The DOX is the most widely used drug in the treatment of CRC as adjuvant chemotherapy. Unfortunately, the use of DOX in the treatment of CRC is limited because of its pronounced toxicity and MDR phenomenon. Therefore the present investigation was carried out to develop and characterize, the novel targeted co-delivery system bearing DOX and VEGF siRNA for its selective and targeted delivery to CRC cells. Engineered nano constructs, namely DOX and siRNA entrapped CMAb anchored ChNPs were developed and characterized for their selectivity and efficacy. CEA, exclusively present on CRC cells was selected as a targeting receptor for CMAb. Hence, the surface of DOX and siRNA entrapped ChNPs was modified by conjugating CMAb as a ligand which could selectively be taken up by the receptors (over-expressed on CRC cells).

In this chapter, preparation, optimization and characterization of ChNPs, DOX-ChNPs, DOX-siRNA-ChNPs and DOX-siRNA-ChNPs-CMAb were carried out. Entrapment efficiency of DOX and siRNA were analyzed by UV-Vis spectrophotometer. siRNA entrapment into ChNPs was confirmed by agarose gel retardation assay. The conjugation efficiency of CMAb to DOX-siRNA-ChNPs was studied by ELISA.

## 4.1 Materials

Low molecular weight Ch (mw 50,000–190,000 Da, degree of deacetylation 75–85%), sodium tripolyphosphate (TPP) was purchased from Sigma-Aldrich (Mumbai, India), acetic acid, Tween 80, 1 M NaOH, HCl, KCl, Agarose gel electrophoresis kit was purchased from Himedia Laboratories Pvt. Ltd., Mumbai, India. DOX hydrochloride was obtained as a gift sample from Sun Pharma Advanced Research co Ltd, India. Targeting human VEGF siRNA (sense: 5'-ACAUCACCAUGCAGAUUAUdTdT-3', antisense: 5'-dTdTUGUAGUGGUAC GUCUAAUA-3') was obtained from Santacruz Biotech, India. All other chemicals used were analytical grade. Double-distilled water (DDW) and RNase-free water were used throughout the study when necessary.

## 4.2 Methodology

**Development and characterization of surface modified DOX and siRNA-loaded chitosan nanoparticles:**

### 4.2.1 Preparation of ChNPs, DOX-ChNPs and DOX-siRNA-ChNPs

ChNPs, DOX-ChNPs and DOX-siRNA-ChNPs were prepared using the ionotropic gelation technique reported by Calvo et al., 1997. Briefly, the Ch was dissolved in 1% aqueous acetic acid at various concentrations (3, 4, 5 and 6 mg). 1 mg TPP was then dissolved in deionized water. The Ch solution was kept at room temperature (R.T.) for continuous stirring and the TPP solution was added dropwise into Ch solution to obtain the ChNPs.

To incorporate DOX into ChNPs, DOX was added to the Ch solution and the solution was stirred at R.T. for 1 h. The TPP solution was added dropwise while stirring. We observed the physical changes that occurred in the solution and the solution that turned into a milky suspension was regarded as a colloidal dispersion containing DOX-ChNPs. Ultracentrifuge the DOX-ChNPs suspension at 10,000 rpm at 10°C for 30 min and the pellet containing DOX-ChNPs was resuspended in PBS (pH 7.4) before further analysis and use. Amber or aluminium foil-covered glassware was used to prevent the photodegradation of DOX (Abdul Ghafoor Raja et al., 2015).

To incorporate DOX and siRNA into ChNPs, DOX was added to the Ch solution and stirred for 1 h at R.T. Then, 2 μl of siRNA (10μg/μl) containing TPP solution was dropwise added under constant magnetic stirring for 1 h at R.T. To avoid RNase contamination, all solutions were prepared in RNase-free water and RNase-free materials and conditions were used throughout the experiment. Amber or aluminum foil-covered glassware was used to prevent the photodegradation of DOX (Abdul Ghafoor Raja et al., 2015).

### 4.2.2 Preparation of surface-modified DOX-siRNA-ChNPs with CEA monoclonal antibody (DOX-siRNA-ChNPs-CMAb)

To perform surface modification of DOX-siRNA-ChNPs with CMAb the carbodiimide chemistry was used (G.T. Hermanson., 1996). DOX-siRNA loaded ChNPs were centrifuged at 10,000 rpm for 30 min and then the pellet was resuspended in 500 μL of MES (2-(N-morpholino) ethanesulfonic acid) buffer (0.1

M). Then, 0.5 mM of EDC and 0.25 mM of NHS were dissolved in MES buffer and added into the DOX-siRNA-ChNPs solution. The resultant mixture was kept for 1 h at R.T. with agitation. To remove the excess EDC and NHS the DOX-siRNA-ChNPs were washed in MiliQ water at 20,000 for 30 min three times and resuspended in 1X PBS (pH 7.4). Then CMAb was added in the ratio 1:0.01 (DOX-siRNA-ChNPs:CMAb) and left for 24 h with agitation at 4°C. To remove excess CMAb, two washes were performed with 1X PBS before storing the DOX-siRNA-ChNPs-CMAb.

### 4.2.3 Optimization of Various Process and Formulation Variables

Various process and formulation variables that may influence the preparation and properties of the NPs were identified and optimized. The optimization was carried out by varying one parameter while keeping others constant. During the process of optimization, various parameters viz. Ch concentrations (3, 4, 5 and 6 mg), stirring speed (500, 1000 and 1500 rpm), stirring time (1/2 h, 1 h and 2h), DOX concentrations (1.0, 1.5 and 2.0 mg) and incubation time of CMAb in surface modification (6, 12, 24 h) were optimized to get small, uniformly distributed, discrete NPs with maximum DOX entrapment efficiency and higher CMAb conjugation efficiency.

### 4.2.3.1 Optimization of polymer (Ch) concentration

For optimizing the Ch concentration, the various concentrations of Ch (3.0, 4.0 5.0, 6.0 mg) were dissolved in 1% v/v glacial acetic acid and fixed concentration of 1 mg TPP were dissolved in deionized water and added drop-wise under magnetic stirring at R. T. for 1 h. Then, opalescence suspension was further observed under a microscope to see the formation of any aggregates. The mixtures which are opalescence and free from any aggregates were taken for particle size analysis using Malvern Zetasizer Ver. 7.12 (Malvern Instruments Ltd, UK).

### 4.2.3.2 Optimization of DOX concentration

The effect of the concentration of Ch on particle size was studied and optimized. Optimized Ch:TPP ratio was selected to the determined effect of DOX concentration on percent entrapment efficiency and particle size. Various concentration of DOX viz. (0.5, 1.0 and 1.5 mg) was used to incorporate DOX into ChNPs and optimized.

**4.2.3.3 Optimization of Stirring speed**

The impact of stirring speed (500, 1000 and 1500 rpm) on the entrapment efficiency and particle size of selected formulations was studied.

**4.2.3.4 Optimization of Stirring time**

The effect of stirring time (1/2, 1 and 2 h) on the entrapment efficiency and particle size of selected formulations was studied. The effect of various concentrations of DOX, the effect of stirring speed and time on DOX entrapment efficiency and particle size were determined. The mixture was observed visually for the formation of opalescence suspension. Then, opalescence suspension was further observed under the microscope to see the formation of any aggregates. The mixtures, which are opalescence and free from any aggregates, were taken for further analysis. The particle size was determined by using Malvern Zetasizer Ver. 7.12 (Malvern Instruments Ltd, UK) and percent DOX entrapment was determined by UV-vis spectrophotometry.

**4.2.3.5 Optimization of incubation time of CMAb in surface modification**

The effect of CMAb incubation time on conjugation efficiency was determined and optimized. Three different time points of incubation such as 6, 12 and 24 h were studied on optimized formulation Ch:TPP ratio with optimized DOX concentration. The CMAb conjugation efficiencies were determined by ELISA.

**4.2.4 Preparation of Optimized Formulation**

Optimized nanoparticulate formulations were prepared with optimized Ch: TPP ratio, the optimized concentration of DOX, the optimized concentration of CMAb incubation time and fixed concentration of siRNA using the same method discussed in the preparation section.

## 4.3 Characterizations

The optimized NPs were evaluated for shape and morphology, particle size, polydispersity index (PDI), zeta potential. Also, DOX entrapment efficiency and in-vitro release studies of DOX in PBS (pH 5.5 and 7.4) were evaluated and siRNA entrapment was confirmed. Conjugation efficiency of CMAb to DOX-siRNA-ChNPs was quantified.

**4.3.1 Morphology of ChNPs**

The transmission electron microscopy was performed at 200 kV (JEOL Model JEM-2100) to examine morphology of ChNPs.

**4.3.2 Particle Size, PDI and Zeta Potential**

The aqueous dispersions of the NPs were measured at 25 °C with a scattering angle of 90° after dispersing the NPs in PBS (pH 7.4) NPs on Malvern Zetasizer Ver. 7.12 (Malvern Instruments Ltd, UK) to determine particle size, PDI, zeta potential.

**4.3.3 Fourier Transform Infrared Spectroscopy (FTIR)**

To investigate the functional groups of ChNPs, DOX and DOX-ChNPs, the samples were mixed with KBr to form a thin pellet. Samples were analyzed in the range 400-4000 cm$^{-1}$ at Alpha Bruker, Germany.

**4.3.4 Entrapment efficiency of DOX**

The entrapment efficiency of DOX and siRNA into ChNPs were measured using a dual-beam UV-vis spectrophotometer. To assess the DOX entrapment efficiency, the prepared solution containing DOX-ChNPs was centrifuged (10,000 rpm at 10°C for 30 min). The free DOX in supernatant recovered from centrifugation was quantified by measuring its absorbance at 480 nm.

The supernatant of un-loaded ChNPs was used as a baseline correction. The percent entrapment efficiency (EE) was calculated from equation 4.1.

$$\textbf{Entrapment efficiency} \, (\%) = \frac{C \, (sample) - C \, (supernatant)}{C \, (sample)} \times 100 \ldots\ldots\ldots\ldots(4.1)$$

Where, C $_{(sample)}$ is the initial concentration of DOX added and C $_{(supernatant)}$ is the concentration of DOX present in the supernatant (Siahmansouri et al., 2016). All measurements were performed in triplicate and data are presented as mean ± standard deviation.

**4.3.5 In-vitro release study of DOX**

A 10 mg pellet from DOX-ChNPs centrifugation was dispersed in freshly prepared PBS (pH 5.5 and pH 7.4) and this suspension was placed in a dialysis membrane bag with a molecular cutoff of 12 kDa. The bag was tied and placed in 100 ml of PBS solution. The entire system was placed in a shaking incubator at 37 ± 1 °C, gently shaken (90–100 rpm) and protected from light. For each sample, 2 ml of

diffusion medium was collected at prefixed time intervals (2, 4, 6, 12, 20, 24, 36, 48 h) and immediately replaced with 2 ml of fresh PBS. The amount of DOX released into the medium was quantified at 480 nm using an Agilent Technologies Cary 60 dual-beam UV-Vis spectrophotometer (Siahmansouri et al., 2016, Alinejad et al., 2016).

### 4.3.6 Confirmation of siRNA entrapment by Agarose Gel Retardation Assay

The entrapment of siRNA into ChNPs was analyzed by agarose gel retardation assay (Katas and Alpar, 2006, Abdul Ghafoor Raja et al., 2015). Naked siRNA, siRNA-ChNPs were incubated and gently shaken at 37°C for 30 min. Then 5 µl of loading buffer was added to all samples. Samples were applied to a 4% (w/v) agarose gel containing EtBr (2 mg/ml) and electrophoresed in 1×TAE buffer at a constant voltage of 120 V for 20 min as shown in Figure 4.1. Results were observed under a UV transilluminator (GeNei, India).
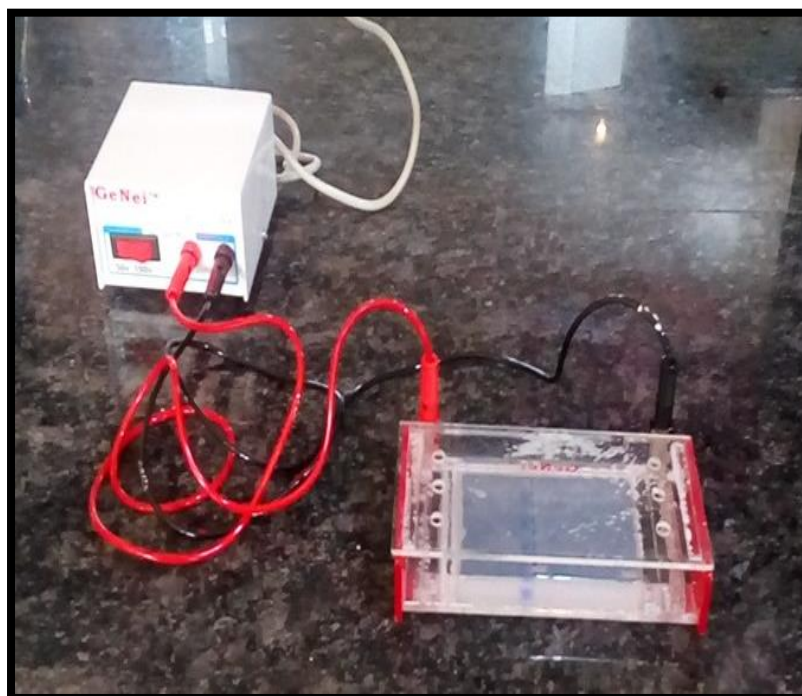


**Figure 4.1: Gel electrophoresis assembly (GeNei, India)**

### 4.3.7 CMAb conjugation efficiency studied by Enzyme-Linked Immunosorbent Assay (ELISA)

The conjugation efficiency of CMAb to DOX-siRNA-ChNPs was evaluated by ELISA (Pereira et al., 2018). For plating, firstly add 40 µl of carbonate coating buffer in a 96-well plate then added 10 µl of each sample, positive control (same

amount of CMAb used in surface modification process), DOX-siRNA-ChNPs-CMAb, supernatant of DOX-siRNA-ChNPs-CMAb and then incubated for 3 h at $37^0$C. After incubation three washes were performed with PBS and Tween-20 (PBST) mixture. To prevent non-specific binding of CMAb to the plate 100 µl of 1% BSA solution was added. Then the plate was incubated at $37^0$C for 1h. Three washes with PBS were performed after incubation. Then, added 50 µl of Goat anti-mouse-HRP Ab (1:2500) and incubated for 45 min at $37^0$C. Again three washes were performed with PBS then added 100 µl TMB substrate solution and left for 30 min. Then sulphuric acid (2M) was added and the plate read at 450 nm on LISA Plus Microplate ELISA reader shown in Figure 4.2. The conjugation efficiency (%) was calculated using equation 4.2.

$$\textbf{Conjugation efficiency} = \frac{\textbf{Abs.of the sample}}{\textbf{Abs.of the input}} * \textbf{100}.............................(4.2)$$

The input is the same amount of CMAb used in the surface modification process. A positive control of this experiment is the amount of CMAb used.
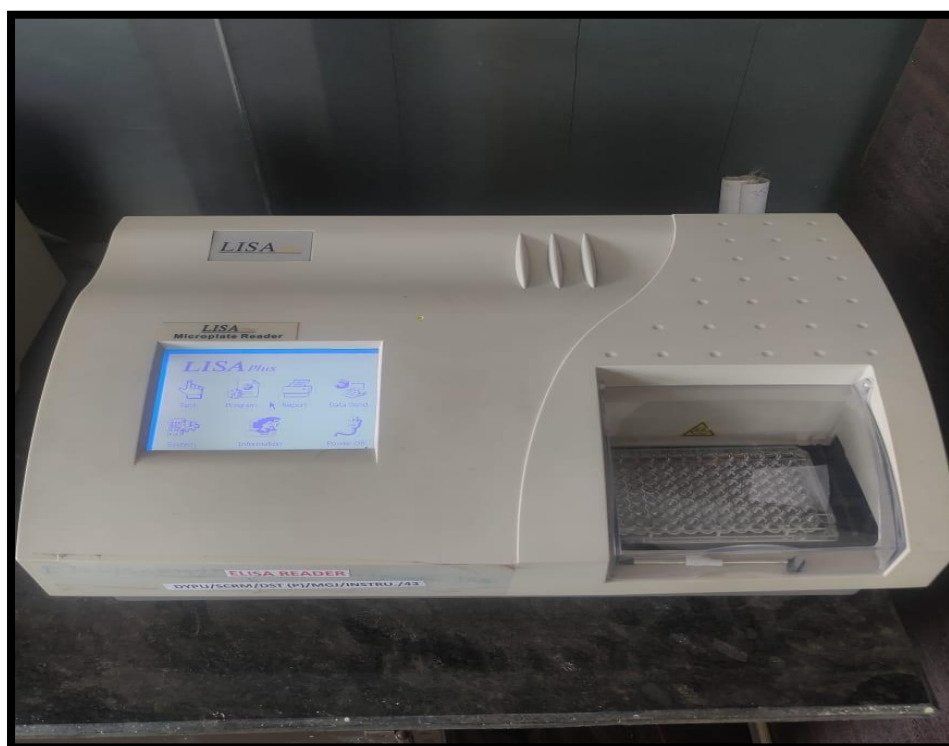


**Figure 4.2: ELISA reader (LISA Plus Microplate ELISA reader)**

**Statistical analysis**

Each experiment was performed in triplicate and presented as mean ± standard deviation (SD). Data were analyzed using one-way analysis of variance (ANOVA) with Tukey's post hoc test (Graph Pad Prism Software v8.0.2 Inc., USA). The significance level was set at probability with $*p < 0.05$. $**p<0.01$ and $***p<0.001$.

## 4.4. Results and Discussion

**Development and characterization of surface modified DOX and siRNA-loaded chitosan nanoparticles:**

Chitosan nanoparticles were prepared by the ionic gelation method. The basic principle behind this method is ionic cross-linking between the positive charge of amine groups of Ch and negative charge groups of TPP. It is a simple and easy method of preparation of ChNPs performed in an aqueous medium without using any organic solvents. ChNPs spontaneously formed under constant magnetic stirring at R.T. by adding TPP to the Ch solution.

For development of an optimal and stable DOX-siRNA-ChNPs-CMAb analyzed various process and formulation variables to getting information about the effects of selected variables on particle size, zeta potential, PDI and DOX entrapment efficiency.

**4.4.1 Optimization of Various Process and Formulation Variables**

**4.4.1.1 Optimization of polymer (Ch) concentration**

It was reported that, particle size has strong impact on biological performance of the NPs and it is indicated that the ratio between Ch and TPP are critical parameter which controls size distribution of ChNPs. To determine stability of NPs suspension, surface charge of the NPs plays an important role and also positively charged NPs facilitate their interaction with cell membranes. The PDI is a measure of homogeneity in NPs dispersion and ranges from 0 to 1 (Zhang and Kosaraju., 2007, Mahdi Karimi et al., 2013, Kiilll et al., 2017)

In this study, ChNPs were optimized by varying Ch concentration (3, 4, 5, 6 mg) while TPP concentration was kept constant (1 mg) based on particle size, zeta potential and PDI values of resulting ChNPs. ChNPs were analyzed by particle size analyzer and their results are recorded in Table. 4.1.

The average size range of Ch**:**TPP from 3:1 to 6:1 were 87.5±0.3 to 251.7±0.8, our results showed that the trend of particle size increased with increasing concentration of Ch, as reported in the literature (Kiilll et al., 2017, Gan et al., 2005). The zeta potential of ChNPs increased with increasing Ch concentration due to $NH^{3+}$ protonated groups of Ch ranged from +25.2±0.6 to +49.8±0.7 and these results are similar to the de Pinho Neves et al., 2014 (de Pinho Neves et al., 2014). According to Neves et al., no agglomeration was observed at zeta potential greater than 30 mV and at less than 28 mV agglomeration was observed during storage (de Pinho Neves et al., 2014). Whereas, another parameter of characterization of ChNPs is PDI were ranges from 0.26±0.03 to 0.54±0.04. According to Zhang and Kosaraju., 2007, PDI values close to zero indicate a homogeneous dispersion and values greater than 0.3 indicate a highly heterogeneous dispersion (Zhang and Kosaraju., 2007). Therefore, ratio 5:1 is selected as the optimized Ch:TPP ratio which indicates that, particle size 187±0.6 with zeta potential +33.6±0.4, 0.29±0.03 PDI values.

**Table 4.1: Effect of Ch : TPP ratio on particle size**

| Ch concentration (mg) | TPP concentration (mg) | Particle Size (nm) | PDI | Zeta Potential (mV) |
|---|---|---|---|---|
| 3 | 1 | 87.5±0.3 | 0.26±0.03 | +25.2±0.6 |
| 4 | 1 | 143.4 ±0.5 | 0.29±0.05 | +27.1±0.2 |
| 5* | 1* | 187.3±0.6 | 0.27±0.03 | +33.6±0.4 |
| 6 | 1 | 251.7±0.8 | 0.54±0.04 | +49.8±0.7 |

*Shows the optimized parameter, Values are expressed as mean±SD, n=3,

**4.4.1.2 Optimization of DOX concentration**

The incorporation of DOX into ChNPs was achieved simply by mixing the DOX solution with Ch solution at R.T. under continuous magnetic stirring at 100 rpm for 30 min. To this solution, TPP was added for the formation of DOX-ChNPs. The effect of DOX concentration on entrapment efficiency and particle size was studied. It was found that on increasing the concentration of DOX from 0.5 mg to 1.5 mg, there were reduction in DOX entrapment efficiency but particle size was increased with

increased concentration of DOX and results are similar with the Jain and Jain., 2010 (Jain and Jain., 2010). Therefore, 0.5 mg was the optimum concentration of DOX selected for further preparation. The results are depicted in Table 4.2.

**Table 4.2: Effect of DOX concentration on particle size and DOX entrapment efficiency**

| Optimized Ch:TPP (mg) | DOX concentration (mg) | Particle size (nm) | PDI | Zeta Potential (mV) | DOX entrapment efficiency (%) |
|---|---|---|---|---|---|
| 5:1 | 0.5* | 227.5±3.4 | 0.23±0.03 | +34.1±0.2 | 62±2.14 % |
|  | 1.0 | 322.2±2.7 | 0.29±0.02 | +39.5±0.4 | 50±2.84 % |
|  | 1.5 | 518.4±4.8 | 0.34±0.05 | +41.1±0.3 | 38±3.24 % |

*Shows the optimized parameter, Values are expressed as mean¬¬±SD, n=3.

## 4.4.1.3 Optimization of Stirring speed

The effect of stirring speed on particle size and DOX entrapment was studied. At low stirring speed (500 rpm) ChNPs were found to be comparatively larger with low DOX entrapment. It was found that increasing the stirring speed to 1000 rpm slightly increased the percentage of DOX entrapment efficiency with decreasing particle size. The NPs formed at this speed also showed uniform and smooth surfaces. High stirring speed (1500 rpm) exerted no significant effect either on percent DOX entrapment or on particle size and results are similar with the Al-Nemrawi et al., 2018 (Al-Nemrawi et al., 2018). The results are recorded in Table. 4.3.

**Table 4.3: Effect of stirring speed on entrapment efficiency and particle size for DOX-ChNPs**

| Ch:TPP (mg) | DOX concentration (mg) | Stirring Speed (rpm) | Particle Size (nm) | PDI | Zeta Potential (mV) | DOX entrapment efficiency (%) |
|---|---|---|---|---|---|---|
| 5:1 | 0.5 | 500 | 269.2±2.5 | 0.23±0.02 | +30.5±0.4 | 36±2.14 % |
|  |  | 1000* | 238.4±1.5 | 0.21±0.06 | +34.3±0.2 | 57±2.50 % |
|  |  | 1500 | 229.7±4.5 | 0.33±0.05 | +38.6±0.5 | 49±3.24 % |

*Shows the optimized parameter, Values are expressed as mean ±SD, n=3.

**4.4.1.4 Optimization of Stirring time**

The impact of stirring time on the DOX entrapment and particle size was studied and results recorded in Table 4.4. The stirring time can affect the rigidity of NPs during/after the cross-linking with polyanion the reaction between the TPP and amino group of polymers is ionic. But, there was less DOX entrapment in ½ h, after extending stirring time up to 1h there was an increase in DOX entrapment and at 2 h there was a decrease in DOX entrapment. Therefore, 1 h stirring time selected for optimized formulation preparation.

**Table 4.4: Effect of stirring time on entrapment efficiency and particle size for DOX-ChNPs**

| Ch: TPP (mg) | DOX (mg) | Stirring Speed (rpm) | Stirring time (h) | Particle Size (nm) | PDI | Zeta Potential (mV) | DOX entrapment efficiency (%) |
|---|---|---|---|---|---|---|---|
| 5:1 | 0.5 | 1000 | ½ h | 152±2.5 | 0.36±0.03 | +29.6±0.4 | 32±2.14 % |
| | | | 1h* | 234±3.6 | 0.21±0.05 | +34.2±0.3 | 58±2.84 % |
| | | | 2 h | 179±4.5 | 0.30±0.05 | +46.6±0.3 | 45±3.24 % |

*Shows the optimized parameter, Values are expressed as mean¬¬±SD, n=3.

**4.4.1.5 Optimization of incubation time of CMAb in surface modification**

In the next step of optimization, the effect of CMAb incubation time in surface modification was studied by ELISA and results are recorded in Table 4.5. It was observed that conjugation efficiency of CMAb to the DOX-siRNA-ChNPs was increased by increasing incubation times as 6, 12 and 24 h. The highest conjugation efficiency was observed at 24 h.

**Table 4.5: Effect of CMAb incubation time on conjugation efficiency**

| Optimized Ch:TPP (mg) | Optimized DOX (mg) | CMAb incubation time (h) | CMAb conjugation efficiency (%) |
|---|---|---|---|
| 5:1 | 0.5 | 6 | 5.2 |
| | | 12 | 9.6 |
| | | 24* | 17.5 |

*Shows the optimized parameter, Values are expressed as mean¬¬±SD, n=3.

**4.4.1.6 Preparation of Optimized Formulation**

Optimized nanoparticulate formulations were prepared with optimized Ch: TPP ratio of 5:1, 0.5 mg of DOX, stirring speed 1000 rpm, stirring time 1 h, fixed concentration of siRNA, 24 h of CMAb incubation time (DOX-siRNA-ChNPs-CMAb) given in Table 4.6 and used for further characterization and in-vitro and in-vivo studies.

**Table 4.6: Optimized Formulation Parameters of DOX-siRNA-ChNPs-CMAb**

| Ch:TPP (mg) | DOX (mg) | siRNA (µg) | Stirring speed (rpm) | Stirring time (h) | CMAb incubation time (h) |
|---|---|---|---|---|---|
| 5:1 | 0.5 | 30 | 1000 | 1 | 24 |

*Shows the optimized parameter, Values are expressed as mean¬¬±SD, n=3.

## 4.4.2 Characterizations

The optimized NPs were characterized for particle size, PDI, zeta potential, shape and morphology. Also confirmed the siRNA entrapment in ChNPs. DOX entrapment efficiency and in-vitro release study of DOX in PBS (at pH 5.5 and 7.4) were studied. Conjugation efficiency of CMAb to DOX-siRNA-ChNPs were quantified

**4.4.2.1 Morphology of ChNPs**
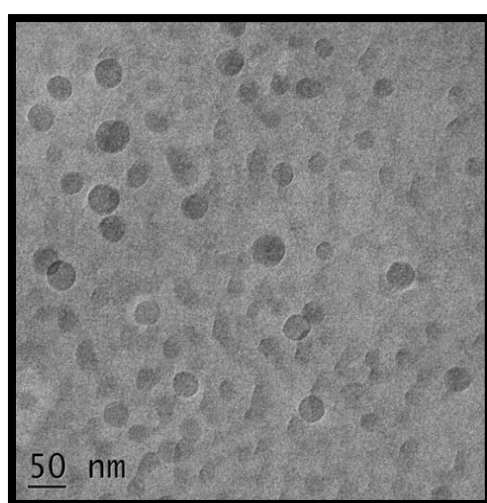


**Figure 4.3: TEM image of ChNPs**

Transmission electron microscopy showed a spherical structure of ChNPs with the solid dense structure shown in Figure 4.3.

**4.4.2.2 Particle Size, PDI and zeta Potential**

The particle size, PDI and zeta potential of prepared formulations were determined and the results are recorded in Table 4.7.

**Table 4.7: Particle size, PDI and zeta potential of optimized NPs formulations**

| Formulations | Particle Size* (nm) | PDI | Zeta Potential (mv) |
|---|---|---|---|
| ChNPs | 189±4.5 | 0.20±0.03 | +30.6±0.3 |
| DOX-ChNPs | 226±6.5 | 0.25±0.05 | +32.5±0.5 |
| siRNA-ChNPs | 218±3.1 | 0.21±0.04 | +31.6±0.4 |
| DOX-siRNA-ChNPs-CMAb | 232±6.5 | 0.22±0.05 | -34.2±0.3 |

**4.4.2.3 Fourier transform infrared spectroscopy (FTIR)**

The formation of NPs and DOX-ChNPs was demonstrated through the FTIR data shown in Figure 4.4, when Ch is crosslinked with TPP, NPs formation occurs and this interaction was shown by the amide I band between 1650-1675 cm$^{-1}$ (C=O stretching), amide II bands between 1550-1590 cm$^{-1}$ (NH bending). A broader peak at 3302 cm$^{-1}$ and a shoulder peak at 1624 cm$^{-1}$ were observed in ChNPs due to the development of hydrogen bonds. For DOX-ChNPs, the absorption bands appearing at 1016 cm$^{-1}$ and 1645 cm$^{-1}$ are related to DOX (Xu and Du, 2003).
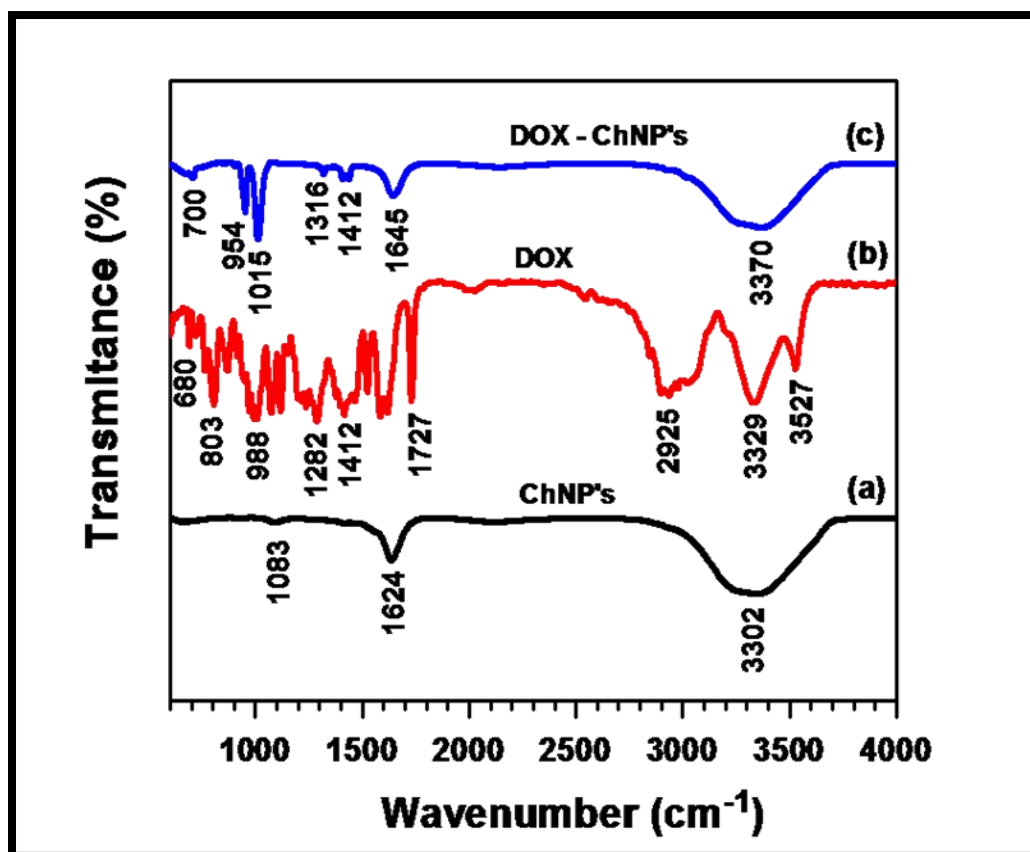
**Figure 4.4: FTIR spectra of ChNPs, DOX, DOX-ChNPs**

## 4.4.2.4 Entrapment efficiency of DOX

The entrapment efficiency of DOX into ChNPs were measured using a dual-beam UV-vis spectrophotometer results are recorded in Table 4.8. It was shown that, 65±1.46% of DOX entrapped in DOX-ChNPs.

**Table 4.8: Entrapment efficiency of DOX into ChNPs**

| Formulations | Entrapment efficiency (%) |
|--------------|---------------------------|
| DOX-ChNPs | 65.42±1.46 % |

## 4.4.2.5 In-vitro release study of DOX

The in-vitro DOX release study was conducted in two different environments: pH 5.5 (simulating the tumor environment) and pH 7.4 (representing physiological pH). Figure 4.5 displays the percentage cumulative release of DOX from DOX-siRNA-ChNPs-CMAb over a specified time interval. At the end of 48 h, total DOX released i.e. 87.55±4.27% and 70.99±4.07% at pH 5.5 and at pH 7.4.
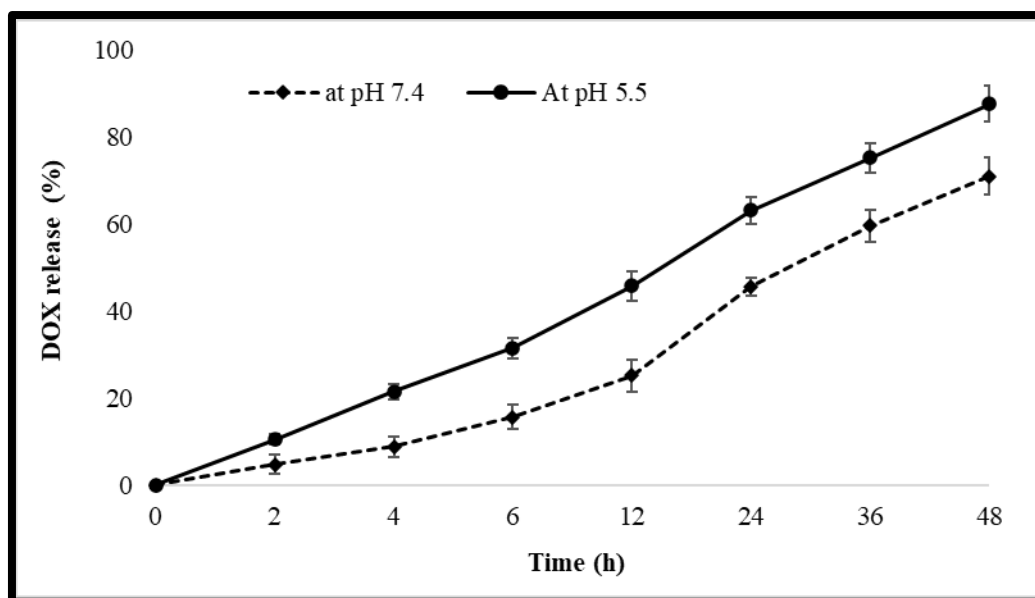
**Figure 4.5: In-vitro DOX release profile at pH 5.5 and pH 7.4 in PBS from DOX-ChNPs**

The developed formulation was engineered to specifically target CRC cells that overexpress CEA. This was achieved by coupling the DOX-siRNA-ChNPs withbCMAb. Upon binding to CEA molecules on the cell surface, the CMAb conjugated formulation was internalized via endocytosis. After being internalized, the formulation containing DOX, siRNA and ChNPs complexed with CMAb was enclosed within endosomal compartments. Leveraging the "proton sponge effect," the DOX-siRNA-ChNPs were able to escape from the endosomes. This phenomenon takes advantage of the ChNPs amino groups, which have a pKa value around 6.5. Within the acidic environment of the endosomes, these amino groups underwent protonation, facilitating disruption of the endosomal membrane. This process led to an influx of water and chloride ions into the endosomes. This influx was believed to be driven by the increased presence of positively charged ions (cations) that entered the endosome to balance its overall charge. Consequently, this osmotic influx of water and ions caused the endosome to swell, eventually leading to its physical rupture. As a result of this rupture, the DOX-siRNA entrapped within the ChNPs were released into the cytoplasm. In summary, the designed formulation was tailored to target CRC cells overexpressing CEA by utilizing CMAb (Chuan et al., 2019, Wang and Zhou, 2015).

**4.4.2.6 Confirmation of siRNA entrapment by Agarose Gel Retardation Assay**

The agarose gel retardation assay was employed to investigate the electrostatic interactions between a positively charged carrier and the negatively charged

phosphate group in siRNA (Ray, 2020, Dhandapani et al., 2019, Sun et al., 2018). In this assay, both the naked siRNA and siRNA-ChNPs were loaded onto an agarose gel, as depicted in Figure 4.6 (a). The results demonstrated that the naked siRNA, which carries a negative charge, readily migrated toward the positive electrode during electrophoresis. This migration was visible as a dark band on the agarose gel. However, when siRNA formed complexes with the positively charged ChNPs, it hindered the mobility of siRNA within the gel. Figure 4.6 (b) provides a densitometry analysis of the agarose gel retardation assay, further illustrating the observed effects.
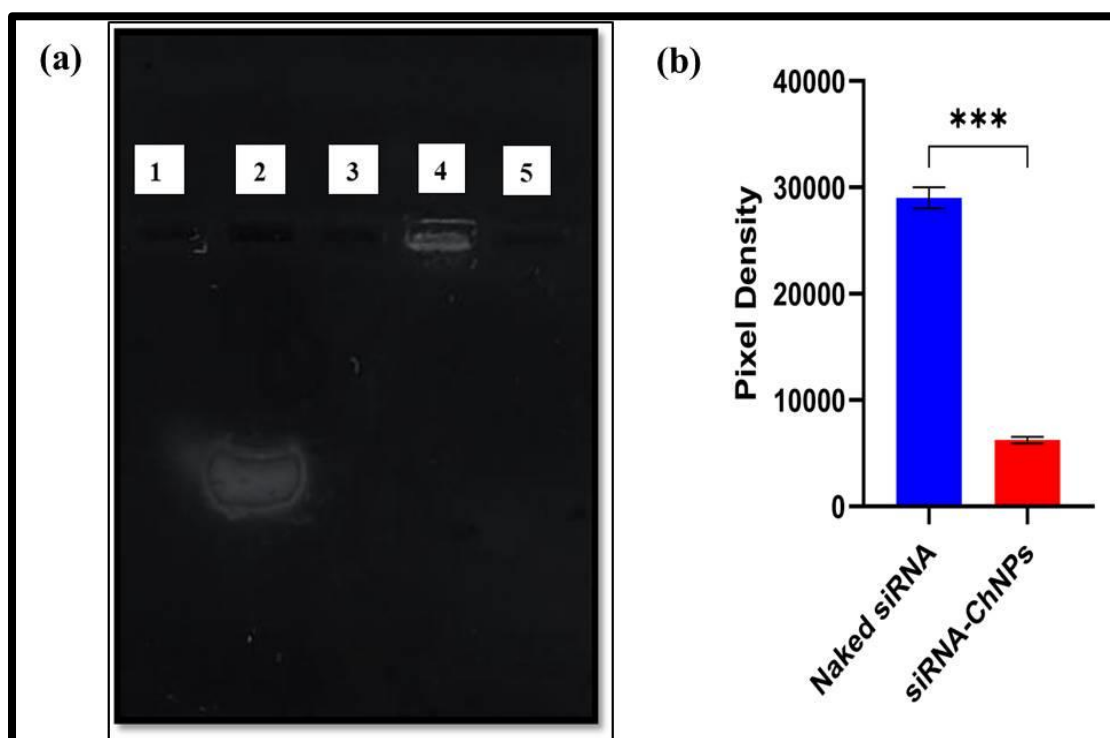


**Figure 4.6: (a) siRNA entrapment confirmed by agarose gel retardation assay, 1. Blank well, 2. Naked siRNA, 3. Blank well, 4. siRNA-ChNPs 5. Blank well, (b) densitometry analysis of agarose gel retardation assay**

**4.4.2.7 CMAb conjugation efficiency studied by Enzyme-Linked Immunosorbent Assay (ELISA)**

ELISA analysis was conducted to assess the conjugation efficiency of CMAb to DOX-siRNA-ChNPs. The findings presented in Figure 4.7 provided confirmation of the presence of CMAb on the surface of DOX-siRNA-ChNPs, indicating that approximately 17±1.5% of the CMAb was successfully conjugated. However, it was noted that a greater quantity of CMAbs remained in the supernatant.

ELISA analyzed the conjugation efficiency of CMAb to DOX-siRNA-ChNPs and these results are similar to Pereira et al., 2018, the positive control utilized the same quantity of CMAb as employed in the surface modification procedure. While the total amount of the positive control should theoretically match the combined Abs levels in both the NPs and supernatant, observations suggest a potential discrepancy. This could potentially be attributed to the loss of Abs during subsequent purification stages of the NPs. An additional factor influencing this lower percentage could be the orientation of the Abs. If the binding sites of the Abs were not adequately available for interaction with the secondary HRP-Ab, it could result in a weaker signal, even though the Abs is indeed present on the NPs surface (Pereira et al., 2018).
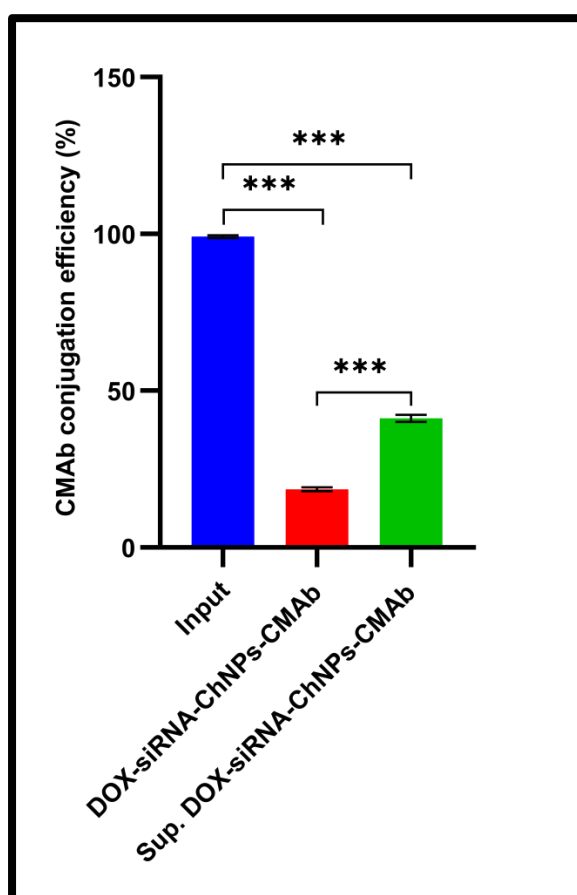


**Figure 4.7: Conjugation efficiency of CMAb to the DOX-siRNA-ChNPs. The initial amount of CMAb used in the surface modification (Input), DOX-siRNA-ChNPs-CMAb, supernatant DOX-siRNA-ChNPs-CMAb were tested using an ELISA assay to assess the presence of the CMAb confirming the surface modification. The presented values as means ± SD (n=3; \*\*P<0.01; \*\*\*P<0.001).**

## 4.5 Conclusions

In conclusion, ChNPs were successfully prepared by the ionic gelation method. Ch:TPP ratios were optimized based on particle size. It was found that 5:1 was the optimum Ch:TPP ratio with optimum particle size. It was selected for optimization of DOX concentration. The effect of DOX concentration on particle size and entrapment efficiency was studied. Their results demonstrated that by increasing the concentration of DOX particle size was increased. But, entrapment efficiency was slightly increased. Hence, 0.5 mg of DOX was selected as the optimum concentration with $65\pm1.46\%$ of entrapment efficiency. Further optimized, the incubation time of the CMAb in the surface modification process. At 24 h, higher CMAb conjugation efficiency was observed.

Optimized formulation was prepared with 5:1-Ch: TPP ratio, 0.5 mg of DOX and 24 h of CMAb incubation and fixed concentration of siRNA. TEM analysis showed the spherical, solid dense structure of ChNPs. In-vitro release study showed initial burst release and then slow and sustained release of DOX from ChNPs. Agarose gel retardation assay confirmed the entrapment of siRNA into ChNPs. Surface modification of ChNPs was performed by using carbodiimide chemistry with CMAb and their conjugation efficiency was evaluated by ELISA. Their results indicated that $17\pm1.5\%$ of antibody was present on the surface of ChNPs.

# References

❖ Abdul Ghafoor Raja M, Katas H, Jing Wen T. Stability, intracellular delivery, and release of siRNA from chitosan nanoparticles using different cross-linkers. PLoS One. 2015 Jun 11;10(6):1-19.

❖ Alinejad V, Somi MH, Baradaran B, Akbarzadeh P, Atyabi F, Kazerooni H, Kafil HS, Maleki LA, Mansouri HS, Yousefi M. Co-delivery of IL17RB siRNA and doxorubicin by chitosan-based nanoparticles for enhanced anticancer efficacy in breast cancer cells. Biomed Pharmacother. 2016 Oct 1;83:229-240.

❖ Al-Nemrawi NK, Alsharif SS, Dave RH. Preparation of chitosan-TPP nanoparticles: the influence of chitosan polymeric properties and formulation variables. Int. J. Appl. Pharm. 2018 Sep 8;10:60-65.

❖ Calvo P, Remunan-Lopez C, Vila-Jato JL, Alonso MJ. Novel hydrophilic chitosan-polyethylene oxide nanoparticles as protein carriers. J Appl Polym Sci. 1997 Jan 3;63(1):125-132.

❖ Chuan, D.; Jin, T.; Fan, R.; Zhou, L., Guo, G. Chitosan for gene delivery: Methods for improvement and applications. Adv. Colloid Interface Sci. 2019, 268, 25-38.

❖ de Pinho Neves AL, Milioli CC, Müller L, Riella HG, Kuhnen NC, Stulzer HK. Factorial design as tool in chitosan nanoparticles development by ionic gelation technique. Colloids and Surfaces A: Physicochemical and Engineering Aspects. 2014 Mar 20;445:34-39.

❖ Dhandapani RK, Gurusamy D, Howell JL, Palli SR. Development of CS-TPP-dsRNA nanoparticles to enhance RNAi efficiency in the yellow fever mosquito, Aedes aegypti. Sci Rep. 2019 Jun 19;9(1):8775.

❖ G.T. Hermanson, Bioconjugate Techniques, I, Academic Press, London, 1996, pp. 169–172.

❖ Gan Q, Wang T, Cochrane C, McCarron P. Modulation of surface charge, particle size and morphological properties of chitosan–TPP nanoparticles intended for gene delivery. Colloids and Surfaces B: Biointerfaces. 2005 Aug 1;44(2-3):65-73.

❖ Jain NK, Jain SK. Development and in vitro characterization of galactosylated low molecular weight chitosan nanoparticles bearing doxorubicin. Aaps Pharmscitech. 2010 Jun;11(2):686-697.

❖ Karimi M, Avci P, Ahi M, Gazori T, Hamblin MR, Naderi-Manesh H. Evaluation of chitosan-tripolyphosphate nanoparticles as a p-shRNA delivery vector: formulation, optimization and cellular uptake study. Journal of nanopharmaceutics and drug delivery. 2013 Sep 1;1(3):266-278.

❖ Katas H, Alpar HO. Development and characterization of chitosan nanoparticles for siRNA delivery. J Control Release. 2006 Oct 10;115(2):216-225.

❖ Kiilll CP, da Silva Barud H, Santagneli SH, Ribeiro SJ, Silva AM, Tercjak A, Gutierrez J, Pironi AM, Gremião MP. Synthesis and factorial design applied to a novel chitosan/sodium polyphosphate nanoparticles via ionotropic gelation as an RGD delivery system. Carbohydrate Polymers. 2017 Feb 10;157:1695-1702.

❖ Pereira I, Sousa F, Kennedy P, Sarmento B. Carcinoembryonic antigen-targeted nanoparticles potentiate the delivery of anticancer drugs to colorectal cancer cells. Int J Pharm. 2018 Oct 5;549(1-2):397-403.

❖ Ray L. Synergistic anticancer activity by co-delivered nanosized dual therapeutic agents and siRNA in colon cancer. J Drug Deliv Sci Technol. 2020 Feb 1;55:101351.

❖ Siahmansouri H, Somi MH, Babaloo Z, Baradaran B, Jadidi-Niaragh F, Atyabi F, Mohammadi H, Ahmadi M, Yousefi M. Effects of HMGA2 siRNA and doxorubicin dual delivery by chitosan nanoparticles on cytotoxicity and gene expression of HT-29 colorectal cancer cell line. J Pharm Pharmacol. 2016 Sep;68(9):1119-1130.

❖ Sun Q, Wang X, Cui C, Li J, Wang Y. Doxorubicin and anti-VEGF siRNA co-delivery via nano-graphene oxide for enhanced cancer therapy in vitro and in vivo. Int J Nanomed. 2018;13:3713.

❖ Wang, X.B.; Zhou, H.Y. Molecularly targeted gemcitabine-loaded nanoparticulate system towards the treatment of EGFR overexpressing lung cancer. Biomed. Pharmacother. 2015, 70, 123-128.

❖ Xu Y, Du Y. Effect of the molecular structure of chitosan on protein delivery properties of chitosan nanoparticles. Int J Pharm. 2003 Jan 2;250(1):215-226.

❖ Zhang L, Kosaraju SL. Biopolymeric delivery system for controlled release of polyphenolic antioxidants. European polymer journal. 2007 Jul 1;43(7):2956-2966.

**Summary**

This chapter summarizes the in-vitro evaluation of CMAb conjugated DOX-siRNA-ChNPs (DOX-siRNA-ChNPs-CMAb) by different in-vitro analyses on the HT-29 cell line. To study the cytotoxicity of DOX-siRNA-ChNPs-CMAb in comparison with ChNPs, free DOX, DOX-ChNPs, naked siRNA, siRNA-ChNPs, DOX-siRNA-ChNPs, DOX-siRNA-ChNPs-CMAb MTT assay was performed. To confirm intracellular entry of DOX and siRNA, DOX fluorescence was analyzed in HT-29 cells. Uptake was compared with free DOX, DOX-siRNA-ChNPs, DOX-siRNA-ChNPs-CMAb after 2, 4, 6, 8, 12 and 24 h. Apoptosis analysis was performed to quantitatively determine the intracellular uptake in HT-29 cells by flow cytometry.

## 5.1 Materials

Human colorectal adenocarcinoma (HT-29) cells were obtained from the National Center for Cell Sciences (NCCS), Pune, India, PBS, Dulbecco's Modified Eagle Medium (DMEM), fetal bovine serum (FBS), antibiotics (streptomycin, penicillin), non-essential amino acids (NEAA), 3-(4,5-dimethylthiazol-2-yl)-2,5-diphenyltetrazolium bromide dye (MTT), acetone, methanol, dimethylsulfoxide ( DMSO) were purchased from Himedia Laboratories Pvt. Ltd., Mumbai, India AlexaFluor® 488 Annexin V/Dead Cell Apoptosis Kit (catalog number V13241) was purchased from Invitrogen, India.

## 5.2 Methodology

### 5.2.1 Cell Culture and maintenance

The HT-29, Human colorectal adenocarcinoma cell line at passage number 8 was sourced from the National Centre for Cell Science (NCCS) located in Pune. These cells were maintained in a culture medium comprising 90% DMEM, supplemented with 10% FBS, 45 UI/mL of penicillin and 45 μg/mL of streptomycin. They were cultured in a standard cell culture environment, which involved incubating them at 37°C in a $CO_2$ incubator set to 5% $CO_2$ concentration.

### 5.2.2 Cytotoxicity study

The cytotoxicity of the prepared nanoformulations were assessed on HT-29 cells by MTT assay.

HT-29 cells were seeded in a 96-well plate at $1 \times 10^5$ cells/ml density. The cells were cultured overnight in DMEM media. This incubation was done in a $CO_2$ incubator under standard cell culture conditions, typically at 37°C with 5% $CO_2$. Different concentrations of formulations were prepared in DMEM media. These formulations include ChNPs, DOX-ChNPs, siRNA-ChNPs, DOX-siRNA-ChNPs, DOX-siRNA-ChNPs-CMAb, free DOX, Naked siRNA. 100 µl of each formulation at the specified concentrations (0.5, 1, 1.5, 2 µg/ml) was added to the respective wells containing the cultured cells. The plate was then incubated for 24 h. After the 24 h incubation period, 20 µl of MTT solution (5 mg/ml) was added to each well. MTT is a yellow tetrazolium salt that is converted into purple formazan crystals by metabolically active cells. The plate was kept in the dark at R.T. for 4 h to allow the MTT to be metabolized by viable cells. After the incubation with MTT, the supernatant was carefully removed from each well. 100 µl of DMSO was added to each well. DMSO helps to dissolve the formazan crystals, resulting in a colored solution. The optical density (OD) of the colored solution in each well was measured at a wavelength of 492 nm using a microplate ELISA reader, such as the LISA Plus Microplate ELISA reader. The OD is directly proportional to the number of viable cells, as formazan production depends on cell metabolism. The cell viability was calculated by equation 5.1.

$$\textbf{\textit{Cell viability}} \, (\%) = \frac{\textit{OD of test compound}}{\textit{OD of control}} * \textbf{100} \ldots\ldots\ldots\ldots\ldots\ldots\textbf{(5.1)}$$

### 5.2.3 Cellular uptake study

Fluorescence microscopy was employed to investigate the internalization of DOX in this study (Yousefpour et al., 2011, Yang et al., 2016). HT-29 cells were initially seeded at a density of 50,000 cells/well in a 24-well plate and incubated for 24 h. Following this incubation period, 1 ml of medium containing 200 µl of DOX-siRNA-ChNPs, DOX-siRNA-ChNPs-CMAb and 1 µg of DOX was added to the cells and they were further incubated for 24 h. After the treatment medium was removed and the cells were washed with cold PBS (pH 7.4), they were stained with DAPI. Subsequently, the cells were fixed with a chilled acetone: methanol mixture (1:1) at 4°C for 30 min and washed again with cold PBS (pH 7.4). The uptake of DOX within the cells was then visualized using fluorescence microscopy with excitation wavelengths set at 488 nm for DOX and 340 nm for DAPI, using a Nikon Inverted

Microscope Eclipse Ti-E, Japan, equipped with imaging software (NIS) as shown in Figure 5.1.
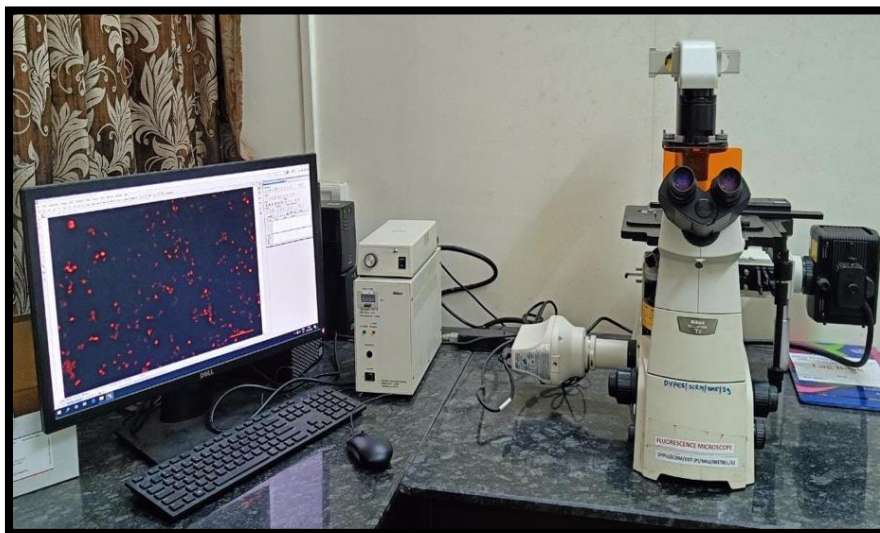


**Figure 5.1: Fluorescence microscopy (Nikon Inverted Microscope Eclipse Ti-E, Japan).**

## 5.2.4 Analysis of apoptosis by flow cytometry

Flow cytometry was employed to assess the apoptotic potential of Free DOX, DOX-siRNA-ChNPs and DOX-siRNA-ChNPs-CMAb on HT-29 cells using an Alexa Fluor 488 annexin V/Dead Cell Apoptosis Kit (Invitrogen, India) (Sadreddini et al, 2017, Gholami et al., 2019, Siddharth et al., 2017). Initially, 50,000 cells/well were seeded into a 24-well plate and allowed to incubate for 24 h. Subsequently, 250 µl of DOX-siRNA-ChNPs and DOX-siRNA-ChNPs-CMAb were added to the respective wells and a negative control group was included for cell incubation. After the incubation period, cells were detached by trypsinization, washed with cold 1X PBS and resuspended in 1X annexin-binding buffer. Next, 5 µl of Alexa Fluor 488 annexin V was added to each sample, followed by a 15 min incubation at R.T. Following this incubation, 1 µl of propidium iodide (PI) solution (100 µg/ml) was added to every 100 µl of cell suspension. After another incubation step, 200 to 400 µl of 1X Annexin binding buffer was added to each sample, mixed gently and kept on ice. Finally, the treated samples were thoroughly mixed and the apoptotic cell population was analyzed using flow cytometry with an Attune NxT acoustic flow cytometer (Invitrogen by Thermo Fisher Scientific, USA) shown in Figure 5.2.

**Figure 5.2: Flow cytometer**

(https://www.thermofisher.com/order/catalog/product/A24858)

**Statistical analysis**

The experiments were conducted in triplicate and the results are expressed as the mean ± standard deviation (SD). Data were subjected to statistical analysis using one-way analysis of variance (ANOVA) with Tukey's post hoc test, utilizing Graph Pad Prism Software version 8.0.2 (Inc., USA). Statistical significance was defined at different levels: $*p < 0.05$, $**p < 0.01$ and $***p < 0.001$.

## 5.3 Results and discussion

Physical interactions between DOX and nucleic acids are well known. Due to the presence of flat aromatic rings, DOX preferentially binds to 5'-GC-3' or 3'-GC-5' sequences. Many researchers have exploited these properties to develop specific formulations by complexing plasmids, apatmers and siRNA with DOX. Most of these conjugates showed significant inhibition of tumor growth when applied as delivery systems (Chen et al., 2019). By taking inspiration from these interesting studies, we hypothesized that DOX could intercalate into the double-stranded region of siRNAs to form physical complexes.

### 5.3.1 Cytotoxicity study by MTT assay

The cytotoxicity of the developed formulations, including ChNPs, DOX-ChNPs, siRNA-ChNPs, DOX-siRNA-ChNPs, DOX-siRNA-ChNPs-CMAb, free

DOX and naked siRNA was assessed on HT-29 cells through MTT assay. The concentration of free DOX, DOX-ChNPs, DOX-siRNA-ChNPs and DOX-siRNA-ChNPs-CMAb were taken on the basis of IC-50 values reported in the literature. The concentration of Ch was used in the preparation of optimized ChNPs and the minimum was used to study their cytotoxicity and HT-29 cells without any treatment was kept as a control. The findings are shown in Figure 5.3, the DOX-siRNA-ChNPs-CMAb was more cytotoxic to HT-29 cells in comparison to other formulations like ChNPs, DOX-ChNPs, siRNA-ChNPs, DOX-siRNA-ChNPs, free DOX and naked siRNA, HT-29 demonstrated a significant decrease in cellular viability after 24 h of treatment with the DOX-siRNA-ChNPs-CMAb formulation. The cytotoxicity assessment of the formulation was conducted using the MTT assay on HT-29 cells. According to Pornpitchanarong et al., 2020, DOX was internalized by the cells to a limited degree due to the presence of hydrophilic polar groups, which impede the molecules from freely penetrating the cell membrane. Nevertheless, the DOX-ChNPs were readily absorbed by cells owing to their extensive surface area, which facilitated interactions with the cell membrane. As a result, the DOX-ChNPs exhibited a greater inclination and were capable of permeating the cytosol more effectively. Furthermore, it has been demonstrated that polymeric NPs can significantly augment cells internalization of entrapped drugs and their subsequent accumulation within the cell interior. This effect is primarily mediated through diverse endocytic pathways, with a notable emphasis on macropinocytosis (Pornpitchanarong et al., 2020). Notably, the IC50 value of DOX-siRNA-ChNPs-CMAb exhibited a significant reduction compared to that of DOX-siRNA-ChNPs alone. This compelling outcome is attributed to the efficient process of receptor mediated endocytosis, through which DOX-siRNA-ChNPs-CMAb is internalized by HT-29 cells. Once inside the cells, the DOX and siRNA moieties are released from intracellular lysosomes and act on cellular components, exerting their distinct therapeutic effects. Specifically, the active form of DOX effectively impedes DNA strand replication, inhibiting cancerous cell proliferation. Concurrently, VEGF-siRNA engages with its target mRNA, facilitating its degradation. This targeted interference effectively hampers the process of angiogenesis and causes cell death. These multi-faceted observations cogently emphasize the remarkable potential of DOX-siRNA-ChNPs-CMAb to amplify the anticancer ability of CEA therapeutics markedly. This augmentation of therapeutic efficacy is especially pronounced against cancer cells that express the target CEA,

thus positioning DOX-siRNA-ChNPs-CMAb as a promising and potent strategy against cancer (Wang and Zhou, 2015).
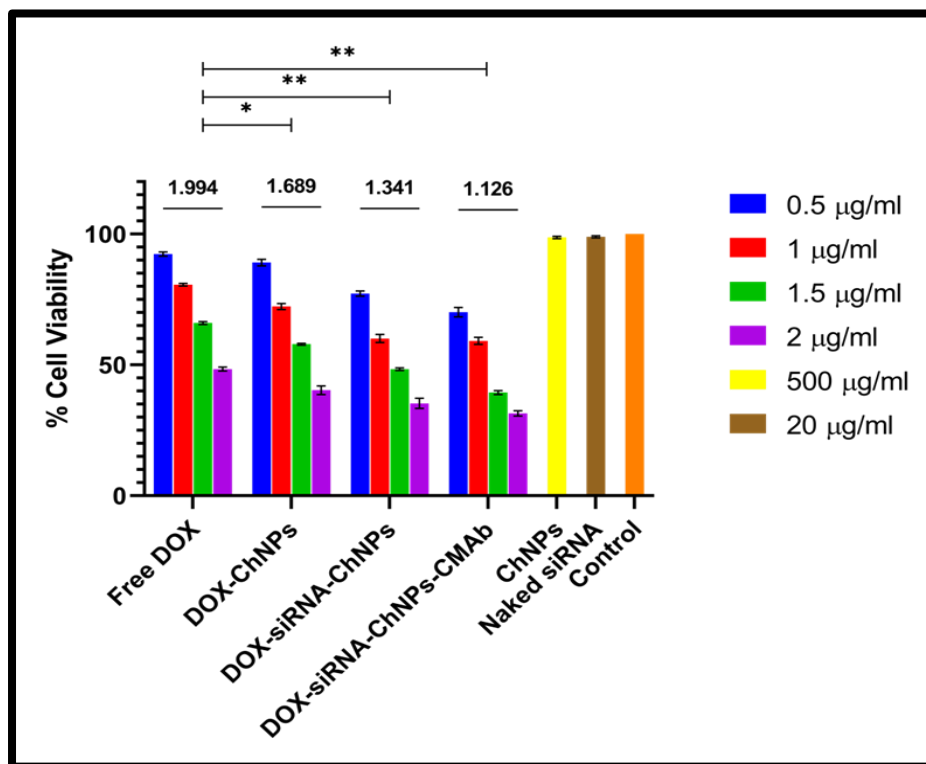


**Figure 5.3: In-vitro cell viability studied by MTT assay in HT-29 cell line following 24 h treatment with free DOX, DOX-ChNPs, DOX-siRNA-ChNPs, DOX-siRNA-ChNPs-CMAb with different concentrations and control, ChNPs, naked siRNA. The presented values as means ± SD (n=3; *P<0.01; **P<0.001)**

**5.3.2 Cellular uptake study**

The time dependent uptake of free DOX, DOX-siRNA-ChNPs, DOX-siRNA-ChNPs-CMAb by HT-29 cells was confirmed by fluorescence microscopy. DOX incorporated into the nuclei of HT-29 cells, shown red fluorescence of DOX, blue fluorescence of DAPI-stained nuclei. In the merged image, pink color is observed in the cytoplasm of the cells and blue color is observed in the nuclei, indicating DOX entry into the cells by white arrows in Figure 5.4.

Various cellular uptake mechanisms for free DOX and DOX-NPs have been extensively documented in the literature, owing to their conspicuous red fluorescence. The main concept is that the acidic environment of the endosomal/lysosomal compartment facilitates the subsequent release of DOX from NPs and then translocated to the nucleus (Li et al., 2014, Chittasupho 2014, Wang and Zhou, 2015).
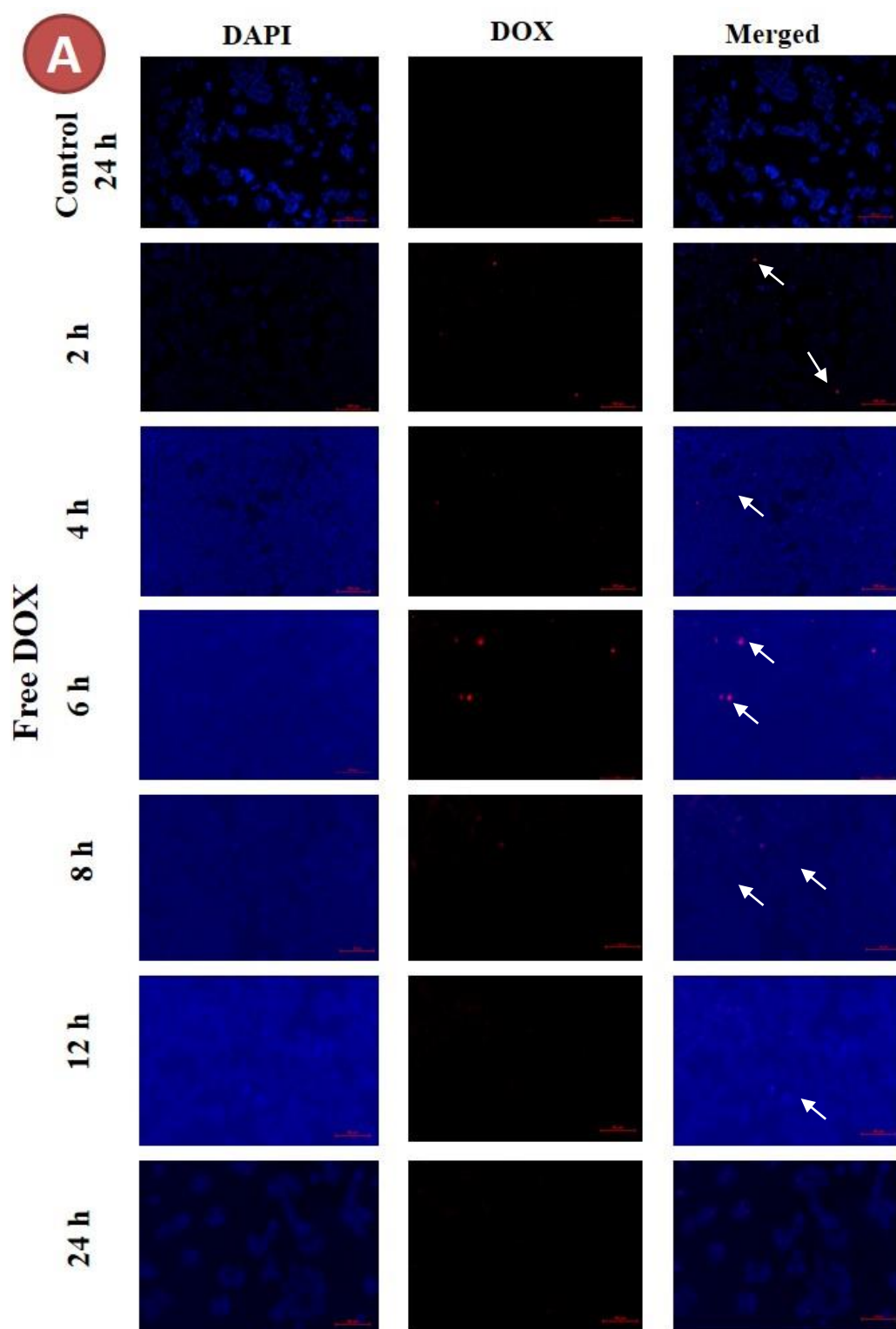
**Figure 5.4: Fluorescence microscopic images for DOX uptake at 2, 4, 6, 8, 12, 24 h of (A) free DOX in HT-29 cells and control HT-29 cells at 24 h.**
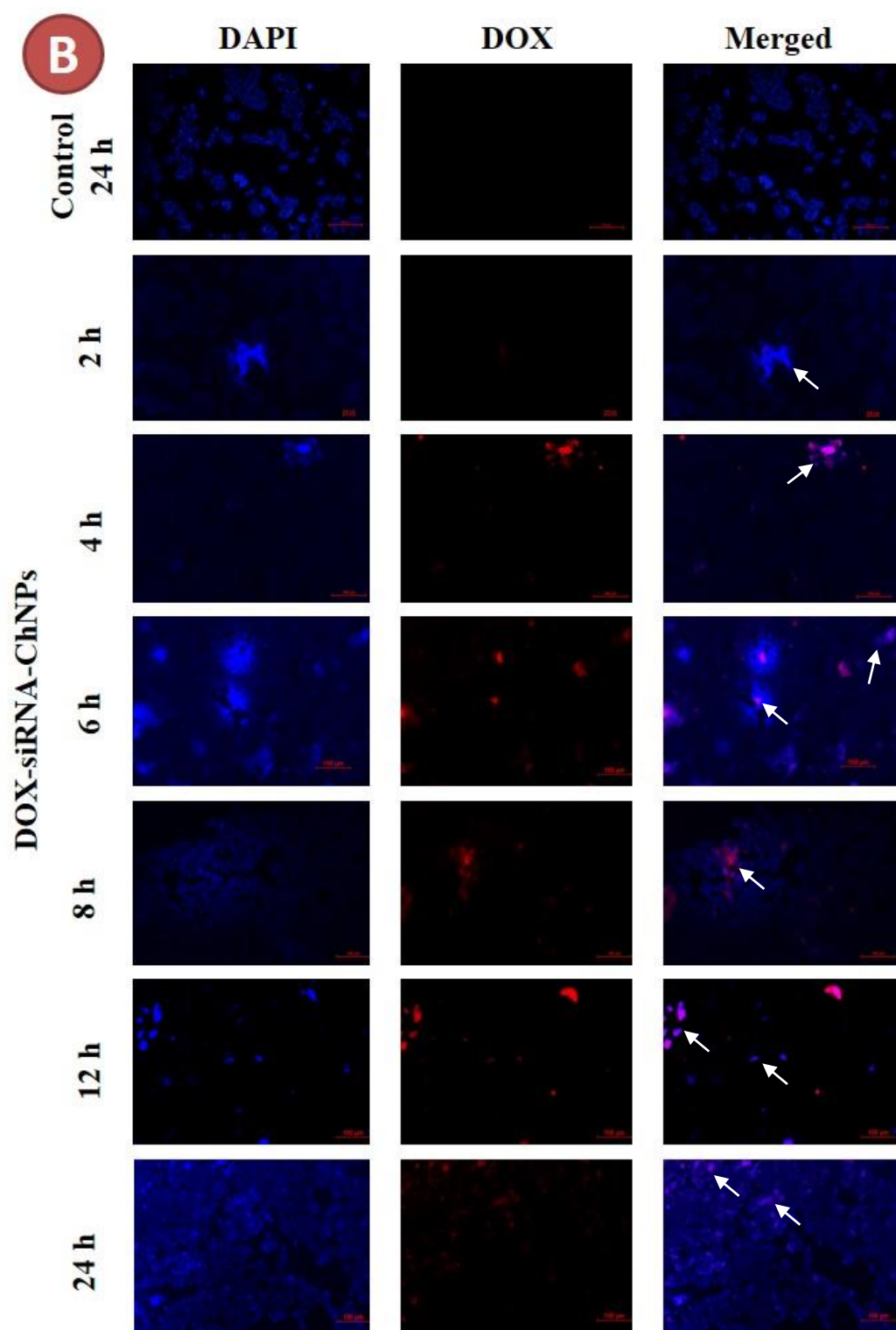
**Figure 5.4: Fluorescence microscopic images for DOX uptake at 2, 4, 6, 8, 12, 24 h of (B) DOX-siRNA-ChNPs in HT-29 cells and control HT-29 cells at 24 h.**
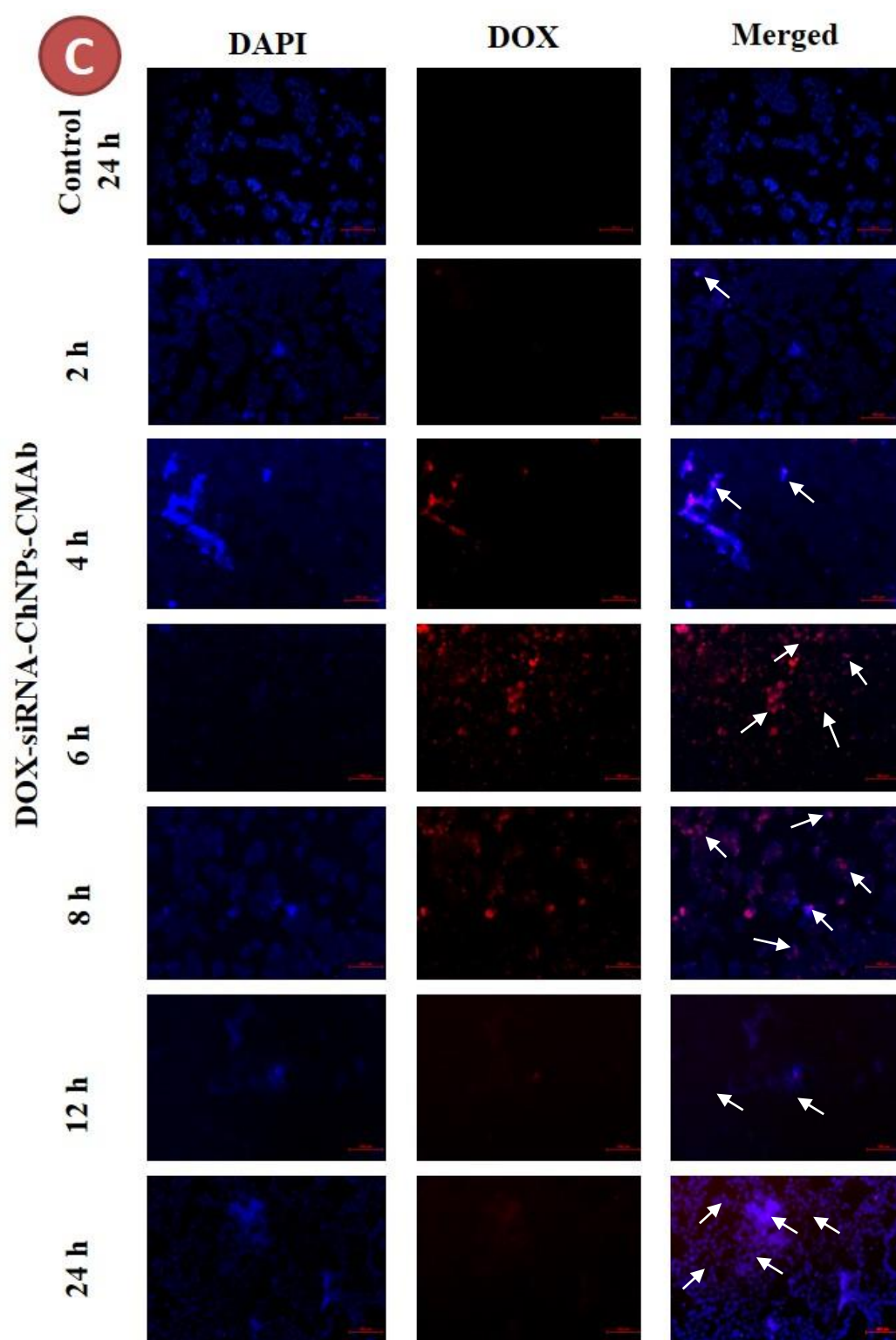
**Figure 5.4: Fluorescence microscopic images for DOX uptake at 2, 4, 6, 8, 12, 24 h of (C) DOX-siRNA-ChNPs-CMAb in HT-29 cells and control HT-29 cells at 24 h.**

The targeting efficacy of DOX-siRNA-ChNPs in combination with CMAbs could be evaluated by studying the cellular uptake of DOX. By evaluating the red fluorescence of DOX, we can say that siRNA can also be absorbed by cells. It shows selective and enhanced uptake of DOX-siRNA-ChNPs-CMAb by HT-29 cells compared with free DOX, DOX-siRNA-ChNPs after 24 h. Up to 6 h, free DOX showed a higher level of absorption, which reduced after 12 h. On the other hand, observations indicated that more DOX localized to the nucleus when in free form compared with DOX entrapped in ChNPs for up to 6 h, but after that, it decreased significantly for 24 h. This may be due to the DOX efflux from the cells. The results revealed that DOX-siRNA-ChNPs-CMAb binds significantly more than DOX-siRNA-ChNPs. DOX-siRNA-ChNPs-CMAb showed a significant increase in DOX uptake over the course of 24 h compared with DOX-siRNA-ChNPs and free DOX uptake in Figure 5.4.

DOX-siRNA-ChNPs-CMAb exhibited a noteworthy enhancement in cellular uptake of DOX over 24 h, surpassing the uptake observed with DOX-siRNA-ChNPs and free DOX. These findings closely align with the outcomes reported by Yousefpour et al., 2011 (Yousefpour et al., 2011). Chittasupho et al., (2014) reported that the presence of a higher quantity of NPs and their rapid binding to the cell surface contribute to the targeting mechanism. This phenomenon is believed to enhance the likelihood of successful localization of DOX-siRNA-ChNPs-CMAb. The co-localization of DOX with cell nuclei implies that both DOX and siRNA were effectively released from ChNPs and evenly distributed within the cells (Chittasupho et al., 2014)

The findings demonstrated a notable increase in binding affinity for DOX-siRNA-ChNPs-CMAb compared to DOX-siRNA-ChNPs. Over 24 h, DOX-siRNA-ChNPs-CMAb exhibited a substantial rise in DOX uptake compared to DOX-siRNA-ChNPs and free DOX. This effect was attributed to a reduction in drug efflux, leading to enhanced intracellular DOX accumulation in the nucleus. The observed selective uptake through CEA receptors suggests that the internalization of NPs may play a crucial role in this process (Butt et. al., 2016, Zhang et al., 2016).

### 5.3.3 Analysis of apoptosis by flow cytometry

In addition, the combined impact of targeting and co-delivery was systematically analyzed using flow cytometry, aiming to assess the efficacy of inducing cellular apoptosis in HT-29 cells and results are shown in Figure 5.5. The analysis revealed the presence of viable cells (-/-), cells in the early stages of apoptosis (+/-), cells in the late stages of apoptosis (+/+) and necrotic cells (-/+) following staining with annexin V labeled with Alexa Fluor® 488. The cells exposed to free DOX at 2µg/ml (IC50 value) had a higher rate of apoptosis (98.84%). Furthermore, the combined delivery of DOX and siRNA (DOX-siRNA-ChNPs) resulted in a notable induction of apoptotic cell death (89.83%). However, the combined action of DOX, siRNA, ChNPs and CMAb demonstrated considerably enhanced apoptosis (96.32%).

Further, the anticancer effect of DOX-siRNA-ChNPs-CMAb was confirmed by Annexin V/PI-based apoptosis assay on a flow cytometer indicating a late apoptosis phase induction within 24 h. The results corroborated the concept that directing CMAb improves apoptotic effects on HT-29 cells with greater efficacy compared to both free DOX and DOX-siRNA-ChNPs. However, it is important to note that the conventional treatment also exhibits higher cytotoxicity towards healthy cells. As the primary mechanism of DOX action against cancer cells is attributed to its ability to inhibit topoisomerase II and generate free radicals (Mizutani et al., 2005). Our innovative targeted formulation addresses this concern by selectively focusing on CRC cells, thereby mitigating these adverse effects.

Confirmatory bright filed images of HT-29 after exposure to different formulations such as DOX-siRNA-ChNPs-CMAb, DOX-siRNA-ChNPs, free DOX was showed viable cells indicated by black arrows and dead cells indicated by red arrows in Figure 5.6.

These images suggested that, cell viability of HT-29 cells were decreased by increasing concentration of DOX-siRNA-ChNPs-CMAb, after 24 h at higher concentration (500 µl) i.e. not observed considerable number of viable cells. But in case of DOX-siRNA-ChNPs there was no significant change in cell viability was observed after 24 h at higher concentration (500 µl). However, at highest concentration of free DOX HT-29 cells were show resistance at 24 h.
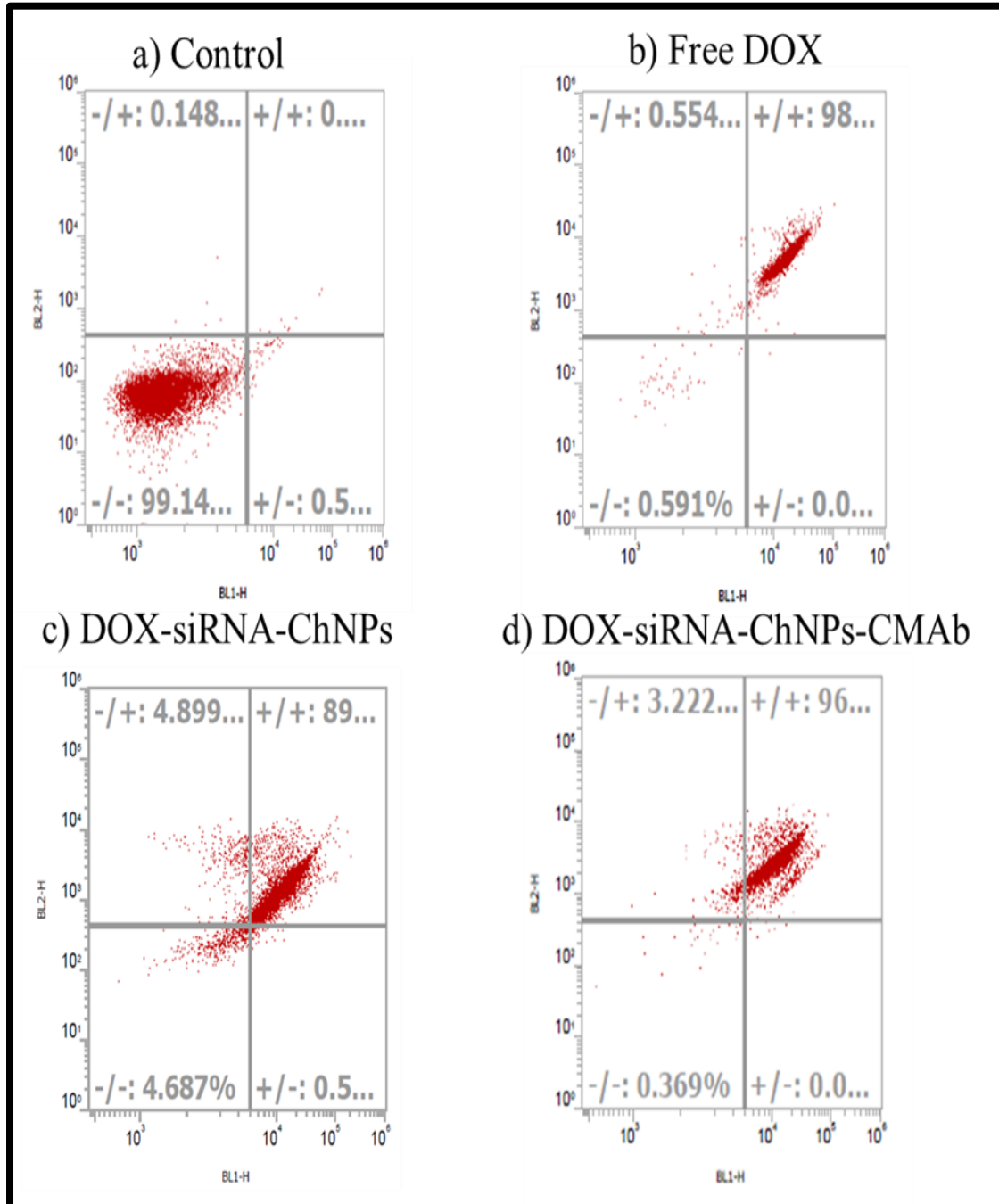
**Figure 5.5: Annexin V/PI analysis to study apoptosis in HT-29 cells at 24 h a) Control, b) free DOX, c) DOX-siRNA-ChNPs, d) DOX-siRNA-ChNPs-CMAb by flow cytometry**
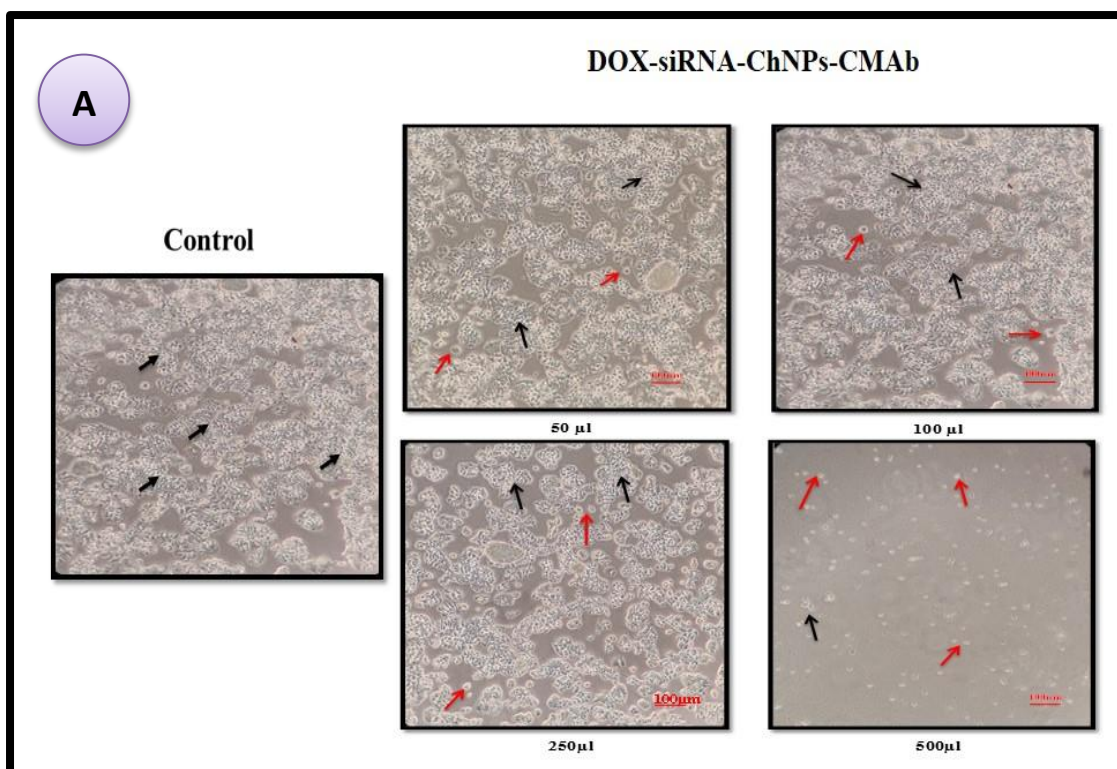
**Figure 5.6: Bright field images of HT-29 cells to confirm the viability of cells after exposure to different quantities of (A) DOX-siRNA-ChNPs-CMAb at 24 h.**
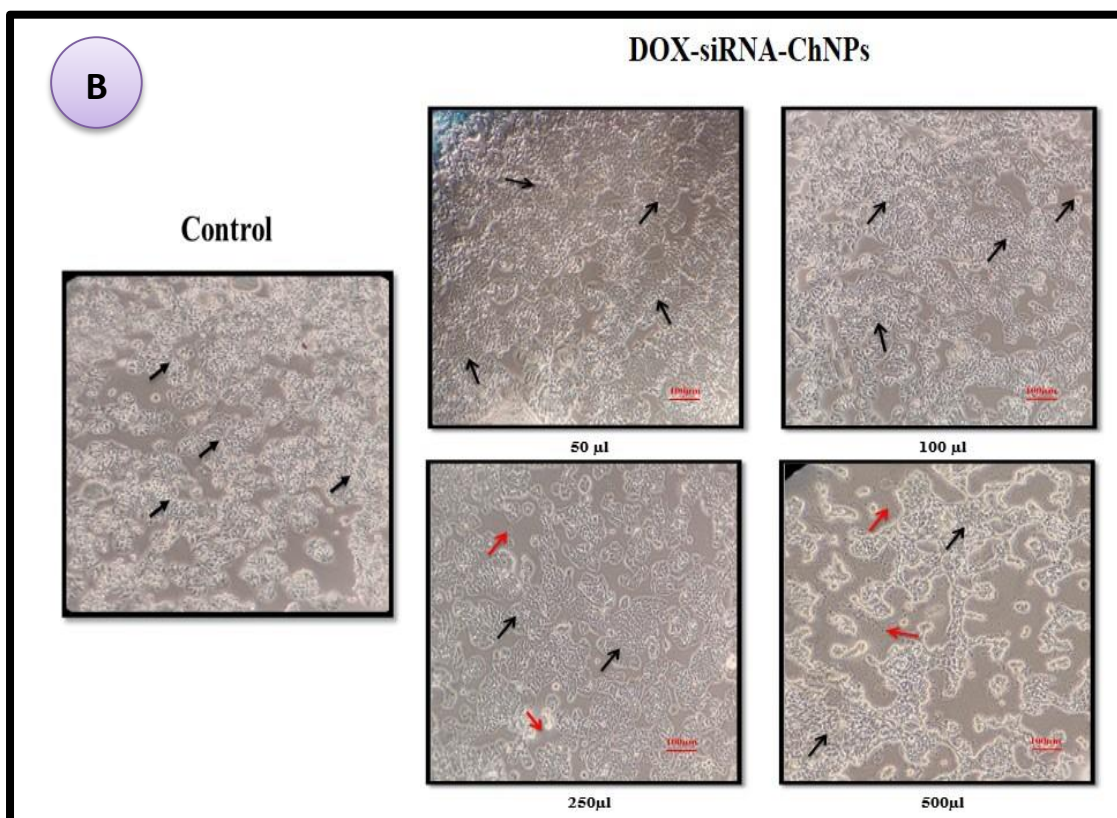


**Figure 5.6: Bright field images of HT-29 cells to confirm the viability of cells after exposure to different quantities of (B) DOX-siRNA-ChNPs at 24 h.**
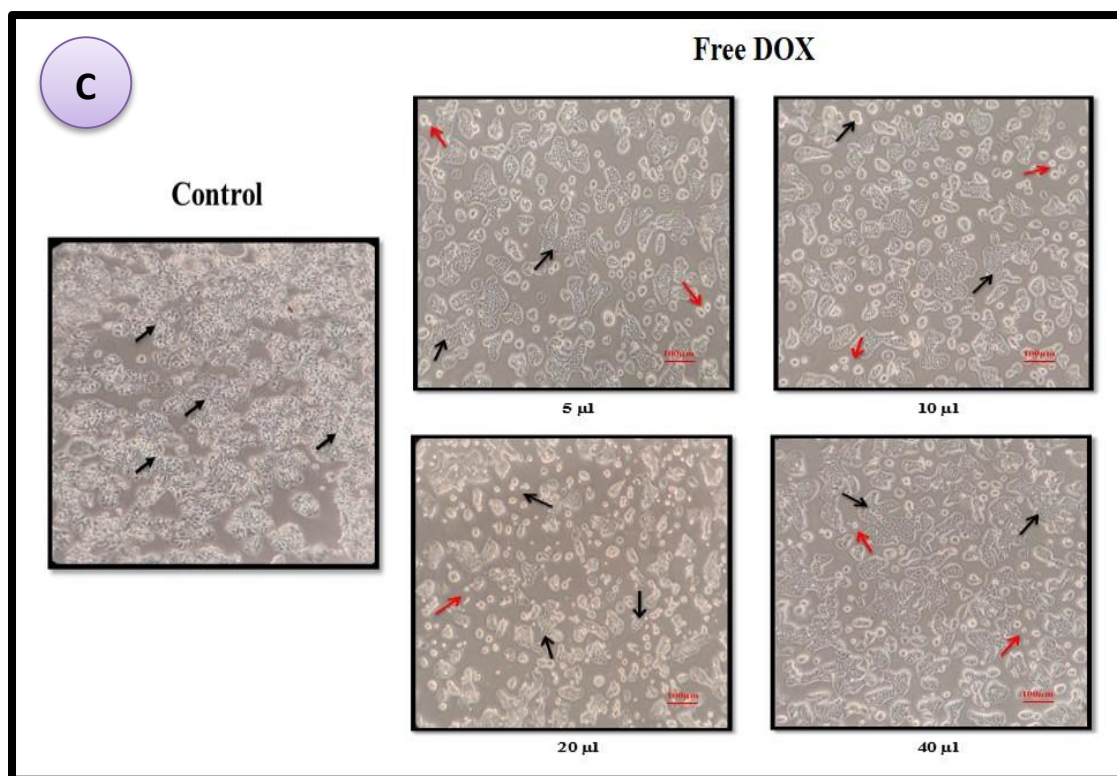
**Figure 5.6: Bright field images of HT-29 cells to confirm the viability of cells after exposure to different quantities of (C) free DOX at 24 h.**

## 5.4 Conclusions

The development of targeted co-delivery systems may improve therapeutic efficacy and reduce side effects. In this work, DOX-siRNA-ChNPs were prepared and surface modified with CMAb for targeting CEA in HT-29 cells. DOX-siRNA-ChNPs-CMAb showed the highest cytotoxicity against HT-29 cells over DOX-siRNA-ChNPs and free DOX. This is likely due to enhanced ligand specific internalization and receptor mediated endocytosis of ChNPs leading to greater cytotoxicity. Cellular uptake of free DOX, DOX-siRNA-ChNPs, DOX-siRNA-ChNPs-CMAb were showed that highest cellular uptake in DOX-siRNA-ChNPs-CMAb than free DOX and DOX-siRNA-ChNPs. Also, 96% apoptosis was observed in DOX-siRNA-ChNPs-CMAb than DOX-siRNA-ChNPs. Taken together all the results make the DOX-siRNA-ChNPs-CMAb formulation an ideal system to explore targeted co-delivery in the treatment of CRC as a more efficient and specific therapy.

# References

❖ Butt AM, Amin MC, Katas H, Abdul Murad NA, Jamal R, Kesharwani P. Doxorubicin and siRNA codelivery via chitosan-coated pH-responsive mixed micellar polyplexes for enhanced cancer therapy in multidrug-resistant tumors. Mol Pharm. 2016 Dec 5;13(12):4179-4190.

❖ Chen M, Wang L, Wang F, Li F, Xia W, Gu H, Chen Y. Quick synthesis of a novel combinatorial delivery system of siRNA and doxorubicin for a synergistic anticancer effect. Int J Nanomed. 2019;14:3557.

❖ Chittasupho C, Lirdprapamongkol K, Kewsuwan P, Sarisuta N. Targeted delivery of doxorubicin to A549 lung cancer cells by CXCR4 antagonist conjugated PLGA nanoparticles. Eur J Pharm Biopharm. 2014 Oct 1;88(2):529-538.

❖ Gholami L, Tafaghodi M, Abbasi B, Daroudi M, Kazemi Oskuee R. Preparation of superparamagnetic iron oxide/doxorubicin loaded chitosan nanoparticles as a promising glioblastoma theranostic tool. J Cell Physiol. 2019 Feb;234(2):1547-1559.

❖ Li Q, Lv S, Tang Z, Liu M, Zhang D, Yang Y, Chen X. A co-delivery system based on paclitaxel grafted mPEG-b-PLG loaded with doxorubicin: preparation, in vitro and in vivo evaluation. Int J Pharm. 2014 Aug 25;471(1-2):412-420.

❖ Mizutani, H.; Tada-Oikawa, S.;, Hiraku, Y.;, Kojima, M.;, Kawanishi, S. Mechanism of apoptosis induced by doxorubicin through the generation of hydrogen peroxide. Life Sci. 2005, 76, 1439-1453.

❖ Pornpitchanarong C, Rojanarata T, Opanasopit P, Ngawhirunpat T, Patrojanasophon P. Catechol-modified chitosan/hyaluronic acid nanoparticles as a new avenue for local delivery of doxorubicin to oral cancer cells. Colloids Surf B Biointerfaces. 2020 Dec 1;196:111279.

❖ Sadreddini S, Safaralizadeh R, Baradaran B, Aghebati-Maleki L, Hosseinpour-Feizi MA, Shanehbandi D, Jadidi-Niaragh F, Sadreddini S, Kafil HS, Younesi V, Yousefi M. Chitosan nanoparticles as a dual drug/siRNA delivery system for treatment of colorectal cancer. Immunol Lett. 2017 Jan 1;181:79-86.

❖ Siddharth S, Nayak A, Nayak D, Bindhani BK, Kundu CN. Chitosan-Dextran sulfate coated doxorubicin loaded PLGA-PVA-nanoparticles caused apoptosis

in doxorubicin resistance breast cancer cells through induction of DNA damage. Sci Rep. 2017 May 19;7(1):1-10.

❖ Wang XB, Zhou HY. Molecularly targeted gemcitabine-loaded nanoparticulate system towards the treatment of EGFR overexpressing lung cancer. Biomedicine & Pharmacotherapy. 2015 Mar 1;70:123-128.

❖ Yang H, Xu M, Li S, Shen X, Li T, Yan J, Zhang C, Wu C, Zeng H, Liu Y. Chitosan hybrid nanoparticles as a theranostic platform for targeted doxorubicin/VEGF shRNA co-delivery and dual-modality fluorescence imaging. RSC Adv. 2016;6(35):29685-29696.

❖ Yousefpour P, Atyabi F, Vasheghani-Farahani E, Movahedi AA, Dinarvand R. Targeted delivery of doxorubicin-utilizing chitosan nanoparticles surface-functionalized with anti-Her2 trastuzumab. Int J Nanomedicine. 2011;6:1977-1990.

❖ Zhang CG, Zhu WJ, Liu Y, Yuan ZQ, Yang SD, Chen WL, Li JZ, Zhou XF, Liu C, Zhang XN. Novel polymer micelle mediated co-delivery of doxorubicin and P-glycoprotein siRNA for reversal of multidrug resistance and synergistic tumor therapy. Sci Rep. 2016 Mar 31; 6(1):1-2.

## Summary

Novel anticancer DDS show their potential for enhanced therapeutic efficacy and reduced non-specific toxicity through the ability to enhance delivery of chemotherapeutic agents to tumors. Novel anticancer DDS reveal potential to increase therapeutic efficacy and reduce nonspecific toxicity with their ability to improve the delivery of chemotherapeutics to tumors tissues. To validate the effectiveness of developed novel DDS, in-vivo study plays a major role. The in-vivo performance is a preliminary step for the clinical evaluation of a drug or formulation. Different animal models are used for evaluating CRC targeted DDS. The anatomy and physiology of experimental animals and humans should be the same to extrapolate animal data to clinical trials. Most published studies on the development of CRC specific DDS have been performed in rats and mice.

In the present study, histopathological examination by H&E staining was performed to evaluate organ toxicity of the developed formulation and immunohistochemistry (IHC) analysis. In-vivo targeting studies were carried out using free DOX, DOX-siRNA-ChNPs, DOX-siRNA-ChNPs-CMAb formulations.

The animal studies have been duly approved by Institutional Animal Ethics Committee, Central Animal House, D. Y. Patil Medical College, Kasaba Bawada, Kolhapur 416 006, Maharashtra, India. (Approval No: (DYPMCK/ IAEC/ 2021/ FEB/09)

## 6.1 Materials

Swiss albino mice, HT-29 cells, Sterile saline, 10% formaldehyde, H&E stain.

## 6.2 Methodology

### 6.2.1 Selection of animals and tumor induction

In this experiment, Swiss albino mice aged between 4-8 weeks were used to establish tumors through subcutaneous injection of $2.3 \times 10^6$ HT-29 cells. The tumor volume was measured using Vernier calliper and mice body weight was monitored and recorded (Sun et al., 2018). After 21 days of tumor induction, the mice were randomly assigned to four different treatments groups as shown in Figure 6.1, a positive control group, a standard group receiving free DOX (at a dosage of 5 mg/kg), a Formulation-1 group receiving DOX-siRNA-ChNPs and a Formulation-2 group

receiving DOX-siRNA-ChNPs-CMAb. One group kept as Negative control (without tumor induction, without any treatment).



**Figure 6.1: Photograph of tumor induced mice groups, Positive control (tumor induced), Std (Free DOX), Formulation-1 (DOX-siRNA-ChNPs), Formulation-2 (DOX-siRNA-ChNPs-CMAb)**

**Table 6.1: Doses and injections schedule**

| Substances | HT-29 cells | Nanoformulations |
|---|---|---|
| **Doses** | Once | Three times per week |
| **Sites** | Subcutaneously | Intravenously (i.v.) |
| **Volumes** | $2.3 \times 10^6$ | 0.2mL |
| **Blood withdrawal** | Not applicable | Not applicable |
| **Volumes** | Not applicable | Not applicable |
| **Sites** | Not applicable | Not applicable |
| **Radiation (dosage and schedules)** | Not applicable | Not applicable |

**6.2.2 Formulations administration**

These treatments, administered injections given in Table 6.1 as 0.2 ml intravenous injections were given once every other day for a weekand shown in Figue 6.2. Throughout the course of the experiment, the mice's body weights and tumor volumes were closely monitored and recorded twice a week for a period of 10 days. At the end of this 10 day treatment period, all the mice were euthanized and their multiple organs were fixed in formalin for subsequent analysis (Sun et al., 2018, Li et. al., 2016, Amjad et al., 2015, Bothiraja et al., 2018).



**Figure 6.2: Photograph of intravenous route administration of formulation**

**6.2.3 H&E staining**

To assess the potential organ toxicity and tumor regression effects of formulations on heart, liver, kidneys, lungs and colon were surgically removed as shown in Figure 6.3 and preserved in 10% neutral buffered formalin. Subsequently, these tissue samples, now fixed in formaldehyde were embedded in paraffin. Thin sections, measuring 3-5 μm in thickness were then cut using a microtome (specifically, the YSI-115 model from Yorco Sales Pvt Ltd. in India) and mounted on slides. These sections were further processed and stained with hematoxylin and eosin (H&E) to enable the analysis of organ toxicity and tumor regression potential. The prepared slides were examined under a Nikon Inverted Microscope Eclipse Ti-E, Japan (Butt et al., 2016, Sun et al., 2018, Motawi et al., 2017, Li et al., 2018, Liu et al., 2018, Liu et al., 2021).
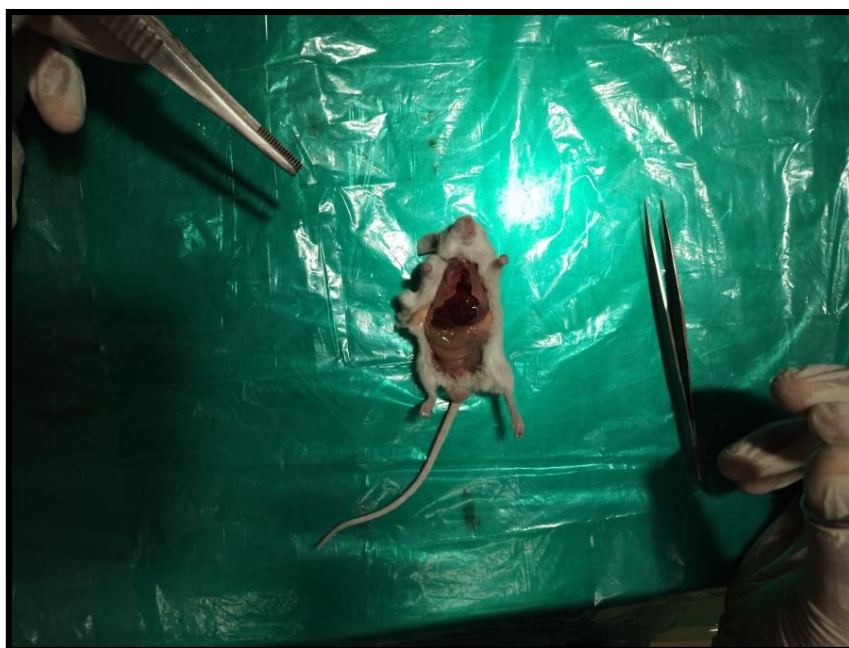
**Figure 6.3: Photograph of sacrificed animal and organs isolation
for further study**

### 6.2.4 Immunohistochemistry study

For the immunohistochemical (IHC) analysis, prepared 3-5 μm thick sections of paraffin-embedded colon tissue using a microtome (YSI-115 Yorco Sales Pvt Ltd. in India). These sections were carefully placed on slides coated with poly-L-lysine. To prepare the tissue for analysis, performed deparaffinization and rehydration. Antigen retrieval was carried out using citrate buffer at a pH-6, followed by the blocking of peroxidase using 3% $H_2O_2$. Next, the tissue sections were incubated with primary Abs, specifically CEA (Invitrogen, USA, diluted at 1:100) and Mib1 (Invitrogen, USA, diluted at 1:150), for a duration of 60 min. Horseradish peroxidase (HRP) was then introduced and allowed to incubate for 45 min. Subsequently, DAB chromogen was applied and left to incubate for 10 min. The sections were then counterstained with hematoxylin and examined using a Nikon Inverted Microscope Eclipse Ti-E in Japan (Ilie et al., 2021, Liu et al., 2021).

To assess the staining results, cells that exhibited positive staining for CEA and Mib1 were evaluated blindly by assigning codes and were manually counted by three different independent observers. The staining intensity was categorized as follows: + (no or weak expression), ++ (mild expression), +++ (moderate expression) and ++++ (high expression). The distribution of staining in epithelial tissue, whether normal or neoplastic mucosa was recorded as even (> 75% stained), focal (25% - 75%

stained), or mini focal (< 25% stained). Additionally, the cellular localization of staining in epithelial tissue was noted, including extracellular staining, luminal and cytoplasmic staining of columnar epithelial cells and goblet cell staining.

**Statistical analysis**

Each experiment was performed in triplicate and presented as mean ± standard deviation (SD). Data were analyzed using one-way analysis of variance (ANOVA) with Tukey's post hoc test (Graph Pad Prism Software v8.0.2 Inc., USA). The significance level was set at probability with *$p < 0.05$. **$p<0.01$ and ***$p<0.001$.

## 6.3 Results and discussion

### 6.3.1 Effect of formulations on tumor volume and body weight

The in-vivo antitumor efficacy of free DOX, DOX-siRNA-ChNPs, DOX-siRNA-ChNPs-CMAb was evaluated in a xenograft mice model. As seen from Figure 6.4.
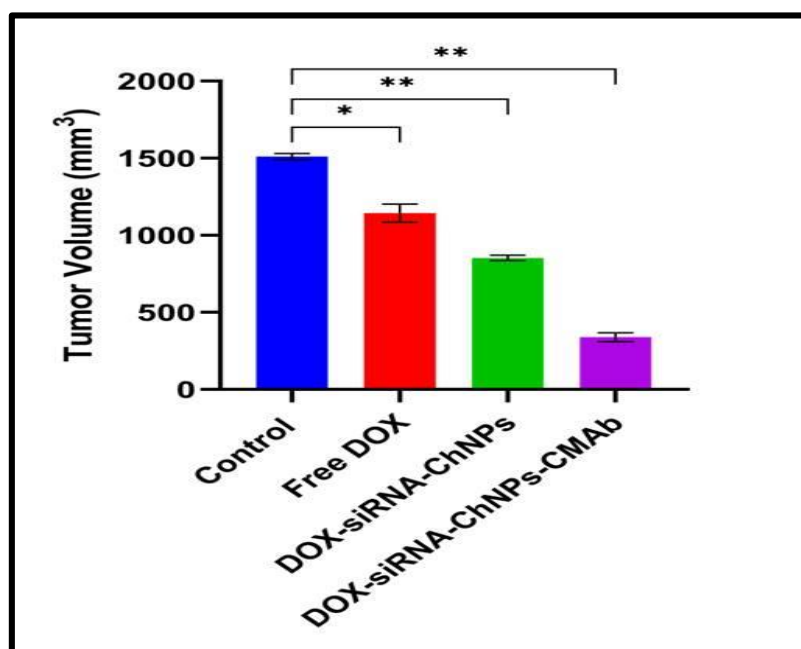


**Figure 6.4: In-vivo antitumor efficacy of positive control, free DOX, DOX-siRNA-ChNPs, DOX-siRNA-ChNPs-CMAb on tumor volume. The mice were treated with formulations at 5 mg/kg.**

The final tumor volume of untreated mice was ~1500 mm³, whereas administration of DOX reduced the tumor volume to an extent but not satisfactorily. Importantly, optimized formulation, DOX-siRNA-ChNPs-CMAb showed appreciable tumor regression and recued the tumor volume by 4-5 folds than comparing to the control and DOX-siRNA-ChNPs. It indicates the DOX-siRNA-ChNPs-CMAb can

enter into the tumor tissue by passive diffusion and deliver the DOX and siRNA to the tumor cells. The final tumor volume of DOX-siRNA-ChNPs-CMAb treated mice was around ~336 mm$^3$.

The safety of formulations was further assessed by the body weight of mice. As seen Figure 6.5, no significant changes in body weight were observed upon administration of any formulations than free DOX. Negative control group mice showed normal growth. However, positive control group mice showed slightly decreasing body weight.
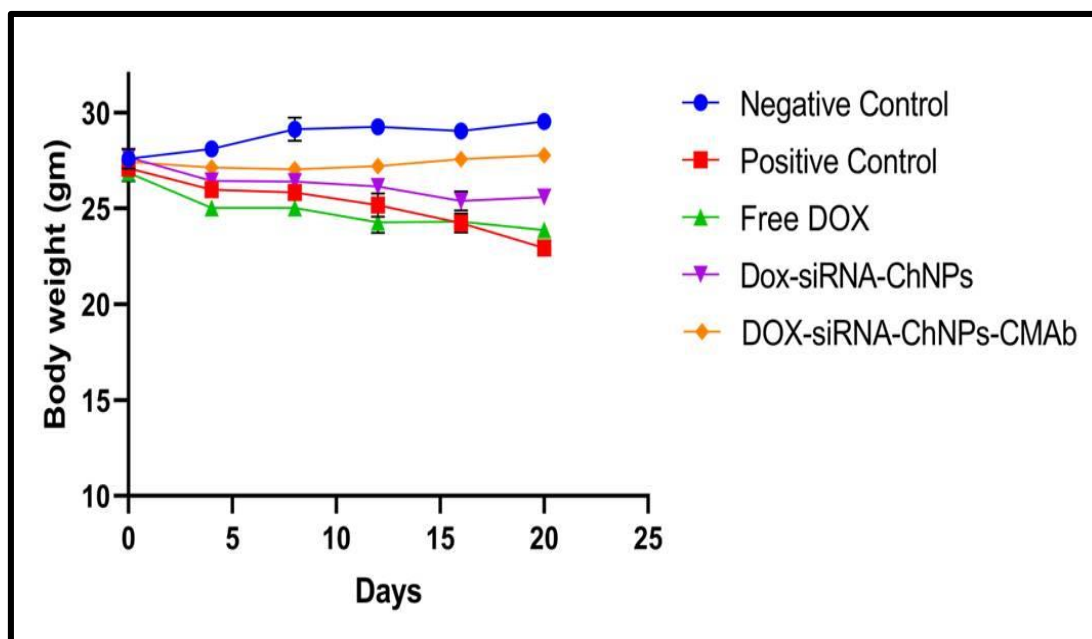


**Figure 6.5: Effect of formulation administration on body weight of mice positive control, negative control, free DOX, DOX-siRNA-ChNPs, DOX-siRNA-ChNPs-CMAb.**

## 6.3.2 H&E staining for organ toxicity

The intravenous administration of the developed formulation allows systemic delivery of the encapsulated DOX and siRNA to the specific and targeted organ. The histopathology studies were performed to assess whether the treatment with free DOX, DOX-siRNA-ChNPs and DOX-siRNA-ChNPs-CMAb formulations would result in any significant recovery in tumor tissue and with minimal or no tissue damage in comparison to free DOX solution. Negative control, positive control and treated mice were euthanized at 15 days and then all organs like heart, liver, kidney and lung were isolated for histological analysis. The formalin-fixed paraffin sections were stained with most conventional stain hematoxylin-eosin. The hematoxylin stains

negatively charged nucleic acids (nucleus and ribosomes) in blue. The eosin stains cytoplasm in pink color. Light microscopy was performed to observe the histological changes in organs of negative control, positive control mice and from mice treated with free DOX, DOX-siRNA-ChNPs and DOX-siRNA-ChNPs-CMAb formulations shown in Figure 6.6.
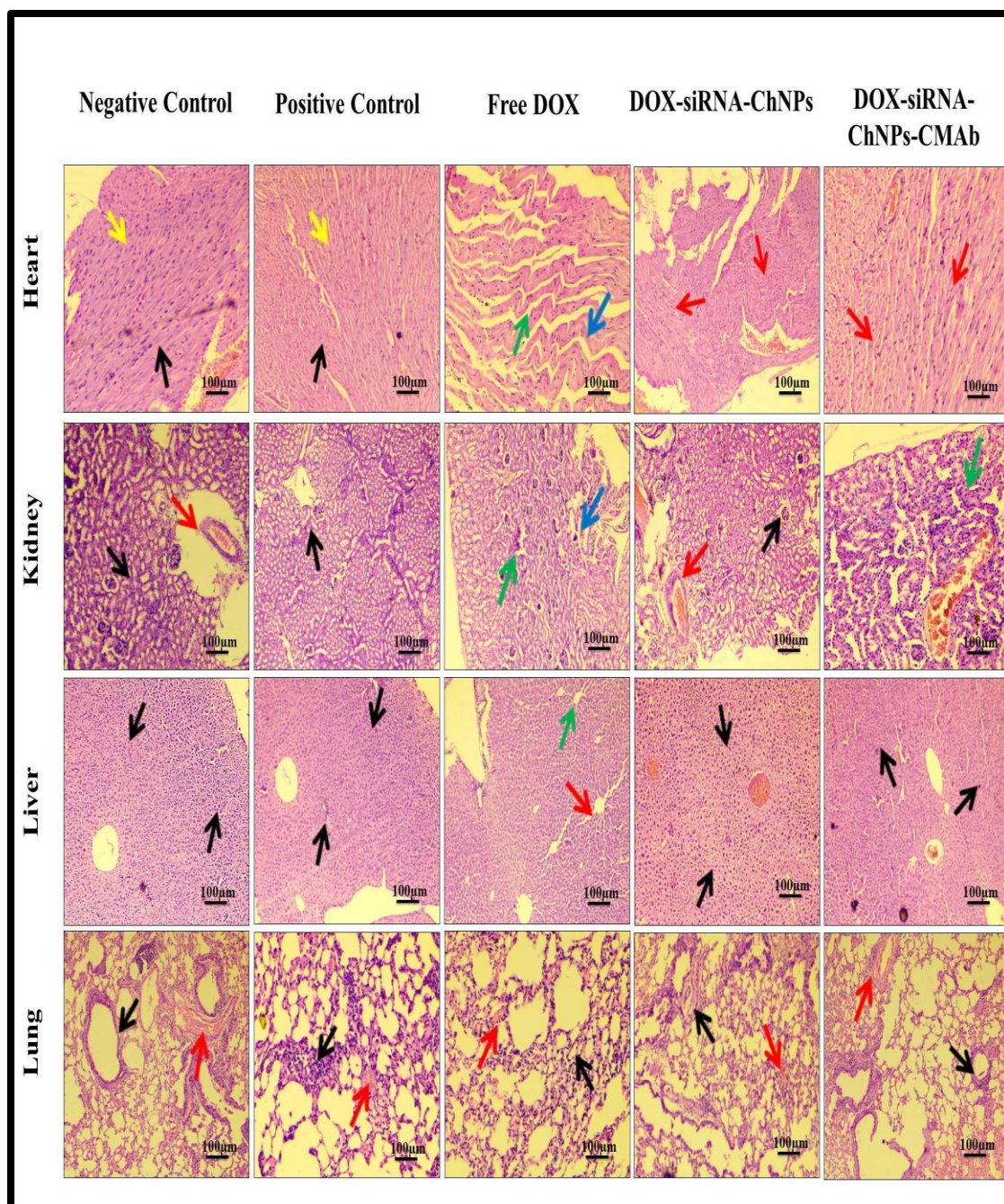


**Figure 6.6 Hematoxylin and eosin (H&E) staining of heart, kidney, liver and lung after treatment with free DOX, DOX-siRNA-ChNPs and DOX-siRNA-ChNPs-CMAb. Positive control (mice induced with HT-29 cells) and negative control (mice without tumor induction).**

H&E staining of the hearts of mice from the negative and positive controls showed normal cardiac cells with normal myocytes (black arrows) and hypertrophic nuclei that can often be found in the papillary muscle ( yellow arrow) is shown in Figure 6.6.

Mice treated with free DOX show damaged myocardium (blue arrows) with altered myocardial structure and congested blood vessels in the heart. Myocardial injury in the form of patchy interstitial fibrosis (green arrows) and myocardial necrosis are signs of DOX cardiotoxicity. After treatment with DOX-siRNA-ChNPs, DOX-siRNA-ChNPs-CMAb normal cardiomyocytes and an intact extracellular matrix were observed.

Renal H&E staining from negative controls showed normal glomeruli (black arrow), normal vascularity (red arrow) with normal cortical epithelial cells. The mice in the positive control group showed normal glomeruli (black arrows). In addition, severe tubular necrosis (green arrow), lymphocyte infiltration and vascular occlusion (blue arrow) were observed in kidneys treated with free DOX.

In the group treated with DOX-siRNA-ChNPs, histology closely resembled normal structure with normal vascularity (red arrow), normal glomeruli (black arrow). The DOX-siRNA-ChNPs-CMAb treated group showed normal histology with cortical epithelial cells (blue arrows).

The liver sections of the negative and positive controls showed normal hepatocellular histology with round to oval nuclei (black arrow). However, the livers of mice treated with free DOX showed pyknotic nucleated cells (green arrows), inflammatory cells, vascular occlusion and hepatocellular necrosis (red arrows) showing damaged cells. Liver sections of mice treated with DOX-siRNA-ChNPs, DOX-siRNA-ChNPs-CMAb showed their normal morphology with normal hepatocytes without any lesions.

The lung portion of the negative control shows normal bronchial structure (black arrow) with normal blood vessels (red arrow). However, the positive control, free DOX, DOX-siRNA-ChNPs showed vascular occlusion (red arrow) and neutrophil infiltration (black arrow). The DOX-siRNA-ChNPs-CMab treated group showed a normal structure of bronchi (black arrows) and blood vessels (red arrows). Mice treated with DOX-siRNA-ChNPs, DOX-siRNA-ChNPs-CMAb did not exhibit significant tissue toxicity on vital organs. The H&E staining images of organ toxicity is shown in (Figure 6.6).
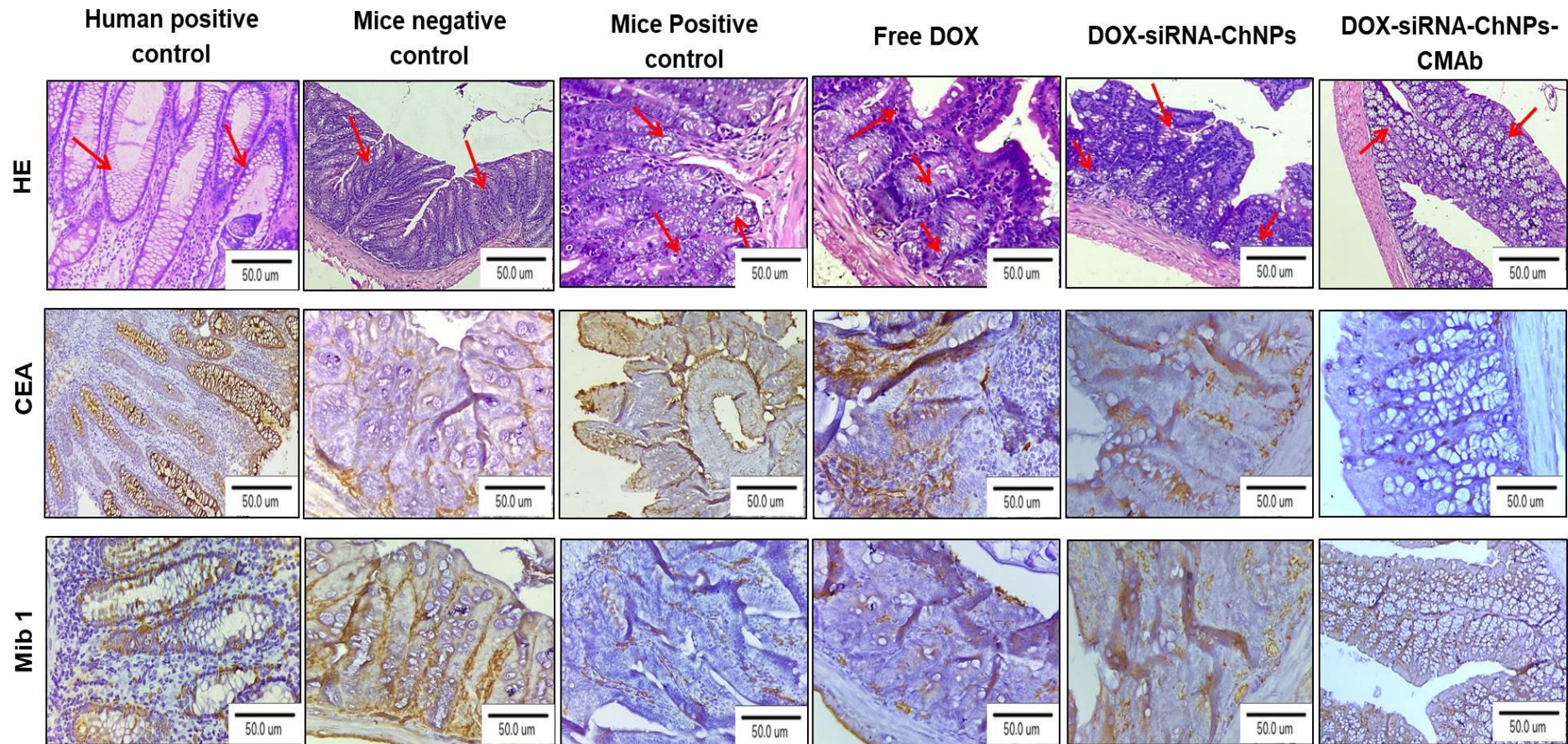
**Figure 6.7 H&E staining and IHC (CEA and Mib 1) of colon sections of human positive control, mice negative control, mice positive control (tumor-induced), free DOX, DOX-siRNA-ChNPs, DOX-siRNA-ChNPs-CMAb showing efficacy of treatment on the inhibition of colon adenocarcinoma in Swiss albino mice injected with HT-29 cells.**

**Table No 6.2 - Observation of CEA and Mib1 expression in different groups**

| Group | 1 | | 2 | | 3 | |
|---|---|---|---|---|---|---|
| | CEA | Mib1 | CEA | Mib1 | CEA | Mib1 |
| **Human positive control** | +++ | ++++ | +++ | ++++ | +++ | +++ |
| **Mice negative control** | + | - | + | - | + | - |
| **Mice positive control** | ++ | +++ | ++ | +++ | +++ | ++ |
| **Free DOX** | ++ | ++ | ++ | ++ | ++ | ++ |
| **DOX-siRNA-ChNPs** | ++ | + | ++ | ++ | ++ | ++ |
| **DOX-siRNA-ChNPs-CMAb** | + | + | + | + | + | + |

**The staining intensity was coded as + (no or weak expression), ++ (mild expression),**

**+++ (moderate expression) and ++++ (high expression)**

### 6.3.3 H&E staining of colon

Negative control group showed normal parenchyma, colonic architecture and mucosa, with intact crypt and many goblet cells.

Human control and positive control colon composed of many cryptic glands lined by columnar cells exhibiting stratified nuclei and vascular chromatin surrounded by pale cytoplasm. Nuclear pleomorphism is seen. Mitotic activity is increased. Its Suggestive of colon adenocarcinoma. Free DOX treated group showed few glands atypical with moderate mitotic activity. Non targeted group showed mild atypical. Targeted group showed normal parenchyma almost shown in HE staining in Figure 6.7.

### 6.3.4 Immunohistochemistry study of colon

Positive control group showed strong expression of CEA and higher proliferation than negative control group. After treatment with free DOX there was no significant change in CEA expression and cell proliferation. However, targeted formulation treated group showed weak expression of CEA and less/no cell proliferation in comparison with non-targeted formulation treated group as shown in Figure 6.7. The results of this study demonstrated that significant suppression of colon

adenocarcinoma in targeted formulation treated group and their graphical representation shown in Figure 6.8.
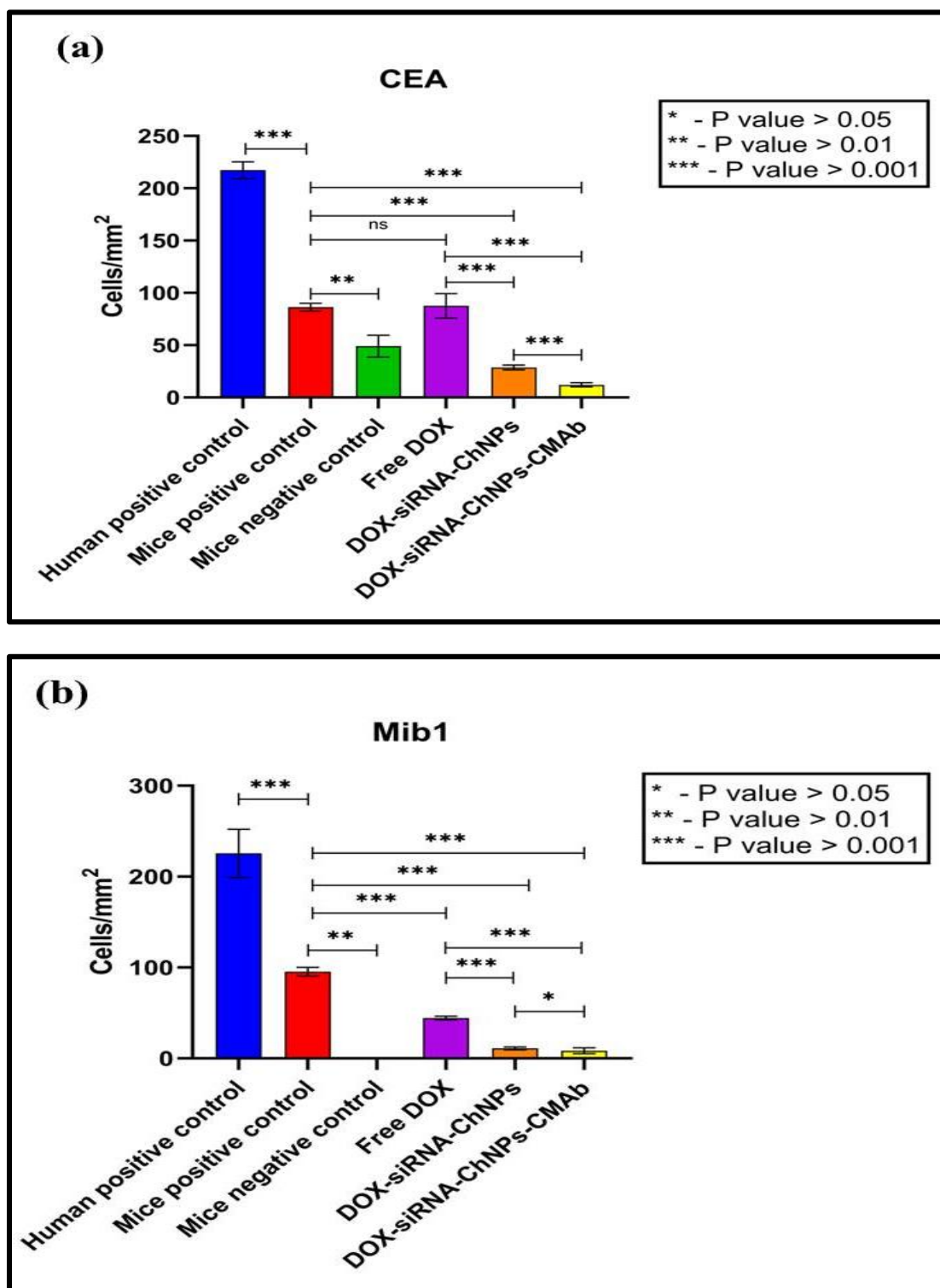


**Figure 6.8 Graphical representation of (a) CEA and (b) Mib1 positive cells in human positive control, mice positive control, mice negative control, free DOX, DOX-siRNA-ChNPs, DOX-siRNA-ChNPs-CMAb.**

## 6.4 Conclusions

It concluded that developed DOX-siRNA-ChNPs-CMAb formulations can deliver the DOX and siRNA to colorectal cancer cells and ensure reduced access of entrapped DOX and siRNA to other organs and thereby increase the therapeutics index by targeting.

It is found that the DOX and siRNA encapsulated in the CMAb conjugated ChNPs administered in-vivo may be able to accumulate in CRC cells actively due to the presence of CEA overexpressed on CRC cells without biodistribution to other tissues, for example, the heart, where DOX mostly accumulates and causes severe cardiotoxicity. Histopathological studies of multiple organs along with tumor post-treatment of free DOX, DOX-siRNA-ChNPs or DOX-siRNA-ChNPs-CMAb in tumor induced mice, demonstrated the targeting ability of DOX-siRNA-ChNPs-CMAb by visualizing the toxic effect of free DOX and DOX-siRNA-ChNPs on multiple organs apart from tumor. The further validation of targeting was provided by IHC of tumor samples which showed a drastic reduction in the population of CEA and Mib1 positive cells after treatment with DOX-siRNA-ChNPs-CMAb, thus showing the ability of CMAb to target CEA expressing CRC.

Therefore, it is concluded that the developed formulations have potential for further clinical trials.

# References

❖ Amjad MW, Amin MC, Katas H, Butt AM, Kesharwani P, Iyer AK. In vivo antitumor activity of folate-conjugated cholic acid-polyethylenimine micelles for the codelivery of doxorubicin and siRNA to colorectal adenocarcinomas. Mol Pharm. 2015 Dec 7;12(12):4247-4258.

❖ Bothiraja C, Rajput N, Poudel I, Rajalakshmi S, Panda B, Pawar A. Development of novel biofunctionalized chitosan decorated nanocochleates as a cancer targeted drug delivery platform. Artif Cells Nanomed Biotechnol. 2018 Oct 31;46(sup1):447-461.

❖ Butt AM, Amin MC, Katas H, Abdul Murad NA, Jamal R, Kesharwani P. Doxorubicin and siRNA codelivery via chitosan-coated pH-responsive mixed micellar polyplexes for enhanced cancer therapy in multidrug-resistant tumors. Mol Pharm. 2016 Dec 5;13(12):4179-4190.

❖ Ilie DS, Mitroi G, Păun I, Ţenea-Cojan TŞ, Neamţu C, Totolici BD, Sapalidis K, Mogoantă SŞ, Murea A. Pathological and immunohistochemical study of colon cancer. Evaluation of markers for colon cancer stem cells. Romanian Journal of Morphology and Embryology. 2021 Jan;62(1):117-124.

❖ Li CF, Li YC, Chen LB, Wang Y, Sun LB. Doxorubicin-loaded Eudragit-coated chitosan nanoparticles in the treatment of colon cancers. J Nanosci Nanotechnol. 2016 Jul 1;16(7):6773-6780.

❖ Li X, Zhao X, Pardhi D, Wu Q, Zheng Y, Zhu H, Mao Z. Folic acid modified cell membrane capsules encapsulating doxorubicin and indocyanine green for highly effective combinational therapy in vivo. Acta Biomater. 2018 Jul 1;74:374-384.

❖ Liu C, Liu T, Liu Y, Zhang N. Evaluation of the potential of a simplified co-delivery system with oligodeoxynucleotides as a drug carrier for enhanced antitumor effect. Int J Nanomedicine. 2018 Apr 20;13:2435-2445.

❖ Liu G, Wang M, He H, Li J. Doxorubicin-loaded tumor-targeting peptide-decorated polypeptide nanoparticles for treating primary Orthotopic Colon Cancer. Front Pharmacol. 2021 Oct 15;12:744811.

❖ Motawi TK, El-Maraghy SA, ElMeshad AN, Nady OM, Hammam OA. Cromolyn chitosan nanoparticles as a novel protective approach for colorectal cancer. Chem Biol Interact. 2017 Sep 25;275:1-2.

❖ Sun Q, Wang X, Cui C, Li J, Wang Y. Doxorubicin and anti-VEGF siRNA co-delivery via nano-graphene oxide for enhanced cancer therapy in vitro and in vivo. Int J Nanomedicine. 2018 Jun 27;13:3713-3728

In the 21st century, cancer is the major leading cause of death. Colorectal cancer is the second leading cause of death due to cancer in the world. Cancer is a complex disease caused by a combination of genetic mutations and cellular abnormalities. Current cancer treatments include surgical intervention, radiation and chemotherapy which often have severe side effects. Chemotherapy is one of the principal modes of cancer treatment, but its effectiveness can be limited by drug resistance. The combination of developing targeted co-delivery delivery by applying nanotechnology may provide more efficient and less harmful therapeutics to overcome the limitations found in conventional chemotherapy.

In the present doctoral research, preparation and characterization of surface modified DOX and siRNA-loaded ChNPs were performed. Preparation parameters were optimized such as Ch concentration, DOX concentration, stirring speed, stirring time for highest DOX entrapment and CMAb incubation time for highest conjugation efficiency to the ChNPs. ChNPs were successfully prepared by the ionic gelation method. Optimized nanoformulation was prepared with 5:1-Ch: TPP ratio, 0.5 mg of DOX concentration, 1000 rpm stirring speed, 1 h stirring time and 24 h of CMAb incubation period with fixed siRNA concentration. These optimized DOX-siRNA-ChNPs-CMAb nanoformulation showed 232±6.5 nm particle size, 0.22±0.05 PDI and -34.2±0.3 mv zeta potential.

The transmission electron microscopic analysis showed the spherical, solid dense structure of ChNPs. DOX-ChNPs showed 65.42±1.46 % DOX entrapment. In-vitro release studies showed that initial faster release and then slow and sustained release of DOX from ChNPs. At the end of 48 h, total DOX released i.e. 87.55±4.27% and 70.99±4.07% at pH 5.5 and pH 7.4 respectively. Agarose gel retardation assay confirmed the encapsulation of siRNA into ChNPs. Surface modification of ChNPs was performed using carbodiimide chemistry with CMAb and their conjugation efficiency was evaluated by ELISA. Their results indicated that 17± 1.5% of antibody was present on the surface of ChNPs.

Developing a targeted co-delivery system could improve the effectiveness of the treatment as well as decrease its side effects. In this work, DOX-siRNA-ChNPs were prepared and surface-functionalized with MAb targeting the CEA overexpressed on CRC cells and on HT-29 is a human colorectal adenocarcinoma cell line with

epithelial morphology. The DOX-siRNA-ChNPs-CMAb showed the highest cytotoxicity to HT-29 cells than free DOX and DOX-siRNA-ChNPs because CEA causes ligand-specific internalization and enhanced endocytosis of NP's which leads to greater cytotoxicity. The successful surface modified and interaction with CEA expressing cells confirmed the targeting ability of DOX-siRNA-ChNPs-CMAb. Cellular uptake of free DOX, DOX-siRNA-ChNPs and DOX-siRNA-ChNPs-CMAb were observed at 2, 4, 6, 8, 12 and 24 h by fluorescence microscopy. Their results showed the highest cellular uptake in DOX-siRNA-ChNPs-CMAb than free DOX and DOX-siRNA-ChNPs. Also, 96 % apoptosis was observed in modified ChNPs than in non-functionalized ChNPs. These entire results combined make the DOX-siRNA-ChNPs-CMAb formulation an ideal system to be considered for targeted co-delivery in colorectal cancer treatment as more efficient and specific treatment.

The in-vivo animal study further confirmed the tumor regression ability of DOX-siRNA-ChNPs-CMAb with the lowest tumor volume. It is suggested that the DOX and siRNA entrapped in the CMAb conjugated ChNPs administered in-vivo may be able to accumulate in colorectal cancer cells actively due to the presence of CEA overexpressed on CRC cells without biodistribution to other tissues, for example, heart, where doxorubicin mostly accumulates and causes severe cardiotoxicity. The histopathological studies revealed that the developed DOX-siRNA-ChNPs-CMAb formulation did not produce any major toxicity in the experimental animals and maintain the normal histological features. Therefore, it could be concluded that the developed formulations have tremendous potential for further clinical trials.

## 8.1 Recommendations

The ultimate target of present research work was to prepare CEA targeted co-delivery of DOX and siRNA by ChNPs. This targeted co-delivery approach improves the therapeutic efficacy in the treatment of CRC. The main objective of this research is preparation, characterization and in-vitro, in-vivo evaluation of CEA targeted co-delivery of DOX and siRNA by ChNPs.

It is recommended that the CEA targeting approach deliver DOX and siRNA specifically in CRC cells may be by receptor-mediated endocytosis. This targeting strategy enhances cytotoxicity, cellular uptake and apoptosis in HT-29 cells. Also, an in-vivo study reveals that this targeting strategy has great potential to reduce tumor volume and metastasis with minimal side effects on other organs.

## 8.2 Conclusions

The conclusions from the present research work are listed as follows:

1. The particle size of ChNPs plays an important role in DOX and siRNA entrapment efficiency. For the highest entrapment there is a need to optimize parameters Ch concentration, DOX concentration, stirring speed, stirring time and CMAb incubation time.

2. Optimized Ch: TPP- 5:1, DOX- 0.5 mg at 1000 rpm for 1 h showed the highest DOX and siRNA entrapment with optimum particle size. CMAb conjugation efficiency was observed at 24 h of incubation time.

3. In-vitro studies of this optimized formulation showed enhanced cytotoxicity, cellular uptake and increased apoptosis rate in HT-29 cells.

4. In-vivo studies suggested that this CEA-targeted co-delivery of DOX and siRNA have greater potential which reduced tumor volume and metastasis with less organ toxicity.

## 8.3 Summary

The present work deals with the preparation of surface modified DOX and siRNA-loaded ChNPs by a simple, organic solvent-free ionic gelation method. The numbers of preparative parameters were optimized to get high DOX and siRNA entrapment, maximum CMAb conjugation efficiency with optimum particle size.

The significance of targeted co-delivery of DOX and siRNA by ChNPs is explained in brief. The different polymers in DDS, Ch polymer and their properties and advantages of ionic gelation method, the introduction of DOX and VEGF siRNA, targeting approach and CEA targeting by MAbs are discussed.

The significance of co-delivery with targeting for cancer treatment is described. The literature survey of ChNPs, DOX-siRNA co-delivery, targeting includes preparation by ionic gelation method, properties, advantages and in-vitro, in-vivo applications. Furthermore, the literature survey of polymers, chemotherapeutic drugs, target genes for siRNA silencing, overexpressed receptors in CRC for targeting and their in-vitro, in-vivo applications is carried out and finally, the orientation and purpose of the thesis are described.

The excipients DOX, VEGF siRNA and CMAb profile are discussed. General information and methods of analysis are discussed and drug identification tests and spectrophotometric estimation of DOX in phosphate buffer saline (pH 7.4) are performed. The product information of VEGF siRNA and CMAb are discussed and performed basic characterizations.

Different parameters affect the particle size, DOX, siRNA entrapment and CMAb conjugation efficiency. Considering this, the optimization of Ch concentration, stirring speed and stirring time in preparation of ChNPs, DOX concentration, CMAb incubation time is a necessary parameter that can be optimized by varying parameters in the preparation method.

From this perspective, the study of the effect of Ch concentration on particle size and DOX entrapment were evaluated. With an increasing concentration of Ch particle size and DOX entrapment was increased but it increases above 5 mg there was a decrease in DOX entrapment and an increase in particle size. Therefore, optimum concentration of Ch is 5 mg was used throughout the study. Then DOX concentration was optimized and it is found that, 0.5 mg showed the highest entrapment with optimum particle size.

In preparation at 1 h of stirring time, 1000 rpm stirring speed was achieved highest DOX entrapment with optimum particle size.

In CMAb conjugation efficiency was optimized by varying CMAb incubation time with DOX-siRNA-ChNPs. It exhibited the highest CMAb conjugation efficiency at 24 h of incubation.

The in-vitro evaluation was assessed on HT-29 cells by MTT assay for cytotoxicity study, fluorescence microscopy for cellular uptake and FACS for apoptosis analysis. The maximum cytotoxicity was shown by DOX-siRNA-ChNPs-CMAb in comparison with other formulations. The cellular uptake studies demonstrated that significantly increased uptake up to 24 h in DOX-siRNA-ChNPs-CMAb than DOX-siRNA-ChNPs and free DOX. The maximum apoptosis was achieved in DOX-siRNA-CMAb than DOX-siRNA-ChNPs at 24 h.

The in-vivo studies were performed on swiss albino mice xenograft to evaluate targeting ability and organ toxicity. It showed that DOX-siRNA-ChNPs-CMAb exhibits the highest tumor regression potential with minimum organ toxicity in comparison to DOX-siRNA-ChNPs and free DOX.

## 8.4 Future Possibilities

In this study, surface modified and non-surface modified DOX and siRNA-loaded ChNPs were prepared by using the ionic gelation method. The surface modification with CMAb improves targeting ability which enhances cytotoxicity, cellular uptake, apoptosis in HT-29 cells and tumor regression with minimum organ toxicity. This overall performance of DOX-siRNA-ChNPs-CMAb indicated that needs more studies to take this formulation into clinical trials. Instead of Ch other biopolymers like alginate and different combination of drug and siRNA can be used. Along with this, the siRNA for MDR genes will also enhance the therapeutic efficiency. To understand the in-vitro gene silencing mechanism quantitatively RT-PCR, ELISA should be performed to study changes in the target gene expression and target protein level. Further, in-vivo gene and protein expression analyses could give a better understanding of the actual processes involved in CRC treatment.